


Advances in functionalization and conjugation mechanisms of dendrimers with iron oxide magnetic nanoparticles

Salma Habib,^{a,b} Mohammed Talhami,^b Amani Hassanein,^b Elsadig Mahdi,^a Maryam AL-Ejji,^c Mohammad K. Hassan,^c Ali Altaee,^d Probir Das^e and Alaa H. Hawari  ^{*b}

Iron oxide magnetic nanoparticles (MNPs) are crucial in various areas due to their unique magnetic properties. However, their practical use is often limited by instability and aggregation in aqueous solutions. This review explores the advanced technique of dendrimer functionalization to enhance MNP stability and expand their application potential. Dendrimers, with their symmetric and highly branched structure, effectively stabilize MNPs and provide tailored functional sites for specific applications. We summarize key synthetic modifications, focusing on the impacts of dendrimer size, surface chemistry, and the balance of chemical (*e.g.*, coordination, anchoring) and physical (*e.g.*, electrostatic, hydrophobic) interactions on nanocomposite properties. Current challenges such as dendrimer toxicity, control over dendrimer distribution on MNPs, and the need for biocompatibility are discussed, alongside potential solutions involving advanced characterization techniques. This review highlights significant opportunities in environmental, biomedical, and water treatment applications, stressing the necessity for ongoing research to fully leverage dendrimer-functionalized MNPs. Insights offered here aim to guide further development and application of these promising nanocomposites.

1. Introduction

Over the past few decades, iron oxide magnetic nanoparticles (MNPs) have been increasingly employed in diverse applications ranging from magnetic resonance imaging and drug delivery to environmental remediation, thanks to their superparamagnetic properties. However, their practical use is constrained by their susceptibility to aggregation and rapid oxidation, which compromises their functionality in biological and aqueous environments.¹ To address these challenges, surface modification techniques using polymers such as dextran, polyethylene glycol, and chitosan have been explored.^{2,3} Among these, dendrimers stand out due to their unique structural and chemical properties.

Dendrimers are highly branched, monodisperse macromolecules characterized by their uniform size and three-dimensional architecture. Unlike linear polymers, dendrimers offer several functional groups on their surface, which can be precisely tailored to enhance the physicochemical and biological properties of MNPs. These groups allow for the conjugation of various chemical entities including drugs, imaging agents, and targeting ligands, making dendrimers a versatile tool in nanomedicine and biosensing applications. Moreover, the internal cavities of dendrimers can encapsulate therapeutic agents, protecting them from the external environment until delivery, thus enhancing the biocompatibility and efficacy of MNPs in biological systems. The biocompatibility of dendrimer-modified MNPs is particularly notable. Dendrimers can be engineered to minimize interactions with cell membranes and reduce cytotoxicity, a significant advantage over other conjugating agents which may elicit adverse biological responses. Furthermore, dendrimers can improve the stability of MNPs in physiological conditions, preventing aggregation and enhancing solubility, which are critical for biomedical applications such as *in vivo* imaging and targeted drug delivery.⁴⁻⁷

Understanding the mechanism of conjugation and functionalization of MNPs with dendrimers is of paramount importance. By working on the underlying processes and interactions, researchers can optimize the loading of functional

groups, enhance dispersibility in solvents, and facilitate the attachment of ligands, scavengers, catalysts, and reagents.

This understanding enables the development of more efficient and fitted applications in fields such as biomedicine, catalysis, environmental remediation, and nanotechnology as a whole. Furthermore, understanding the conjugation and functionalization mechanisms can contribute to the design of novel materials with enhanced properties and performance.

In brief, the functionalization and conjugation of MNPs with dendrimers provides promising possibilities to develop efficient and biocompatible nanomaterials for advanced biomedical applications. This review will further explore the synthesis techniques, particularly focusing on the divergent and convergent methods, and the biomedical applications of dendrimer-based MNPs, emphasizing recent advancements and the future potential of these complexes.

2. Magnetic nanoparticles pre-functionalization with dendrimers

2.1 Magnetic nanoparticles surface modification using anchoring agents

Surface functionalized MNPs can be categorized into three primary types: hydrophobic, hydrophilic, and amphiphilic. This classification is based on the distinct surface properties

of MNPs that are coated with these functional groups. To attach various functional groups (*e.g.*, $-\text{OH}$, $-\text{COOH}$, $-\text{NH}_2$, or $-\text{SH}$) onto the surface of bare MNPs, organic or inorganic coupling agents could be employed (Fig. 1). These agents facilitate the conjugation of MNPs with dendrimers, imparting stability, protection, and functionality enhancement properties; this renders them well-suited for diverse research domains and applications. Inorganic or organosilane coupling agents such as TEOS (tetraethyl orthosilicate), primary amine-containing silanes like APTMS (3-aminopropyltrimethoxysilane) and APTES (3-aminopropyltriethoxysilane), epoxy modified silane like 3-(glycidyloxypropyl) trimethoxysilane (GLYMO),⁸ thiol modified silane(3-ercaptopropyltrimethoxysilane),⁹ and carboxyl modified silane such as (OPTBA).¹⁰ Various organic coupling molecules such as long chain hydrocarbons (octyl¹¹ and octadecene),¹² long chain fatty acids (oleic acid), organic acids (succinic anhydride, maleic anhydride, Barium acetate,¹³ citric acid),^{14,15} along with some peptides containing COOH like Glutamic acid¹⁶⁻¹⁸ and L-arginine¹⁹ have been used as surface modifiers for MNPs. The coupling between MNPs and silane groups takes place when the hydroxyl groups that exist on the MNPs initiate an attack on the methoxy or ethoxy group ($-\text{OCH}_3$, $-\text{OC}_2\text{H}_5$) located on the silane coupling agents respectively and replace it by forming a covalent bond ($-\text{Si}-\text{O}-$) between MNPs and silane coupling agent and another bond forms when silane groups crosslink between each other in the

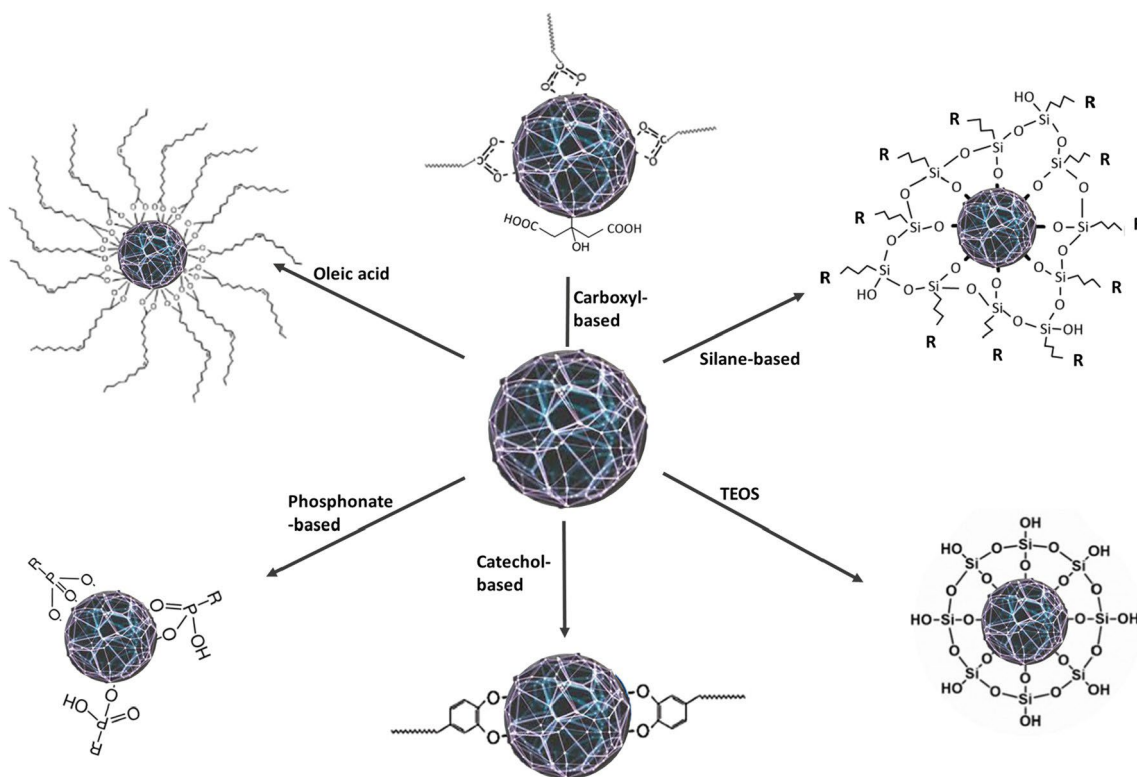


Fig. 1 (A) MNPs coated with TEOS and APTES,³³ (B) fabrication process and thermal decomposition of iron(III) oleate complexes leading to mono-dispersed MNPs,²⁶ (C) phosphonate chelation on MNPs surface, (D) carboxylation of MNPs, (E) chelation and bridge dentation of carboxylate groups onto MNPs surface.

form of (Si–O–Si). This process of salinization coats the MNPs' surface with the functional group that the coupling agent has (–NH₂, –OH, or –COOH), thus resulting in the formation of surface functionalized MNPs. Consequently, the coated MNPs will be able to form stable coordination with dendrimers or their monomers (methacrylate) to propagate further into dendrons. The coordination will be covalently through various types of chemical bonds depending on the anchored groups on the MNPs surface. The chemical bonds will be mentioned in section 3.1. Phosphonates are another anchoring group that are used as strong covalent binder to connect MNPs with dendrimers. Phosphonates groups can bind to MNPs through mon-, bis-, or tri-phosphonate dentation in which ate bis and tri-dentation they provide a stable nanoparticle colloidal with MNPs over a long time.

Organic molecules that bind to MNPs' surface have two main factors: long hydrocarbon chain to stabilize the surface of MNPs, and active functional groups that would help in anchoring on MNPs surface from one side and bind to dendrimers from the other side of the chain. Oleic acid is a long-chain fatty acid that is often used to functionalize the surface of MNPs in organic solvent-based processes.²⁰ Oleic acid coated MNPs are hydrophobic and, therefore, useful in organic solvents and provide a protective coating for the MNPs to prevent oxidation and aggregation, thereby enhancing their dispersion characteristics. In terms of connection and binding with MNPs, oleic acid mostly forms a physical adsorption layer on the surface of MNPs^{21–25} as well as chemical coordination through thermal decomposition of iron oleate.^{20,26,27} Covalent bonding provides a stable and robust linkage between the surface modifier and the MNP, and it happens when the carboxylic group of OA binds chemically to the centers of MNPs.²⁰ Physical adsorption is weaker than coordination and thus can be influenced by the surrounding environment. Mainly, the oleic acid on MNPs produced are further replaced by other anchoring groups (through ligand exchange process) to enable stable functionalization with dendrimers for a wide range of biomedical, catalytic, and water treatment applications. In some cases, OA is kept as a stabilizer to further have dendrimer physically attached to OA coated MNPs to manage hydrophobicity or amphoteric effects.^{20,28,29} Carboxylates are other common organic molecules that are capable of stabilizing MNPs through mon- or bi-dentation (Bridging or chelation).^{26,30} Furthermore, depending on the type and connection of the carboxylate form, organic compounds with two or more carboxyl groups are essential to help MNPs to be coordinated with dendrimers peripheral groups accordingly. For instance, citric acid, succinic acid, L-arginine amino acid,^{14,15} and glutamic acid^{16–19} along with organic salts such as Barium acetate (Ba (CH₃COO)₂),¹³ sodium citrate¹⁴ and trisodium citrate¹³ are examples of the carboxylates that form a bond with MNPs. Another form of carboxylation is by using organic acids or carboxylate to function dendrimer surface, then coordinating with MNPs such as succinic anhydride³¹ and maleic anhydride.³²

2.2 Magnetic nanoparticles surface modification using nanocomposites

Magnetic nanocomposites (MNCs) are composite materials that incorporate MNPs into a matrix material of core-shell and subsequently introduce dendrimers on the top shell of MNCs. Their synthesis can be done using a variety of methods, but one common approach is to use a mixture of magnetic particles and a polymeric matrix. The magnetic core is surrounded by a polymeric network that provides various benefits such as flexibility, control over chemical composition, storage, non-toxicity, and allowing the attachment of functional groups on the MNPs' surface. These functional groups can physically adsorb bio molecules or metals and can be coupled with affinity ligands to modify the surface properties of the superparamagnetic NPs. This surface functionalization enhances the biocompatibility between the nanoparticles and aqueous medium and safeguards against the oxidation of the particle surface.

A case of a magnetic nanocomposite using 4-methylstyrene (4MS), divinyl benzene (DVB), and glycidyl methyl acrylate (GMA) was done by ref. 23 and a similar polymerization with ref. 34. The procedure involved mixing the magnetic particles with a solution of the monomers in a suitable solvent. The mixture is then polymerized, typically using a radical initiator such as 2,2-azobisisobutyronitrile (AIBN). 4-Methylstyrene is a vinyl aromatic monomer that can improve the solubility of the polymer in non-polar solvents and provide thermal stability to the composite. Divinyl benzene is a crosslinking agent that can contribute to enhancing the rigidity and mechanical strength of the nanocomposite. Glycidyl methyl acrylate is a monomer that contains epoxy functionality, which can be used to anchor the polymer to the surface of the magnetic particles and improve the compatibility between the polymer and the particles. The chemical structure of poly (4 methyl styrene-co-divinylbenzene-co-GMA) is a random copolymer consisting of three monomers: 4-methylstyrene, divinylbenzene, and glycidyl methacrylate. The polymer chain consists of repeating units of these monomers arranged in a random sequence. The structure of the polymer can be represented using a polymerization formula, such as: $-\text{[CH}_2\text{-C(CH}_3\text{)Ph-CH}_2\text{-CH(C}_6\text{H}_5\text{)}_2\text{-CH}_2\text{-CH}_2\text{-OC(O)CH}_2\text{CH(CH}_3\text{)}_2\text{]}-$, where "Ph" represents the phenyl group, and "C₆H₅" represents the benzene ring (see Fig. 2 and Table 5).

Other magnetic nanocomposite core-shell structure was made out of methacrylate (MA) and *N,N*-methyl-enebisacrylamide (MBA) with the aid of (AIBN) as the initiator producing cross-linked poly (methyl acrylate) that could make vacancies to contain MNPs in the core of the polymeric matrix.³⁵ The resulting magnetic nanocomposite can additionally serve as a core for the growth of dendrimers on their surfaces, resembling a tree-branch-like system. PAMAM dendrimer was propagated from both nanocomposites and triblock polymeric dendronization^{7,36} with different generations (G0, G1, and G2), refer to Table 6.

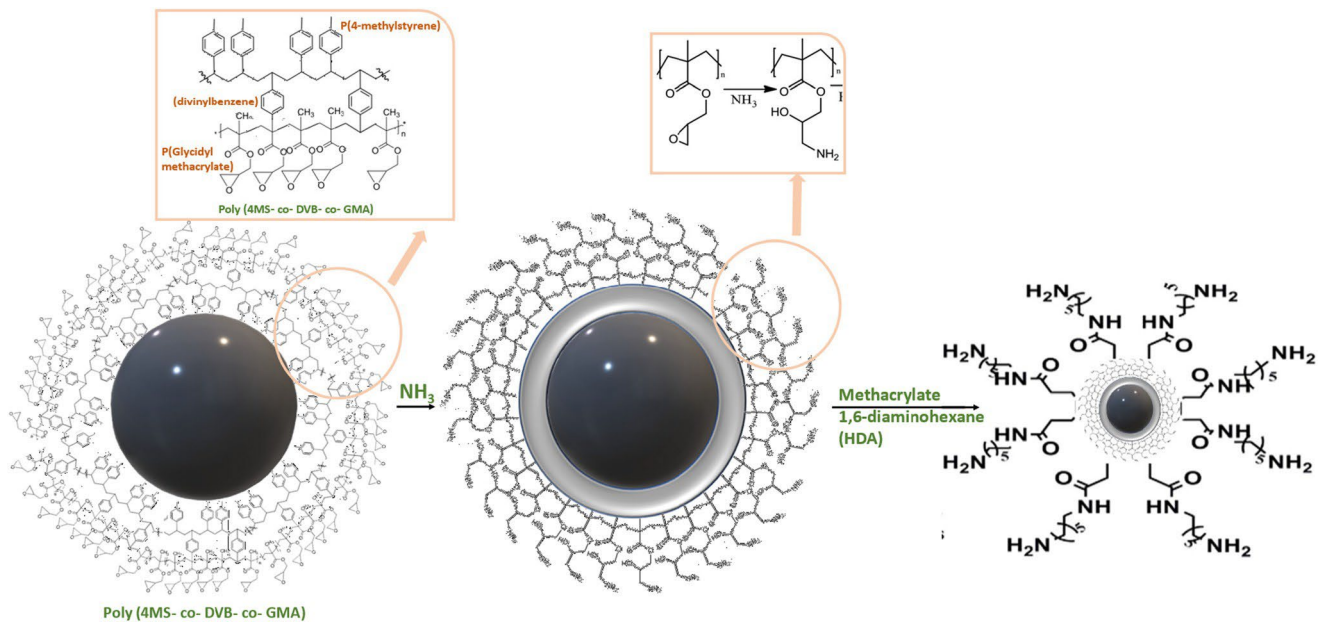


Fig. 2 IOMNPs core-shell amino nanocomposite with P (4-MS-co-DVB-co-GMA) and propagation of PAMAM dendrimer on the surface.²³

Murugan *et al.* (2018)³⁴ used a straightforward method to create four distinct types of magnetic core-shell nanocomposites, which were stabilized using gold/palladium NPs. The initial step involved preparing a matrix of crosslinked copolymer that consists of styrene-divinylbenzene-vinylbenzyl chloride (ST-DVB-VBC) as coating of MNP@oleic acid. The matrix was then functionalized with COOH group through binding 3-aminobenzoic acid with vinylbenzyl chloride on the nanocomposite surface side, followed by conjugation with a ready-made PPI-G (2) and PPI-G (3), respectively dendrimers through amidation reaction (OvC-NH-). Each core-shell matrix was then immobilized separately with AuNPs and PdNPs. Due to an increase in active sites for adsorption, the grafted dendrimer aids in improving the adsorption and catalytic capacities of (dendrimers-MNC) matrix in comparison to other composites in the elimination of heavy metals,³⁵ degradation of organic dyes,²³ or cleaving abilities of biomolecules.³⁴

3. Magnetic nanoparticles bonding type with dendrimer

3.1 Chemical bonding (covalent bonding)

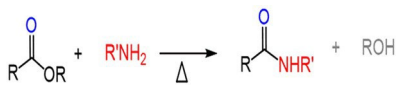
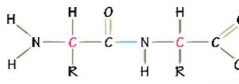
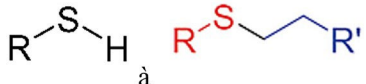
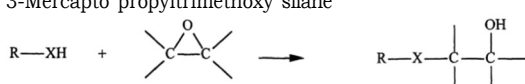
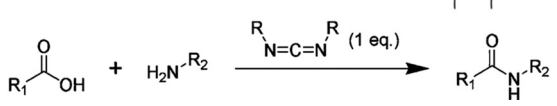
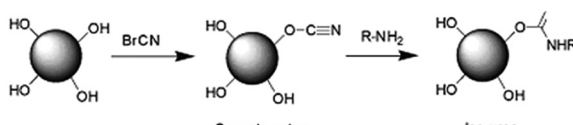
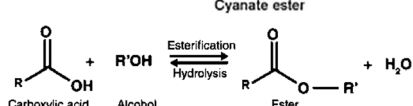
To efficiently conjugate magnetic nanoparticles (MNPs) with dendrimers, several covalent bonding strategies have been developed. These methods ensure the stability and functionality of the conjugated system across various conditions, making them ideal for a wide range of applications from biomedical imaging to water remediation. Table 1 summarizes the different types of covalent bonds utilized in the conjugation process, along with their respective advantages and applications.

3.2 Physical bonding

Alternatively, dendrimers can also be physically attached to MNPs through electrostatic interactions. For example, dendrimers with positive charges can interact with negatively charged MNPs through electrostatic attraction, forming a stable electrostatic complex. The attachment of dendrimers to MNPs can be tuned by adjusting the size, surface functionalization, and concentration of both the dendrimer and MNP. The charge of MNPs can vary depending on several factors, such as the surface chemistry, pH of the solution, and the type of coating. MNPs can be positively charged, negatively charged, or neutral. When the surface of MNPs is functionalized with cationic groups (*e.g.*, amine or quaternary ammonium), the nanoparticles tend to become positively charged. On the other hand, when the surface is functionalized with anionic groups (*e.g.*, carboxylate or sulfonate), the nanoparticles tend to become negatively charged. In both cases, the charge on the nanoparticle surface is due to the presence of ionizable functional groups. Generally, the electrostatic interactions between MNPs and other charged particles or surfaces are complex and depend on several factors, such as the magnitude and distribution of surface charge, the distance between the particles, and the ionic strength of the solution.

3.2.1 Encapsulation. The mechanism of encapsulation of MNPs in dendrimers involves the use of electrostatic interactions and hydrogen bonding between the dendrimer and the MNP. In the case of electrostatic interactions, positively charged dendrimers can encapsulate negatively charged MNPs, while negatively charged dendrimers can encapsulate positively charged MNPs. Hydrogen bonding occurs between the functional groups of the dendrimer and the surface of the MNP. Different types of dendrimers can be used to encapsulate

Table 1 Types of covalent bonds used in literature to conjugate MNPs with dendrimers

Bond type	Reaction	Advantages	Structure	Ref.
Amide	Carboxyl groups react with amino groups	Stable		37 and 38
Peptide linkage	Carboxyl groups react with amino groups (amino acids involved)	Biocompatible		10, 21 and 39
Thiol bonding	Thiol groups react with functional groups	Efficient bonding		22, 40 and 41
Silane coupling	Alkoxysilane groups react with OH groups on MNPs	Effective bonding and optimized surface coverage	Tetraethyl orthosilicate (TEOS) Aminopropyltriethoxy silane (APTES) 3-(Glycidoxypropyl)trimethoxy silane (GLYMO) 4-Oxo-4-(3-(triethoxysilyl)propylamino) butanoic acid (OPTBA) 3-Mercapto propyltrimethoxy silane	13 and 41-43 41 and 44-50 8 10 9
Epoxy	Epoxy groups react with the hydroxyl groups	Reacting with multiple functional groups		8, 23 and 51-53
Carbodiimide	Carboxylic acid groups react with amino groups using a carbodiimide coupling agent	Robust and stable conjugates, optimized surface coverage		4, 10, 46 and 54-57
Cyanate	Isocyanate groups react with hydroxyl groups	Rapid and efficient under mild conditions		58-60
Esterification (carboxylic linkage)	Carboxyl groups react with hydroxyl groups	Relatively stable		16, 22, 61 and 62

MNPs, including poly(amidoamine) (PAMAM),^{62,63} poly(propylene imine) (PPI),^{5,64} and other types of dendrimers as coatings⁶⁵⁻⁶⁷ The choice of dendrimer depends on the size and shape of the MNP, as well as the desired application. The generation of the dendrimer also plays a crucial role in encapsulation efficiency and stability. Generally, higher-generation dendrimers have more cavities for interaction with the MNP, resulting in higher encapsulation efficiency. However, higher-generation dendrimers also have a higher degree of branching, which can lead to steric hindrance and reduce the stability of the encapsulated MNPs. Therefore, the optimal generation of dendrimer for encapsulating MNPs depends on the specific application and the size and surface chemistry of the MNP. In general, MNPs that are smaller than the diameter of the dendrimer cavities can be encapsulated. For example, for a PAMAM dendrimer of generation 4 (G4) with an internal diameter of approximately 3 nm, MNPs with a diameter of less than 3 nm can be encapsulated. However, larger MNPs may be encapsulated by attaching them to the surface of the dendrimer or by using a dendrimer with a larger internal diameter. The size of the dendrimer is also important for efficient encapsulation. Dendrimers with larger internal diameters can accommodate larger MNPs, but they may also have a higher

degree of branching, which can lead to steric hindrance and reduce the encapsulation efficiency. The optimal size for encapsulating MNPs in dendrimers also depends on the desired application. For example, for biomedical applications, the size of the dendrimer and MNP should be small enough to allow for efficient cellular uptake while also being large enough to avoid rapid clearance by the kidneys. Therefore, the size of MNPs and dendrimers that allows encapsulation of MNPs in dendrimers varies depending on multiple factors and needs to be optimized for each specific application.

One example of MNPs encapsulated in dendrimers is the encapsulation of MNPs within a poly(propylene imine) (PPI) dendrimer.^{5,68} The encapsulation was achieved through a three-step synthesis process conducted in a dry THF solution under an argon atmosphere. In the first step, iron hydroxide was formed within the dendrimer matrix as an intermediate product. Subsequently, oxidation of the intermediate product was carried out in the presence of oxygen, resulting in the conversion of iron hydroxide (Fe(OH)₂) to iron oxide (Fe₃O₄). Oxygen bubbling was performed at room temperature and atmospheric pressure. After the completion of the final stage, the reaction mixture was filtered and washed with dry tetrahydrofuran. In some cases, two types of dendrimer-encapsu-

lated magnetic nanoparticles (DENPs) were obtained. Type 1 DENPs corresponds to MNPs being encapsulated within the dendritic structure, with particle sizes not exceeding 4 nm. These particles exhibited solubility in tetrahydrofuran, benzene, chloroform, and methylene chloride. On the other hand, type 2 DENPs represented dendrimers surrounded by larger MNPs (20–30 nm) and were insoluble. The completion of the oxidation reaction was confirmed by changes in the UV spectra, indicating the absence of iron ions in the final products.

Another form of encapsulation is dendrimer entrapping iron magnetic ions in the form of iron(II)⁶⁹ and iron(III).⁷⁰ The potential coordination of dendritic sites allows the entrapping of these ions, thus creating magnetic phase transitions and generating dendritic magnetic fields. They are scientifically named “magnetic mesogens”. These mesogens can be found in mesophase (liquid crystalline form) and possess the characteristics of low viscosity, high orientation control, and huge anisotropy of magnetic susceptibility.^{69,70}

3.2.2 Layer by layer assembly. The MNPs can be coated through a layer-by-layer (LbL) assembly technique. In this technique, the MNPs are alternately dipped into solutions of oppositely charged polyelectrolytes which results in the formation of multilayer coatings of different charges on the surface of the

MNPs. Once the desired number of layers is achieved, the MNPs can be functionalized with dendrimers through a surface modification process. This process was initiated when MNPs were coated with polystyrene sulfonate (PSS) salt by ref. 71 (Fig. 3) and similar to it done by ref. 57 with slight modifications. In this technique, the MNPs were alternately dipped into solutions of PSS, which resulted in the formation of a multilayer coating of PSS with fluorescein isothiocyanate-folic acid (FITC-FA) functionalized PAMAM G5 dendrimers through a surface modification process. The FITC-FA functionalized PAMAM G5 dendrimers were then adsorbed onto the surface of PSS-MNP through electrostatic attraction between the positively charged amine groups on the PAMAM dendrimer and the negatively charged sulfonate groups on the surface of the MNP. The excess dendrimer was then washed away, leaving behind a layer of FITC-FA functionalized PAMAM G5 dendrimers on the surface of the PSS-MNP. Afterward, a multilayer coating was tested with polypeptides polyglutamic acid (PGA) and poly L-lysine (PLL) on the surface of the MNPs.⁵⁷ (PGA) and (PLL) are two oppositely charged polyelectrolytes commonly used in layer-by-layer (LbL) assembly techniques to coat and functionalize MNPs. In LbL assembly, the first layer of PGA is adsorbed onto the MNPs due to electrostatic interactions between the negatively charged carboxylic acid groups

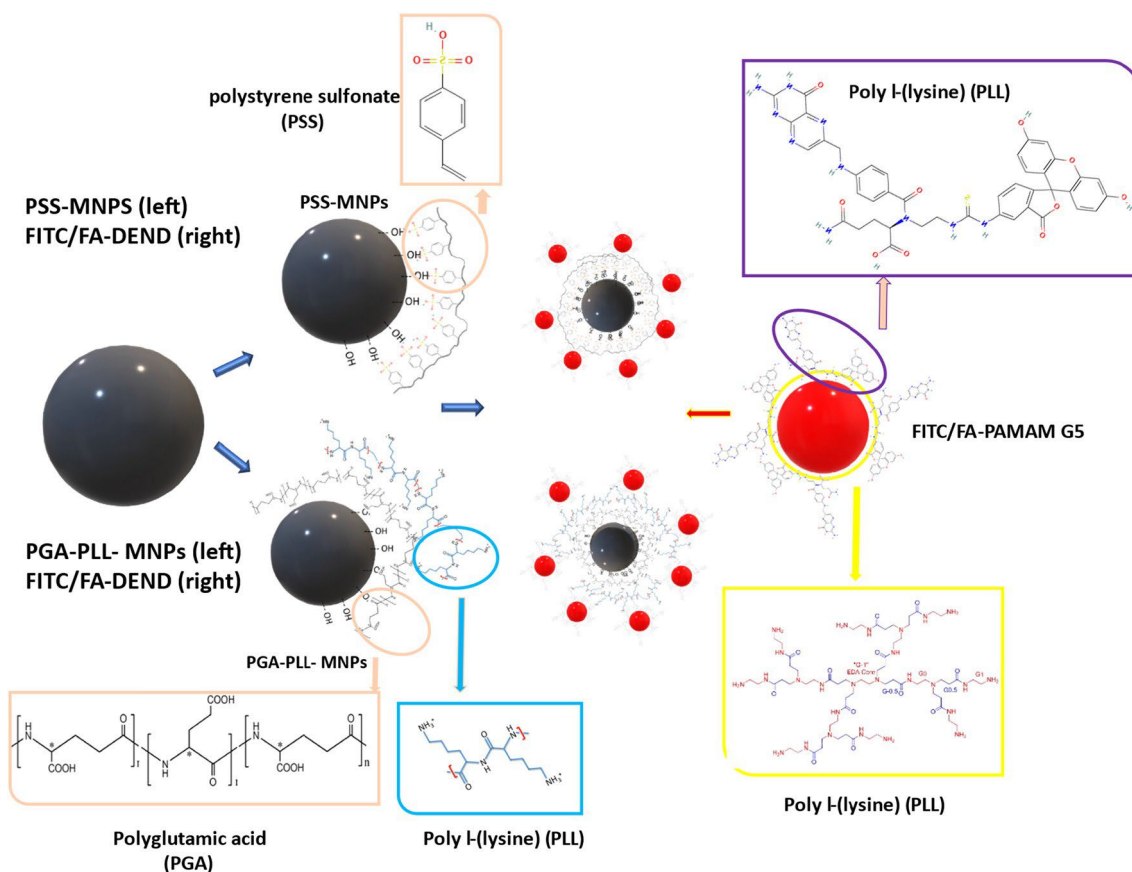


Fig. 3 Layer by layer assembly of MNPs with different polymeric materials through electrostatic interactions then modification with FITC-FA functionalized PAMAM dendrimer G5.^{57,71}

Table 2 Various types of dendrimers and dendritic systems conjugated with MNPs based on the reviewed literature

Type of dendrimer	Monomers	Description	Common conjugation method with MNPs	Functionality	Section
Polyamidoamine (PAMAM) dendrimers	<ul style="list-style-type: none"> ■ Methyl acrylate ■ Methylene diamine 	<ul style="list-style-type: none"> ■ Widely studied ■ Well-defined branching structures ■ Used for various applications 	Covalent bonding, electrostatic interaction	High density of amine and ester groups facilitating versatile bioconjugation and stability in bio-applications	4.1
Polypropylenimine (PPI) dendrimers	<ul style="list-style-type: none"> ■ Butylenediamine ■ Ethylenediamine 	<ul style="list-style-type: none"> ■ Commonly used type ■ Highly branched structures ■ Employed in applications such as gene delivery and drug encapsulation 	Electrostatic interaction, surface adsorption	Amine groups enhance interaction with negatively charged biological molecules and MNPs	4.2
Poly(<i>N</i> -propylethane-1,2-diamine) (PNPEDA) dendrimer	<ul style="list-style-type: none"> ■ Reduced forms of methyl acrylate and methylene diamine 	<ul style="list-style-type: none"> ■ Derived from PAMAM reduction ■ Tailored as stabilizing agents for nanoparticles 	Covalent bonding, surface modification	Reduced amine groups lead to less reactivity but improved biocompatibility and solubility	4.3
Polyethyleneimine (PEI) dendrimers	<ul style="list-style-type: none"> ■ Ethylenediamine (EDA) 	<ul style="list-style-type: none"> ■ High amine density ■ Excellent binding and encapsulation properties ■ Useful for gene transfection and drug delivery 	Electrostatic interaction, surface adsorption	High amine content provides strong nucleic acid binding for gene delivery applications	4.4
Triazin-based dendrimers	<ul style="list-style-type: none"> ■ Ethanolamine-trichlorotriazine ■ Diethanolamine-triazine ■ Diethylenetriamine-triazine ■ Cyanuric chloride-triazine 	<ul style="list-style-type: none"> ■ Incorporate triazine rings into their structure explored for applications like drug delivery and nanocomposite materials. 	Covalent bonding, surface adsorption	Triazine groups offer unique electronic properties beneficial in drug delivery systems	4.5
Peptide dendritic MNPs	<ul style="list-style-type: none"> ■ Poly <i>L</i>-lysine 	<ul style="list-style-type: none"> ■ Dendrimers functionalized with peptides specific targeting of cells or tissues 	Covalent bonding, peptide interaction	Peptide surfaces designed for targeted delivery and diagnostics, enhancing cellular uptake	4.6
Polyglycerol (PG) dendrimers	<ul style="list-style-type: none"> ■ Polyglutamic acid (glutamate) ■ <i>L</i>-Arginine ■ Glycidol 	<ul style="list-style-type: none"> ■ Targeted drug delivery, diagnostics, and imaging ■ Biocompatibility ■ Applications like drug delivery, bioconjugation, and as stabilizers for nanoparticles 	Covalent bonding, surface adsorption	Hydroxyl groups offer multiple sites for bioconjugation, improving biocompatibility and solubility	4.7
Dendritic hyperbranched polyesters (HBPE)	<ul style="list-style-type: none"> ■ 2,2-Bis(hydroxymethyl) propionic acid (bis-MPA) ■ Citric acid 	<ul style="list-style-type: none"> ■ Highly branched, macromolecular structures applications, including drug delivery, nanocarriers, and as contrast agents in imaging 	Covalent bonding, surface modification	Ester groups provide biodegradable options for drug delivery systems, enhancing payload control	4.8
Pyridyl phenylene dendrimers	<ul style="list-style-type: none"> ■ Phenylene ■ Pyridylene 	<ul style="list-style-type: none"> ■ Contain pyridylphenylene units in their structure ■ They are explored in fields like catalysis, molecular recognition and nanotechnology 	Covalent bonding, surface modification	Pyridyl groups enhance molecular recognition and binding, useful in sensors and catalysis	4.9
Carbosilane dendritic systems	<ul style="list-style-type: none"> ■ Amine ■ Allyl group, isocyanate ■ 3-Mercaptopropionic acid 	<ul style="list-style-type: none"> ■ Contain silane in their dendritic systems ■ Well-defined structures and biocompatibility ■ Used in drug delivery, gene therapy, and as carriers for bioactive molecules 	Covalent bonding, electrostatic interaction	Silane groups contribute to strong covalent bonds with MNPs, enhancing stability and functionality	4.10
Methoxyphenyl triallyl-based catalytic dendrons	<ul style="list-style-type: none"> ■ Cyclo- and dicyclohexyldiphosphinopalladium 	<ul style="list-style-type: none"> ■ Designed for catalytic applications and can be functionalized to enhance catalytic activity. They are used in various catalysis processes 	Covalent bonding, surface modification	Allyl groups can be utilized to anchor catalytic sites, enhancing the reactivity of MNPs	4.11

Table 2 (Contd.)

Type of dendrimer	Monomers	Description	Common conjugation method with MNPs	Functionality	Section
Phosphonate-containing dendrimers	■ V	<ul style="list-style-type: none"> ■ Contain phosphonate groups ■ Unique surface properties ■ Applications in materials science, catalysis, and as stabilizers for nanoparticles 	Covalent bonding, surface adsorption	High density of amine and ester groups facilitating versatile bioconjugation and stability in bio-applications	4.12
Magnetic graphene oxide with dendrimers	■	<ul style="list-style-type: none"> ■ Dendrimers are combined with magnetic graphene oxide ■ Multifunctional applications, such as drug delivery, imaging, and environmental remediation 	Covalent bonding, surface modification	Amine groups enhance interaction with negatively charged biological molecules and MNPs	4.13

of PGA and the positively charged surface of the nanoparticles. The excess PGA is then rinsed off to leave behind a monolayer of PGA on the surface of the nanoparticles. Next, a layer of PLL is adsorbed onto the PGA-coated nanoparticles *via* electrostatic attraction between the amino groups of PLL (*i.e.*, carrying a positive charge) and the carboxylic acid groups of PGA (*i.e.*, carrying a negative charge). The resulting PGA/PLL-coated MNPs could be functionalized with FITC-FA functionalized PAMAM G5 dendrimers through electrostatic attraction between the positively charged amine groups on the PAMAM dendrimer and the negatively charged carboxylate groups on the surface of the PGA/PLL-MNP. The FITC label on the surface of the PAMAM dendrimer provides fluorescence for imaging and tracking the MNPs *in vivo*. The FA moiety on the surface of the dendrimer binds specifically to folate receptors on the surface of specific targeted molecules, allowing for targeted delivery of drugs or imaging agents to the tumor site. (Acetylation process follows up to enhance surface function by carboxyl group.)

4. Dendrimer types and monomers variations (Table 2)

4.1 Polyamidoamine (PAMAM) dendrimers

Polyamidoamine (PAMAM) dendrimers stand out as the predominant choice of dendrimers employed for the conjugation and stabilization of MNPs. PAMAM renowned for their intricate three-dimensional structures, are synthesized from amide and amine groups within their branches and terminal sites. The commonly employed monomers for crafting PAMAM dendrimers are ethylenediamine and methyl acrylate. These monomers undergo a stepwise series of reactions, encompassing Michael addition and amidation reactions, which ultimately lead to the formation of the dendrimer structure. The conjugation between MNPs with PAMAM can be done through various strategies, as illustrated in Fig. 4.

- Grafting assembly of PAMAM to MNPs: The most prevalent approach involves grafting MNP-cored PAMAM, which is propagated from MNP cores through amino silane bonds as binding agents. This process, often utilizing silane anchoring groups such as TEOS, APTES, APTMS, and silanes with different tails (SH-COOH, and CH₂CH), has been employed extensively to create different generations of PAMAM-coated MNPs,^{44,48,51,72-78} refer to Table 3.

- MNPs assembled and stabilized by PAMAM: In this method, PAMAM serves as a protective coating for MNPs, with MNPs being generated *in situ*^{79,80} This process involves attaching functionalized PAMAM onto preformed MNPs through specific physical^{8,11,31,57,71,81,82} or chemical interactions,^{83,84} ensuring their stability and functionality (Table 4).

- MNPs entrapped and shielded by PAMAM: Different generations of PAMAM, such as G3, G5, and G6, act as templates for the synthesis and encapsulation of MNPs *in situ*.¹⁷ This encapsulation not only enhances the stability of MNPs but also provides a platform for further functionalization (Table 4).

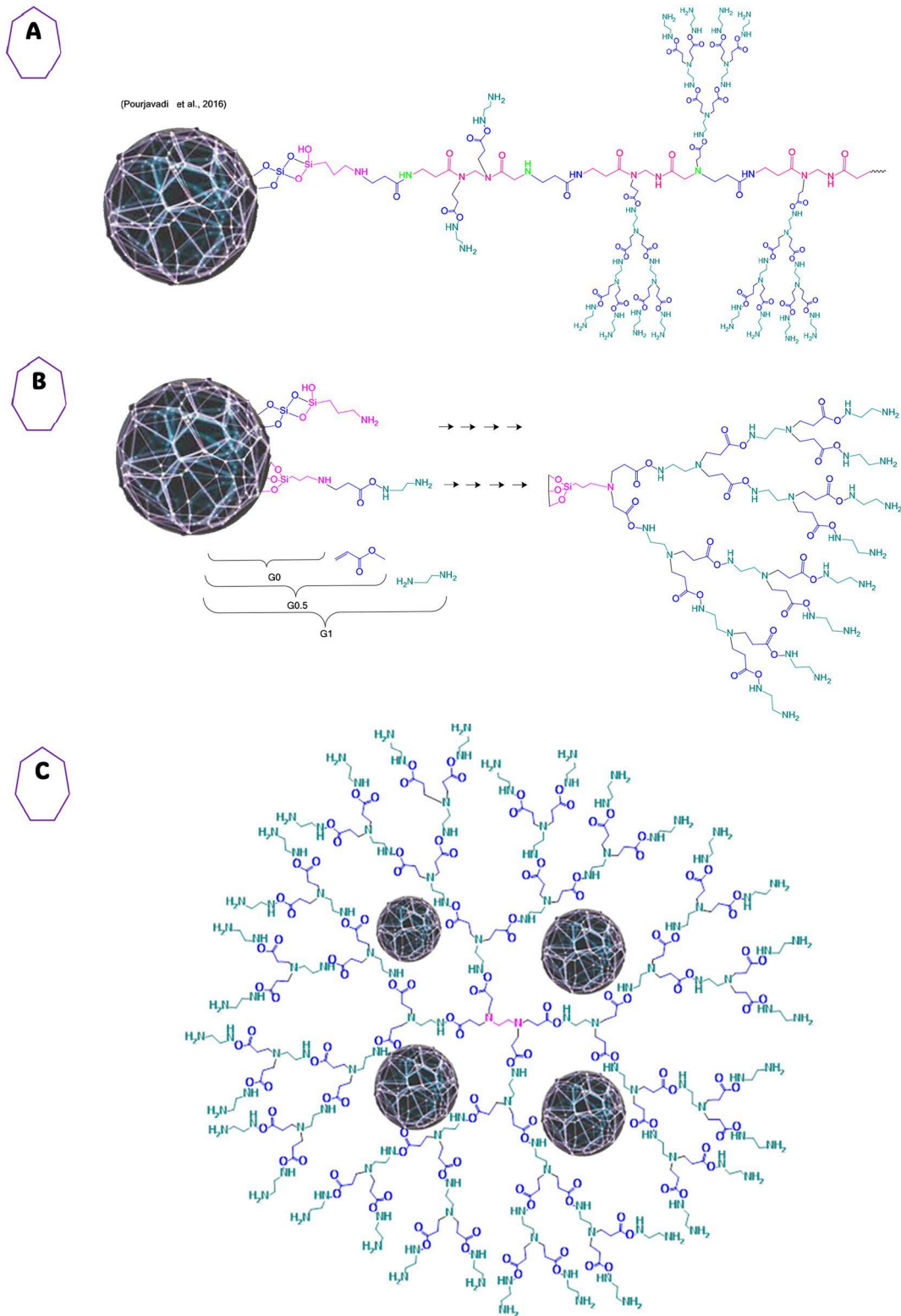


Fig. 4 Various conjugation possibilities of PAMAM dendrimer with MNPs. (A) The common divergent synthesis (grafting from) of PAMAM dendrimer from covalent bonding through silane coupling agent, (B) nanocomposite divergent propagation of PAMAM from polymerized tails on MNPs,³⁵ (C) MNPs encapsulated within PAMAM dendrimer³⁶ (D) MNPs conjugated with PAMAM dendrimer through covalent and physical assembly and stabilization of MNPs' surface using various linking and coupling agents.

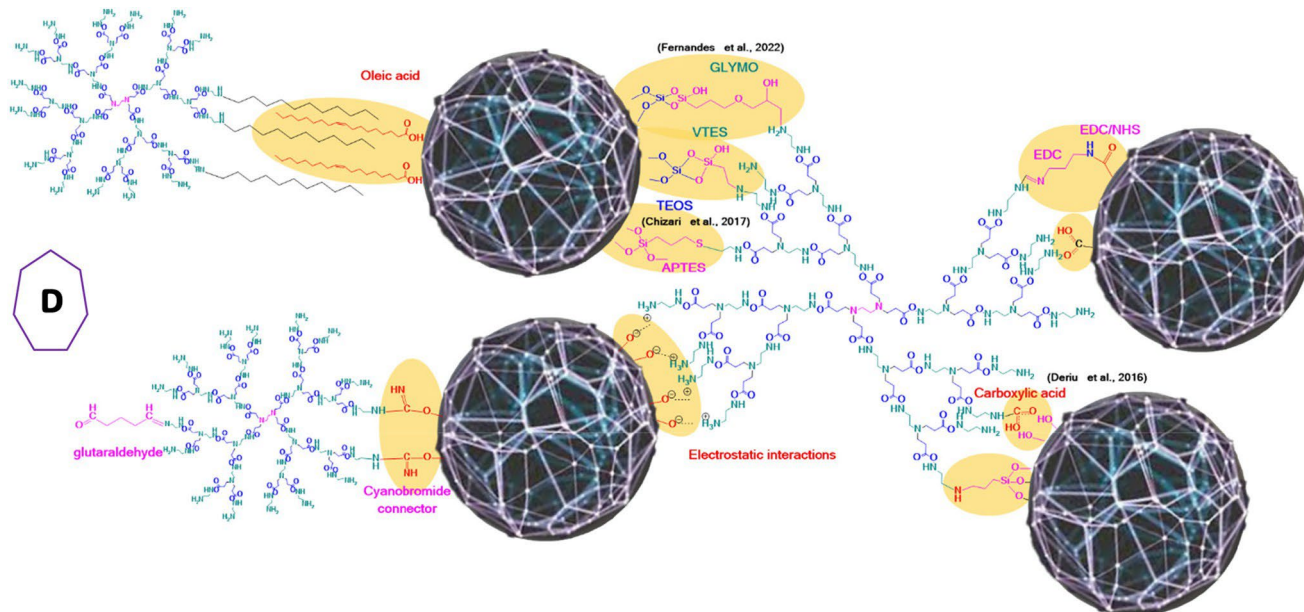


Fig. 4 (Contd).

Additionally, for Stabilization and encapsulation methods, it is essential to note that the core of PAMAM comprises open-chain molecules with primary amines, and the core multiplicity corresponds to the number of branches. For instance, a core multiplicity of three is found in the case of core molecules like ammonia (NH_3), whereas ethylenediamine ($\text{H}_2\text{N}-\text{CH}_2-\text{CH}_2-\text{NH}_2$) core molecules have a core multiplicity of four.⁸⁵ PAMAM dendrimers exhibit remarkable versatility as ligands for different ions, leading to high adsorption capacity. The efficiency of PAMAM dendrimers in adsorption and electrostatic attractions is affected by numerous factors such as the dendrimer generations, pH, temperature, and surface modifications, which alter PAMAM's behavior and application potential.^{24,86}

The PAMAM macromolecules are terminated with multi-functional chemical groups, which provide the dendrimer with several physiochemical features. Notably, ester- or carboxyl-terminal groups are typically used for PAMAM half-generations such as G0.5, G1.5, and G2.5, while primary amine groups are used for the termination of PAMAM full generations such as G1, G2, and G3. Through synthetic manipulation, these reactive terminal groups can be altered to incorporate various functionalities like carboxyl groups, alkyl groups, hydroxyl groups, and other diversified end groups, customizing the dendrimer's performance to suit specific applications (see section 5.4).^{85,87} This adaptable material has found extensive utility in various scientific domains, including gene therapy,^{78,88,89} drug delivery,^{7,17,36,77} bio-imaging,⁹⁰ catalysis,⁹¹ dye degradation,^{23,92-94} heavy metals and pollutants removal,^{43,86,95} as well as probes and sensors for biomedical applications (Boni *et al.*, 2015).²⁹ Researchers often make minor modifications to adapt PAMAM dendrimers to suit the unique requirements of each application.

4.2 Polypropylenimine (PPI) dendrimers

PPI dendrimers, a type of cationic dendrimers, have proven to be valuable in the functionalization of MNPs, offering enhanced stability and improved effectiveness across a range of applications. Synthetic approaches of MNPs with PPI quite differ from encapsulation^{5,64,68} to covalent conjugation with the aid of functionalized MNPs with silanes¹⁰⁴ or other anchoring groups.³⁴ The synthesis of magnetic NPs involved the preparation of maghemite ferrofluid through a controlled alkaline coprecipitation method of Fe(II) and Fe(III) ions, followed by oxidation to maghemite ($\gamma\text{-Fe}_2\text{O}_3$). This sequential process ensured consistent iron oxide cores, avoiding variations from magnetite to maghemite. To achieve covalent grafting of dendrimers onto the $\gamma\text{-Fe}_2\text{O}_3$ NPs, reactive functional groups such as $-\text{Si}(\text{OEt})_3$ were introduced *via* optimized reaction conditions using partially silylated dendritic precursors. This enabled the subsequent formation of covalent bonds with the $\text{Fe}-\text{OH}$ groups present on the MNPs' surface. The surface modification of $\gamma\text{-Fe}_2\text{O}_3$ NPs was accomplished using a sol-gel process based on wet-chemistry techniques in a basic pH environment, resulting in the formation of core-shell hybrid structures.¹⁰⁴

In a separate study, superparamagnetic $\gamma\text{-Fe}_2\text{O}_3$ NPs, with a mean diameter of 2.5 nm, were effectively encapsulated within poly(propylene imine) dendrimers and analyzed using Electron Magnetic Resonance (EMR). The recorded EMR measurements, conducted at different temperatures, indicated that an $S = 30$ spin value model, representing the total magnetic moment of the nanoparticles, successfully interpreted the experimental results, providing compelling evidence of the quantum behavior exhibited by $\gamma\text{-Fe}_2\text{O}_3$ nanoparticles.^{68,105} PPI dendrimers of varying generations (ranging from 1 to 4)

Table 3 Summarized details of magnetic PAMAM dendritic systems in a grafting assembly procedure (grafting from) found in literature. (Main monomers are Methacrylate (MA) & Ethylenediamine (EDA).)

Dendrimer generation/size	Dendrimer core	Dendrimer terminal group	MNPs synthesis	MNPs pre-surface functionalization	Dendritic attachment approach	Bond type between MNPs & dendrimer	Dendritic MNPs post-surface modification	Targeted application	Ref.
G1-G15	MNPs@SiO ₂	NH ₂	Coprecipitation	Amino-silane (TEOS with (3-mercaptopropyl) trimethoxysilane (MTPMS))	Grafting assembly	MNP-O-Si-O-Si-SH	G10-aminophenol	Nonylphenol	97
G3	MNPs@SiO ₂	NH ₂	Coprecipitation	(3-Aminopropyl) triethoxysilane (APTES)	Grafting assembly	MNP-O-Si-NH ₂	G3-4-mercaptopbenzoic acid	PAHs	46
—	MNPs@SiO-SH	—	Coprecipitation	3-Mercaptopropyl-trimethoxysilane (MTPMS)	Grafting assembly	MNP-O-Si-NH ₂	Allyl glycidyl ether	PAHs	98
G10	MNPs@SiO ₂	NH ₂	Coprecipitation	Tetraethylorthosilicate (TEOS) & aminopropyl triethoxysilane (APTES)	Grafting assembly	MNP-O-Si-O-Si-NH ₂	Benzaldehyde	Naphthalene	43
G3	MNPs@SiO ₂	NH ₂	Coprecipitation	3-Aminopropyltriethoxysilane (APTES)	Grafting assembly	MNP-O-Si-NH ₂	—	Chlorophenol	99
G1 & G2	MNPs@SiO ₂	NH ₂	Coprecipitation	Tetraethylorthosilicate (TEOS) & aminopropyl triethoxysilane (APTES)	Grafting assembly	MNP-O-Si-O-Si-NH ₂	Murexide (Mu)	Lead Pb(II)	100
G1	MNPs@SiO ₂	NH ₂	Coprecipitation	3-Aminopropyltriethoxysilane (APTES)	Grafting assembly	MNP-O-Si-NH ₂	—	Lead Pb(II) and cadmium Cd(II)	101
G3	MNP@chitosan	NH ₂	Coprecipitation	Chitosan	Grafting assembly	MNP-O-NH ₂	—	Reactive Blue 2 Dye	92
G2 (MA & EDA) × 1	MNP@SiO	NH ₂	Coprecipitation	3-Aminopropyltrimethoxysilane (APTMS)	Grafting assembly	MNP-O-Si-NH-PAMAM-	Carboxylated chitosan	Methylene blue, methylene orange	54
G3	MNP@SiO	NH ₂	Coprecipitation	Sol gel process with TEOS & (3-aminopropyl) triethoxysilane	Grafting assembly	MNP-O-Si-O-Si-NH-PAMAM-	COONa	Pb(II), Cd(II), and Cu(II)	86
G3	MNP@SiO ₂ @SNH ₂	NH ₂	Coprecipitation	TEOS and (3-aminopropyl) triethoxysilane (APTES)	Grafting assembly	MNP-O-Si-O-Si-NH-PAMAM-OS ₃ H	Sulfamic acid, OS ₃ H	Aminophosonate reaction	91
G0-G3	MNP@SiO ₂ @Si-NH ₂	NH ₂	Coprecipitation	TEOS and (3-aminopropyl) triethoxysilane APTES	Grafting assembly	MNP-O-Si-O-Si-NH-PAMAM-DNA	DNA fragments (herring sperm DNA)	Mercury Hg(II) and methylmercury(I)	95
G6	MNP@Si@NH (G0)	NH ₂	—	APTMS	Grafting assembly (conventional method)	MNPs-O-Si-NH-PAMAM-NH ₂ -(DNA-PEI)s	DNA fragments (pGL-3 and pEGFP-C1 plasmids) & PEI	For magnetofection	90
G1-G5	MNP@Si@NH	NH ₂	Coprecipitation	3-Aminopropyl-trimethoxysilane (APTMS)	Grafting assembly (sonication)	MNP-O-Si-NH-PAMAM	—	Reactive Black 5 (Dye)	102
G1	MNP@Si@NH	NH ₂	Coprecipitation	(3-Aminopropyl) triethoxysilane (APTES)	Grafting assembly (sonication)	MNP-O-Si-NH-PAMAM	Encapsulation of Ag nanoparticles	Catalytic reduction of 4-nitrophenol	44
G1	MNP@Si@NH (G0)	Diethyl carbonate (DEC)	Coprecipitation	3-Aminopropyl-trimethoxysilane APTMS	Grafting assembly Sonication	MNP-O-Si-NH-PAMAM-TiO ₂	TiO ₂ nanoparticles	Photocatalytic decolorization of methyl orange (MO)	73
G0-G5 (G3 was chosen)	MNP@Si@NH (G0)	NH ₂	Coprecipitation	3-Aminopropyl-trimethoxysilane APTMS	Grafting assembly	MNP-O-Si-NH-PAMAM	—	Zinc(II)	74

Table 3 (Contd.)

Dendrimer generation/size	Dendrimer core	Dendrimer terminal group	MNPs synthesis	MNPs pre-surface functionalization	Dendritic attachment approach	Bond type & dendrimer	Dendritic MNPs post-surface modification	Targeted application	Ref.
G0-G3 (G2 was chosen)	MNP@Si@NH (G0)	NH ₂	Coprecipitation	(3-Aminopropyl) triethoxysilane (APTES)	Grafting assembly sonication	MNP-O-Si-NH-PAMAM	—	Cd ²⁺ and Hg ²⁺	103
G1-G7	MNP@Si@NH (G0)	NH ₂	Coprecipitation	3-Aminopropyltrimethoxysilane (APTMS)	Grafting assembly sonication	MNP-O-Si-NH-PAMAM	—	Cellular internalization, cancer targeting	75
G3	MNP@Si@NH (G0)	NH ₂	Coprecipitation	3-Aminopropyltrimethoxysilane (APTMS)	Grafting assembly (reflux, shaking and sonication)	MNP-O-Si-NH-PAMAM-EDTA	Ethylenediaminetetraacetic acid (EDTA)	Precious metals (Pd(IV), Au(III), Pt(II) and Ag(I)) in water	76
G1-G7	MNP@Si@NH (G0)	NH ₂	Coprecipitation	3-Aminopropyltrimethoxysilane (APTMS)	Grafting assembly sonication	MNP-O-Si-NH-PAMAM	Doxorubicin (either on the surface through amide bonding or electrostatically in the cavities)	Drug loading and delivery	77
G4	MNP@Si@NH (G0)	NH ₂	Coprecipitation	3-Aminopropyltriethoxysilane (APTES)	Grafting assembly sonication & reflux	MNP-O-Si-NH-PAMAM	—	Magnetic hyperthermia treatment of breast	78

have been employed in the preparation and stabilization of ferromagnetic Fe₂O₃ NPs. This involved the reduction of Fe(III) and subsequent oxidation of Fe(II), leading to the creation of iron oxide nanocomposites (MNCs) that are highly soluble and well-dispersed within the dendrimer structure. These nanocomposites demonstrated remarkable stability over a wide temperature range. The synthesis process yielded two types of dendrimer-encapsulated MNPs: one type featured MNPs encapsulated within the PPI dendrimer, while the other type involved MNPs gathered around the PPI dendrimer⁵ (see Fig. 5).

Additionally, innovative magnetic core-shell nanocomposites were stabilized using gold/lead NPs and synthesized through a simple process. The resulting nanocomposites exhibited catalytic activity in the cleavage of certain aptamers (pBR322 DNA).³⁴ The synthesis process involved the initial preparation of Fe₃O₄-poly(styrene-divinylbenzene-vinylbenzyl chloride) (ST-DVB-VBC) nanocomposites *via* suspension polymerization. The resulting matrix was then functionalized with 3-aminobenzoic acid, followed by separate grafting of PPI-G(2) and PPI-G(3) dendrimers onto the matrix. The successful grafting of dendrimers onto the matrix was confirmed by Fourier-transform infrared spectroscopy. Subsequently, each core-shell matrix was immobilized with either Au NPs or Pd NPs. The matrix grafted with PPI-G(3) dendrimer exhibited a thick shell, which effectively reduced magnetic attraction on the outer layer. Notably, Fe₃O₄-poly(ST-DVB-VBC)-PPI-G(3)-AuNPs displayed the highest activity for DNA cleavage compared to the other four candidates studied.³⁴

4.3 PNPEDA (poly(*N*-propylethane-1,2-diamine)) dendrimer

Poly(*N*-propylethane-1,2-diamine) dendrimer is a derivative dendrimer from PAMAM that has been used for the functionalization of MNPs. PNPEDA dendrimer is made according to the basic propagation of PAMAM dendrimer from ethylenediamine and methacrylate monomers up to 3 generations from silane-coated MNPs. The amide groups of PAMAM are then reduced into amine groups using a strong reducing agent (lithium aluminum hydride (LAH)) by removing all oxygen from the dendrimer branches along with amine functional groups on the surface (see Fig. 6). The resultant polyamine dendrimer is named poly(*N*-propylethane-1,2-diamine). PNPEDA has the capability of capturing heavy metals from water through the chelation mechanism either from the carboxylic peripheral groups or by entrapping the metal ions in the cavities using the secondary amine groups.²⁴

4.4 Polyethyleneimine (PEI) dendrimers

PEI dendrimers are cationic dendrimers that can bind to anionic MNPs electrostatically (in main cases) or covalently (with the aid of anchoring agents), resulting in stable coatings and functionalization. MNPs can be coated with PEI through various synthesis methods, such as the one-pot hydrothermal route,¹⁰⁶⁻¹⁰⁸ solvo-thermal method,¹⁰⁹ and chemically by

Table 4 Summarized details of magnetic PAMAM dendritic systems (stabilization, grafting onto, encapsulation) procedure in literature

Dendrimer generation/size	Dendrimer monomers	Dendrimer core	Dendrimer terminal group	MNPs size	MNPs synthesis	MNPs pre-surface functionalization	Dendritic attachment approach	Bond type between MNPs & dendrimer	MNPs : dendrimer ratio	Dendritic MNPs post-surface modification	Targeted application	Ref.
G4 & G4-lipid 2-hydroxydodecyl (C ₁₂) moieties	Methacrylate & Ethylenediamine (EDA)	Ethylenediamine (EDA)	NH ₂ , and lipid 2-hydroxydodecyl (C ₁₂) moieties (25%)	TEM 8.3 nm, DLS: 70 nm	Thermal decomposition in the presence of oleic acid	Oleic acid (2 : 1 MNPs)	Stabilization hydrophobic interactions	MNP-COO-OA- (electrostatic interactions on the surface)-then hydrophobic interactions with PAMAM	Diameter 9 nm; ratio, 2.5 : 1	Fluorescein isothiocyanate (FITC) & Rhodamine B Isothiocyanate (RITC)	Water dispersal of hydrophobic MNPs	20
G4-(C ₁₂)	Methacrylate & Ethylenediamine (EDA)	Ethylenediamine (EDA)	NH ₂ , and lipid 2-hydroxydodecyl (C ₁₂) moieties (25%); N-hydroxy succinimide (NHS)	2.6-14.1 nm	Thermal decomposition in the presence of oleic acid	Oleic acid (2 : 1 MNPs)	Stabilization hydrophobic interactions	Hydrophobic interactions	13 mg MNPs- OA : 0.25 mL PAMAM-C ₁₂	Gadolinium or Atto 633 labelled NPs	Probes for biomedical applications	29
G4 (25% C12) labeled with rhodamine	Methacrylate & Ethylenediamine (EDA)	Ethylenediamine (EDA)	NH ₂ and (25%) lipid 2-hydroxydodecyl and rhodamine	2.6-14.1 nm	Thermal decomposition in the presence of oleic acid	Oleic acid (2 : 1 MNPs)	Stabilization hydrophobic interactions	Hydrophobic interactions	1 : 1 ratio	Carboxy-derivatized peptide (T-7: HAIYPRH-amide)	Selective delivery of doxorubicin to cancer cells	55
G2-G4		1,4-Diaminobutane core (4-carbon core)	Succinamic acid surface groups NHCOCH ₂ CH ₂ COOH	Crystallography open database (COD), 4 nm	Hydrothermal (<i>in situ</i> with PAMAM-SAH), SAH: succinamic acid	Direct with PAMAM-SAH modified surface	Stabilization; hydrothermal	PAMAM (electrostatic interactions on the surface)	1 : 1 ratio	Succinamic acid surface groups	—	79
G5	Methacrylate & Ethylenediamine (EDA)	Ethylenediamine (EDA)	Fluorescein isothiocyanate (FITC) & folic acid (FA)	8.4 nm	Coprecipitation (oleic acid)	Polystyrene sulfonate sodium salt (PSS)	Stabilization (ligand exchange & Electrostatic LbL assembly)	Electrostatic interaction between PSS@MNPs and PAMAM	5 mg MNPs : 1 mg PAMAM	Acetylation to neutralize the remaining amine groups of G5.NH2-FI-FA dendrimer	Targeting and imaging of cancer cells	71
G5	Methacrylate & Ethylenediamine (EDA)	Ethylenediamine (EDA)	Fluorescein isothiocyanate (FITC) & folic acid (FA)	8.4 ± 1.4 nm	Coprecipitation (oleic acid)	Poly(glutamic acid) (PGA) and poly(L-lysine) (PLL)	Stabilization (ligand exchange & Electrostatic LbL assembly)	Electrostatic interaction between Glu@Lys@MNPs and PAMAM	5 mg MNPs : 1 mg PAMAM	Acetylation to neutralize the remaining amine groups of G5.NH2-FI-FA dendrimer	Magnetic resonance imaging of tumors	57
G3, G5, and G6	Methacrylate & Ethylenediamine (EDA)	Ethylenediamine (EDA)	PEG	10 to 15 nm	Soft chemical route coprecipitation (<i>in situ</i> with glutamic acid)	Glutamic acid	Stabilization	Electrostatic interaction between Glu@MNPs and PAMAM-PEG	1 mg mL ⁻¹ Glu@MNPs : 0.1 mg mL ⁻¹ PEG-PAMAM	Poly (ethylene glycol) PEG and doxorubicin (DOX)	Drug loading and retention	17
G2	Methacrylate & Ethylenediamine (EDA)	Diethylenetriamine (DETA) core with redox centers	NH ₂		Coprecipitation (<i>in situ</i> with NH-PAMAM)	Direct stabilization by PAMAM-NH ₂	Stabilization	MNP-O...NH PAMAM	—	—	Electron storage	80
G0.5-G6.5	Methacrylate & Ethylenediamine (EDA)	Ethylenediamine (EDA)	NH ₂	5.4 ± 1.2 nm	Coprecipitation	Octylamine and trioctylamine then (13,13-bis-hydroxymethylpentacosane)	Stabilization	MNP-O-NH... (electrostatic with PAMAM)	~10 mg mL ⁻¹ MNPs : 1.5 × 10 ⁻³ M PAMAM	—	—	11

Table 4 (Contd.)

Dendrimer generation/size	Dendrimer monomers	Dendrimer core	Dendrimer terminal group	MNPs size	MNPs synthesis	MNPs pre-surface functionalization	Dendritic attachment approach	Bond type between MNPs & dendrimer	MNPs : dendrimer ratio	Dendritic MNPs post-surface modification	Targeted application	Ref.
G3	Methacrylate & ethylenediamine (EDA)	Ethylenediamine (EDA)	NH ₂	8.4 ± 1.4 nm	Coprecipitation	—	Stabilization (shaking, sonication)	Electrostatic interaction with COOH of PAMAM	5 mg MNPs : 1 mg PAMAM G3	Succinic anhydride SAH COOH (100%) Folic acid FA ₃ -SAH (COOH) Glycidol (GlyOH) ₁₅ FA ₃ -SAH (GlyOH) ₁₅ SAH (GlyOH) ₁₅ NH ₂	Intracellular uptake	31
G0–G3	Methacrylate & ethylenediamine (EDA)	Ethylenediamine (EDA)	NH ₂	300 nm	Purchased and used as it is	COOH-modified poly-styrene shell	Stabilization (chemisorption)	MNP–PS–COOH–NH–PAMAM–NH ₂ –Fc	1 MNPs : 0.2, 0.5, 1, and 2 PAMAM	Ferrocenecarboxylic acid (Fc-conjugated MNPs)	Electron transfer	4
G5 5.4 nm	Methacrylate & ethylenediamine (EDA)	Ethylenediamine (EDA)	NH ₂ then reacted with 3-(glycidyl-oxypopyl) trimethoxysilane (GLYMO)	45 nm ± 5 nm	Oxidative hydrolysis	TEOS	Stabilization	MNP–O–Si–O–Si–NH–PAMAM–NH ₂ –Au NP	15 mg of MNP@SiO ₂ : 150 mg (1 : 10)	Anisotropic Au nanoparticles	Optical sensors	8
G2 (10NH ₂)	Methyl acrylate (MA), ethylenediamine (EDA)	Diethylenetriamine (DETA)	NH ₂	—	Coprecipitation	—	Stabilization (sonication)	—	2.5 g MNPs : (7 ml in 10 ml) Dend	Bisphenol A (DGEBA) epoxy resin	Improving thermal and mechanical properties of DGEBA/IPD epoxy networks	82

Table 5 Summarized details of nanocomposite magnetic PAMAM dendrimer in literature

Dendrimer generation/size	Dendrimer monomers	Dendrimer core	Dendrimer terminal group	MNPs size	MNPs synthesis	MNPs pre-surface functionalization	Dendritic attachment approach	Bond type between MNPs & dendrimer	Dendritic MNPs post-surface modification	Targeted application	Ref.
G0–G2	4-Methylstyrene (4-MS), divinylbenzene (DVB), glycidylmethacrylate (GMA)	MNP@MS@DVB@GMA (core-shell nanocomposite)	NH ₂	8 nm	Coprecipitation	Oleic acid	Grafting PAMAM onto nanocomposite (sonication)	MNP–O–CH ₂ –@CH@CH@O–PAMAM	Encapsulation of gold nanoparticles AuNP	Rhodamine B (Dye)	23
G3	Methacrylate (MA), <i>N,N</i> -methylenebisacrylamide (MBA)	MNPs@MA@MBA (core-shell nanocomposite)	NH ₂	10–15 nm	Coprecipitation	Composite of TEOS, APMTS,	Grafting PAMAM onto nanocomposite	MNP–O–Si–O–Si–NvC–vN–PAMAM	—	Pb(II)	35

Table 6 Summarized details of magnetic PAMAM tri-block copolymer dendritic system in literature

Dendrimer generation/size	Triblock copolymer	G2 propargyl PAMAM	Dendrimer terminal group	MNPs size	MNPs synthesis	MNPs pre-functionalization	Dendritic attachment approach	Bond type between MNPs & dendrimer	MNPs : dendrimer ratio	Dendritic MNPs post-surface modification	Targeted application	Ref.
G2 propargyl PAMAM	Polyamidoamine-type dendron- <i>b</i> -poly(2-dimethylaminoethyl methacrylate)- <i>b</i> -poly(<i>N</i> -isopropylacrylamide)	Two-step copper-mediated atom transfer radical polymerization (ATRP) method	Carboxylic acid (COOH)	10 nm	Thermal decomposition	MNP@OA	Grafting onto (ligand with exchange)	Click chemistry with 20-azidoethyl-2-bromoisobutyrate (AEBIB)	0.08 g Oa@MNP : 1.22 g PAMAM-COOH	PAMAM- <i>b</i> -PDMAEMA- <i>b</i> -PNIPAM	Thermosensitive drug release of DOX	7
	Poly(2-(dimethylamino)ethyl methacrylate)- <i>b</i> -poly(methyl ether methacrylate)									(PAMAM- <i>b</i> -PDMAEMA- <i>b</i> -PPEGMA)	Drug delivery systems for therapeutic applications	36

amide reaction.¹⁴ The covalent conjugation by functionalizing MNPs with citric acid (CA) before binding them to PEI. The amide interaction between the terminal amino groups of PEI and the carboxyl groups of citric acid (CA) present on the surface of MNPs allows for the creation of MNPs-PEI.¹⁴ The binding between PEI and MNPs allows for the conjugation of other molecules, such as fluorescein isothiocyanate (FI) and folate-conjugated polyethylene glycol (PEG),¹⁰⁶ folic acid (FA),¹⁰⁸ polyethylene glycol (PEG), acetic anhydride, and succinic anhydride.¹⁰⁷ The binding of MNPs to biomacromolecules, such as DNA, can be achieved through ion exchange binding.¹¹⁰ These dendrimers have found various applications: the PEI-coated Fe₃O₄ NPs can be multi-functionalized with other biological ligands for MR imaging of different biological systems.¹⁰⁶ PEI-MNPs have shown promise as a delivery system for plasmids encoding CRISPR/Cas9 and template DNA, enhancing the safety and utility of gene editing.¹¹⁰ PEI-coated MNPs have demonstrated efficient removal of emulsified oil from aqueous systems, with the potential for multiple reuse.¹⁰⁹ PEI-MNPs serve as a potential non-viral vector for gene delivery.¹⁴ MNPs coated with PEI and folic acid (FA) are suitable for magnetic field hyperthermia and active targeting.¹⁰⁸ PEGylation and acetylation of Fe₃O₄-PEI NPs can significantly reduce macrophage cellular uptake and make them suitable for targeted cancer imaging and therapeutics (Table 7).¹⁰⁷ A summary of the synthesis and modification processes is represented in Fig. 7.

4.5 Triazin-based dendrimers

Triazin-based dendrimers are a class of dendrimers that contain triazine units as the core and can have amine or carboxylic acid functional groups on the surface. The use of a triazine-based dendritic structure provides numerous benefits as it allows for chemical functionality diversification without requiring protective groups. Additionally, the nucleophilic aromatic substitution process occurs in a sequential and temperature-dependent manner on the ring, eliminating the need for manipulating functional groups. These dendrimers have been shown to be useful for the adsorption of heavy metals alone¹¹⁶ and were successfully conjugated with MNPs to provide high stability, biocompatibility, and functional groups on the surface. Triazine dendrimers can be synthesized in different generations and sizes, allowing for tunable properties and enhanced binding to MNPs. Functionalization of MNPs with triazine dendrimers can be achieved through different methods, such as covalent conjugation or electrostatic adsorption.¹¹⁷ Their performance was impressive in terms of attaching to metal ions Pb(II) and Cd(II), with a strong ability to filter these contaminants from water-based substances (with an efficiency of 93.6% and 98.5%, respectively). Their mechanism of adsorption is realized by using both the hydroxyl and amine functional groups of the ethanolamine component, as well as the triazine amine groups, to coordinate and capture the heavy metal ions, along with utilizing electrostatic interactions.¹¹⁸ (Monomers: ethanolamine-trichlorotriazine, diethanolamine-triazine, diethylenetriamine-triazine and cyanuric chloride-tri-

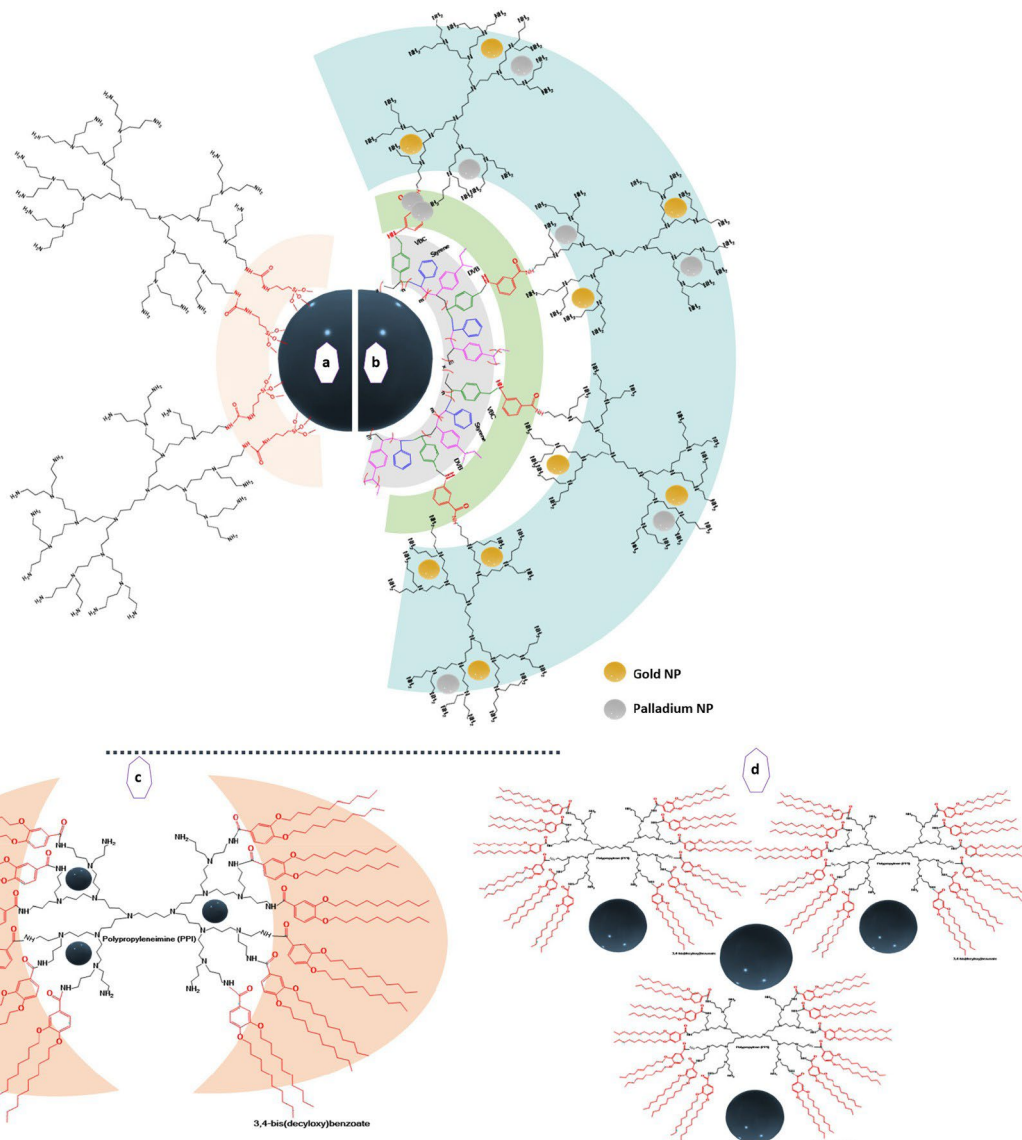


Fig. 5 Synthesis of PPI-MNPs (A) ref. 104, (B) ref. 34, and (C) ref. 5, 68 and 105.

azine,¹¹⁷ triethanolamine-melamine with carbon disulfide bridges, etc.)

Ref. 13 used Barium-iron oxide as the MNPs core and conjugated it with melamine as triazine-based dendrons to remove lead(II) and rhodamine B (RB) dyes from water. The dendrite structure contained three primary functional groups (N, O, and S) that were capable of capturing Pb(II) ions. It was claimed that the hydroxyl groups interacted with Pb(II) ions through an electrostatic attraction or ion exchange. However, the sulfur and amine groups formed complexes with Pb(II) ions, as these functional groups serve as soft ligands for the adsorption of lead ions. The results showed that the adsorption efficiency of RB is high (75%) in acidic solutions due to multiple mechanisms acting simultaneously, including hydrophobic interactions between the outer surface of the dendrite and RB, as well as the π - π interactions between the bulk π systems on the dendrite and RB molecules. The π - π bonds are

formed between the RB having π electrons (benzene ring) and the dendrite structure since the melamine contains π electron orbit. Furthermore, the density of electrons is increased due to the presence of carboxylate groups in the structure of RB, thus enhancing the π - π bonding capacity with the dendrite's triazine rings. The hydrogen bonds present between the functional groups on the dendrite's surface also contribute to promoting the adsorption capacity of Pb(II) ions. Overall, the dendrite structure can either act as an electron-donor or acceptor, and the adsorption efficiency relies upon the tendency of the dendrite and RB to accept or donate electrons.^{119,120} A summary of the conjugation of triazine-based dendrimers with MNPs can be found in Fig. 8 and Table 8.

4.6 Peptide dendritic MNPs

Peptide dendritic MNPs are a nanocomposite type consisting of MNPs coated with peptide dendrimers. These dendri-

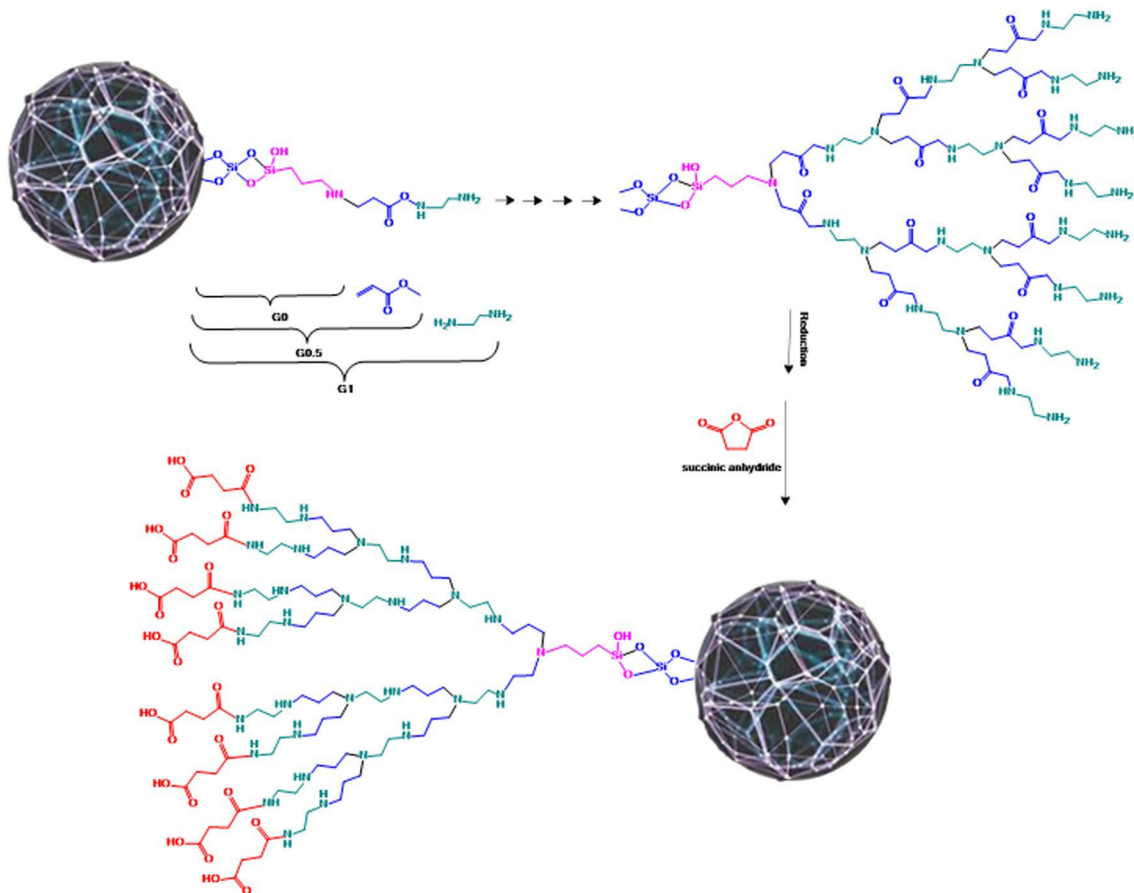


Fig. 6 Synthesis of poly(*N*-propylethane-1,2-diamine) dendrimer from PAMAM and functionalization with succinic anhydride.

mers are composed of amino acid monomers linked together in a branched structure, allowing for the creation of a variety of functional groups on the surface. Peptide dendritic MNPs have been shown to be useful for biomedical applications such as drug delivery, imaging, and biosensing. The binding between peptide dendrimers and MNPs occurs through electrostatic interactions, hydrogen bonding, and coordination between the amino acid residues on the dendrimer and the surface of the IOMNPs (Table 9). The lysine–arginine dendrimer conjugated with Glutamic acid coated IOMNPs,¹⁸ lysine–glutamic acid dendrimers^{10,21} (Fig. 9). (Monomers: glutamic acid (Glu), di-Boc-*L*-lysine, di-Fmoc-arginine.) Poly-*L*-lysine (PLL) dendrimers: PLL dendrimers are cationic dendrimers that can interact with anionic MNPs through electrostatic interactions. These dendrimers have been used for drug delivery and imaging applications. Another type of peptide dendritic coating was done using Arginylglycylaspartic acid (RGD).^{121,122} The acyclic form of RGD dendritic peptide gets attached onto the surface of modified IOMPs (with 4-methylcatechol (MC)). The ring structure of 4-MC can directly bond with an amine group through a chemical reaction known as Mannich reaction when placed around Fe₃O₄ nanoparticles.¹²¹

4.7 Polyglycerol (PG) dendrimers

Glycerol-based polymers are a member of the aliphatic polyether family and are often prepared as linear or branched structures (hyperbranched, dendritic) using anionic ring-opening polymerization. Branched dendritic polyglycerols (dPG) are obtained through a synthetic procedure that uses the latent hydroxyl group in glycidol. Dendritic polyglycerols have a high number of hydroxyl groups, which can be utilized for crosslinking, labeling, and incorporating targeting and grafting moieties. These hydroxyl groups can also be modified before or after polymerization to adjust the physical and chemical properties of the polymer. Polyglycerol dendrimers are neutral, highly water-soluble, and biocompatible. When PGs are grafted onto MNPs, they exhibit an excellent dispersibility of the nanoparticles in water, resulting in water-based stable and non-toxic ferrofluids suitable for further bio-applications. Moreover, these PG@MNPs can be further modified with various moieties (sulfate groups,¹² folate, fluorescents (FITC),⁴¹ and methotrexate functionalities²²) for different functionalities. This modification will enable the targeting of particular molecules (*e.g.*, proteins, antibodies, drugs, *etc.*) for biological-related applications,^{123,124} and heavy metals and dyes for water remediation purposes.^{125–127} The conjugation

Table 7 Summarized details of magnetic PEI dendritic and hyperbranched systems in literature (the main monomer used was Ethylenediamine (EDA))

Dendrimer core	Dendrimer terminal group	MNPs size	MNPs synthesis	MNPs pre-surface functionalization	Dendritic attachment approach	Bond type between MNPs & dendrimer	MNPs : dendrimer ratio	Dendritic MNPs post-surface modification	Targeted application	Ref.
MNPs@COOH	NH ₂	TEM 68 nm	Coprecipitation	Sodium citrate (citric acid CA)	Stabilization (grafting onto)	Covalent interaction (EDC/NHS)	100 mg MNPs : 200 mg PEI	DNA fragments	Gene delivery	14
MNPs@PEG	NH ₂ -COOH	11 nm	(Oil/water) single emulsion/ solvent and evaporation method	3,4-Dihydroxy-L-phenylalanine (DOPA) subsequently conjugated with poly(ethylene glycol) (PEG)	Stabilization (grafting onto)	Carbodiimide coupling chemistry (EDC)	PEI : MNPs, 0.1 : 1, 0.5 : 1, 1 : 1 or 5 : 1, respectively	Small interfering RNAsi-RNA	Intracellular siRNA delivery	111
EDA	NH ₂	Various sizes	Crystallization and entrapping within PEI	—	Encapsulation	Electrostatic interaction	PEI 0.7, 1.0, 1.25	Plasmid DNA	MNPs size control and stabilization synthesis	113
MNPs	NH ₂ , NHAc, COOH	13.5 nm	One-pot hydrothermal route with PEI	—	Encapsulation	Electrostatic interactions	1.25 g Fe precuresor : 0.5 g PEI	Fluorescein isothiocyanate (FITC), folic acid PEG	<i>In vivo</i> magnetic resonance (MR) imaging of tumors	106
MNPs	NH ₂	12–18 nm	One-pot hydrothermal method in the presence of PEI	—	Encapsulation	Electrostatic interactions	1.25 g Fe precuresor : 0.54 g PEI	mPEG-COOH, acetic anhydride, succinic anhydride	Magnetic resonance imaging and therapy.	115
MNPs	NH ₂	DLS 259 nm	One-step solvothermal	Carboxylate groups on Fe ₃ O ₄	Grafting onto	Amide bonding H-N-CvO (Nitrogen in PEI-coated MNPs/ phosphorus in DNA)	2 g Fe precuresor : 3 g PEI	—	Demulsification of oil	109
MNPs	NH ₂	20 nm	Co-precipitation	—	Encapsulation (circular coating)	Aminated MNPs by PEI	100 µl of bare MNP (200 µg mL ⁻¹): 50 µl of PEI (40 µg mL ⁻¹) : 2 µg of DNA	CRISPR/Cas9	Genome editing (plasmids encoding CRISPR/Cas9 and template DNA)	110
MNPs	NH ₂	DLS 190-250 nm	One-pot solvothermal method in the presence of PEI	Sodium acetate (NaAc) electrostatic stabilizer (to prevent particle agglomeration)	Grafting onto and stabilization	Aminated MNPs by PEI	1 g Fe precuresor : 2 g PEI	—	Magnetic field hyperthermia and active targeting	108

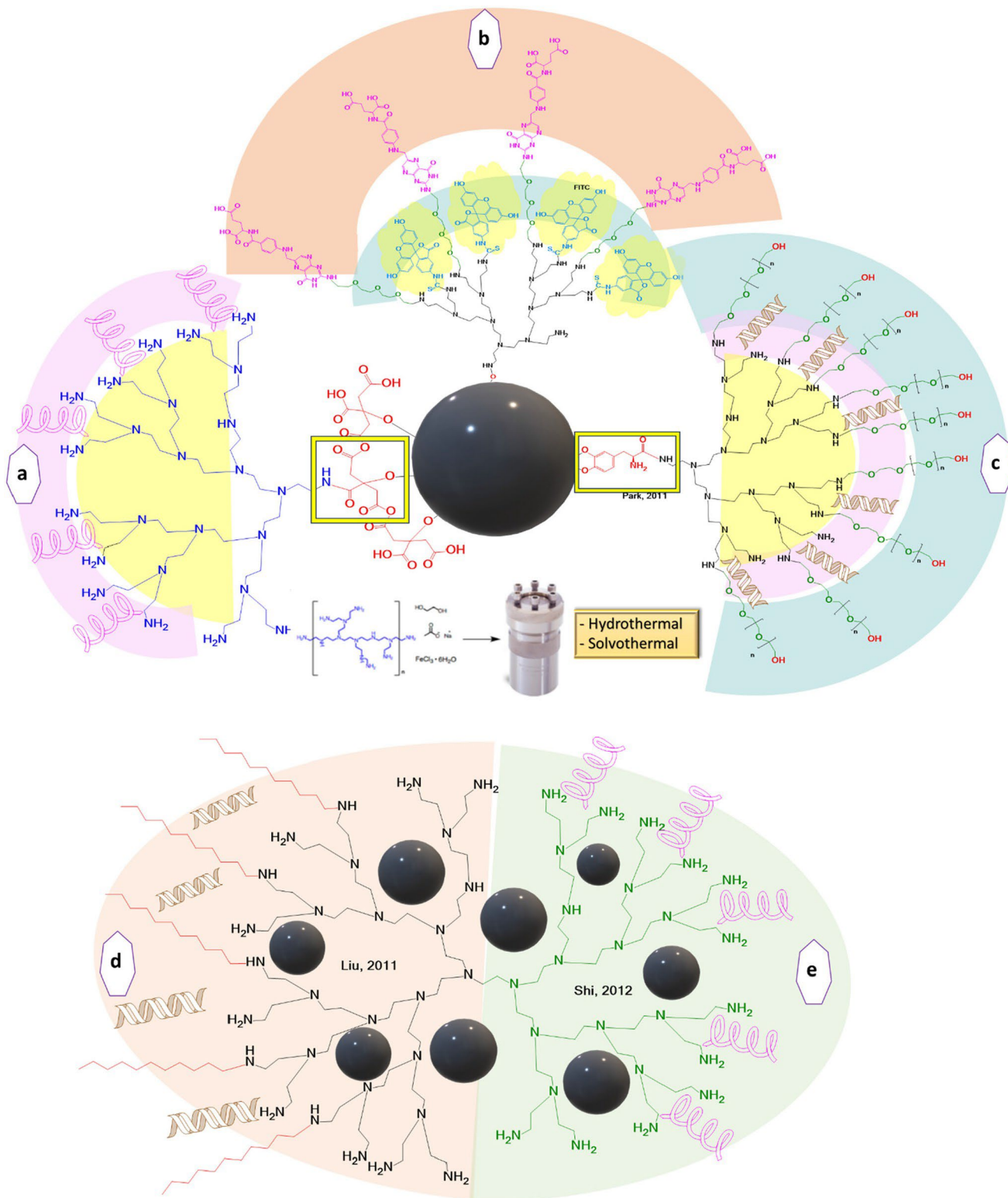


Fig. 7 Synthesis and modification processes of MNPs-PEI dendritic and branched systems (a) DNA attached and encapsulated on magnetic PEI,¹⁰⁶ (b) ref. 108, (c) ref. 109, (d) & (e) MNPs synthesized within PEI and encapsulated with DNA and si-RNA entrapped on the prephiral sites for gene editing and delivery.^{14,107,111-114}

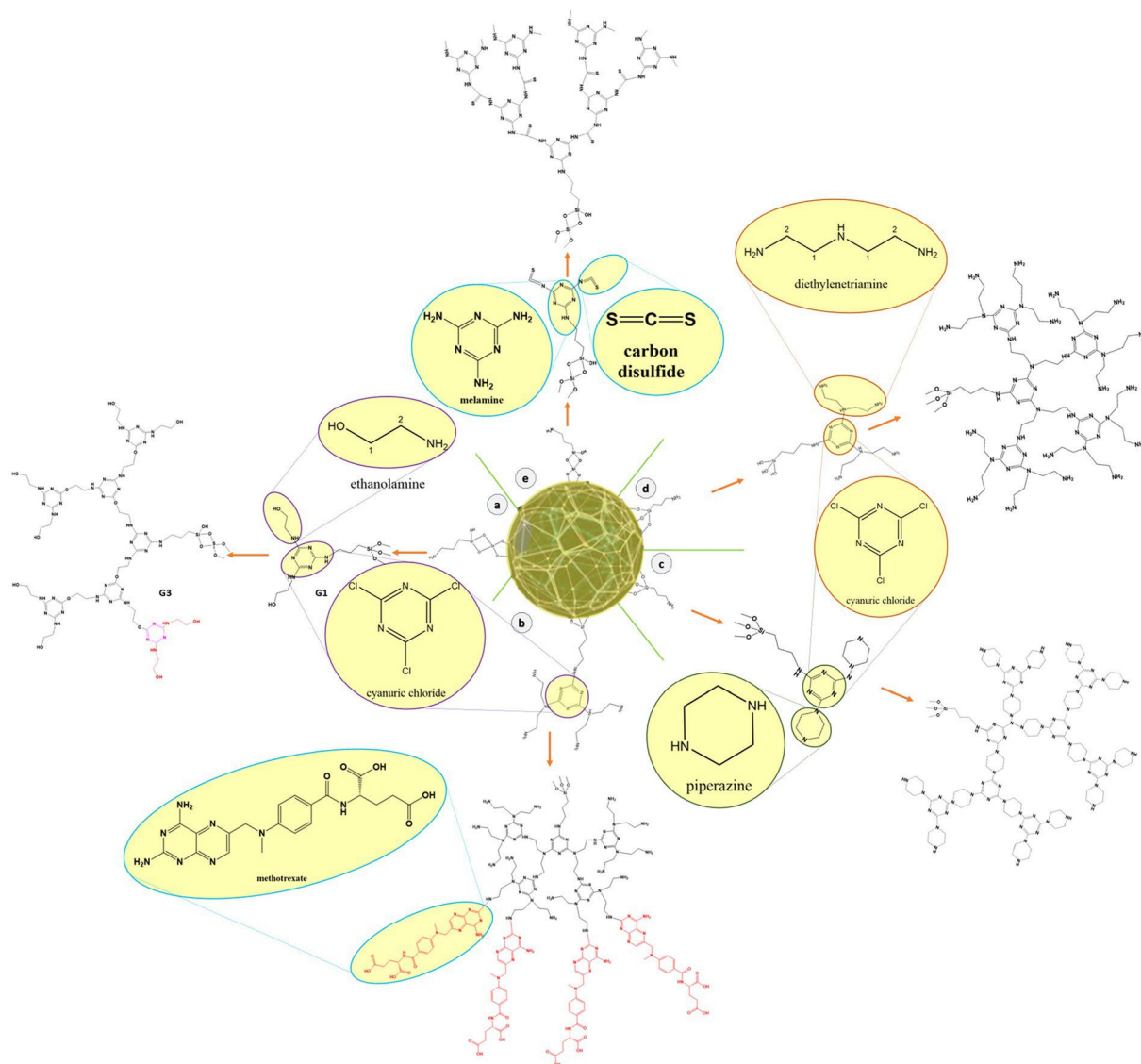


Fig. 8 Triazine-based dendrimer conjugated with MNPs. (a) ref. 118 and 119, (b) ref. 120, (c & d) ref. 117, and (e) ref. 13.

between PG with MNPs can be done either by growing PG from MNPs through glycidol polymerization^{40,41,125,128,129} or stabilizing the MNPs by grafting the polymerized dendron onto their surface.^{12,22} The grafting-from process starts with the initial coating of MNPs with anchoring groups that allow the linkage between the hydroxyl group of glycidol and the anchored groups on the MNPs' surface. Anchoring groups such as amine-containing groups (APTES)-,^{41,128} and Hexanediamine¹²⁵ have been used to link with PG by opening the ring of glycidol and binding *via* direct *N*-alkylation of amines. Li *et al.* (2013) used an acrylate silane(3-(trimethoxysilyl)propylmethacrylate) to bind with thiol functionalized PG to form a C-S *via* "thiol-ene" click reaction.²² The phosphonate-containing groups (sodium(prop-2-ynoxy)methylphosphonate) have been investigated as linkers with mono and trivalent chelation to test the stability of PG@MNPs. It was found that the binding affinity of multivalent ligands con-

taining more than one phosphonate binding site per polymer surpasses that of monovalent ligands. This effect is primarily maintained when three phosphonate ligands are present, as the spatial extension of both ligands provides significant steric stabilization. Consequently, such ligands exhibit colloidal stability in ultrapure water for more than a year.¹² In Jafari *et al.* (2010)⁴⁰ work, gold nanoparticles (AuNP) were used efficiently as a shell of MNPs to provide nontoxic coated MNPs. PG and Au-MNPs were connected through 2-mercaptoethanol, where the thiol site is linked to AuNP surface, forming Au-S bonds. Then, the glycidol is linked by opening the ethoxy ring and forming S-O bond.⁴⁰ Large quantity production of MNPs@PG for various utilization was achieved in a simpler approach through a direct one-pot polymerization reaction of glycidol on MNPs surface by thermally decomposing ferric oxalate pentahydrate precursor with the aid of triethyleneglycol (TEG) and then polymerizing glycidol directly

Table 8 Summarized details of magnetic triazine-based dendrimers in literature

Dendrimer generation/size	Dendrimer monomers	Dendrimer core	Dendrimer terminal group	MNPs size	MNPs synthesis	MNPs pre-surface functionalization	Dendritic attachment approach	Bond type between MNPs & dendrimer	Dendritic MNPs post-surface modification	Targeted application	Ref.
G1, G2	Cyanuric chloride (CC), piperazine (p) Cyanuric chloride (CC), diethylenetriamine (DETA)	MNPs@Si-NH ₂	-NH		Co-precipitation	(Aminopropyl) trimethoxysilane (APTMS)	Grafting assembly	MNPs-Si-NH-CC-P MNP-Si-NH-CC-DETA	—	Drug delivery	117
G3 poly (-aminoethanol) (PAMET)	Cyanuric chloride (CC) & Ethanolamine (EA)	MNPs@SiO ₂ @PrNH ₂	-OH	21 nm	Coprecipitation	TEOS, (aminopropyl) triethoxysilane APTES (PrNH ₂) TEOS, APTES	Grafting assembly	MNPs-Si-O-Si-NH-CC-EA	—	Removal of Cadmium Cd(II), and lead Pb(II) Drug delivery	118 119
Polytriazine-thiourea G2	Melamine (M), carbon disulfide (CS)	MNPs@Ba@Si-NH ₂	-NH	50 nm	Combustion	BaFe ₂ O ₄ , (APTES)	Grafting assembly	MNPs-Ba-Si-NH-M-CS	—	Removal of rhodamine B (RB)-Pb (II)	13
G2	Cyanuric chloride (CC), bis(3-aminopropyl) amine	MNPs@SiO ₂ @Si-NH ₂	NH ₂	46 nm	Coprecipitation	APTES			Folic acid (FA) & methotrexate (MTX)	(ii)	120

Table 9 Summarized details of magnetic peptide dendrimers in literature

Dendrimer generation/size	Dendrimer monomers	Dendrimer core	Dendrimer terminal group	MNPs size	MNPs synthesis	MNPs pre-surface functionalization	Dendritic attachment approach	Bond type between MNPs & dendrimer	MNPs : dendrimer ratio	Dendritic MNPs post-surface modification	Targeted application	Ref.
L-Lysine, polypeptide G1-G3, and L-glutamic acid, polypeptides G1-G3	L-Lysine & L-glutamic acid	MNPs@Oleic acid (ligand to be replaced)	Lys-NH ₂ , Glu-COOH	>30 nm by DLS	Thermal decomposition	Dopamine, catecholamine	Stabilization (ligand exchange), (grafting before coordination)	MNP-O-NH-L-lysine-NH ₂ & MNP-O-NH-L-glutamic acid-COOH	2: 1, dendrimer : MNPs@OA	—	—	21
EDA-KR2 dendrimer G2	L-Lysine, polypeptide, and L-arginine, polypeptides	EDA	Lys-NH ₂	8-12 nm by TEM	Coprecipitation	Glutamic acid-modified iron oxide nanoparticles (Glu-MNPs)	Stabilization, grafting onto	NH-CvO peptide bonding	2 mg ml ⁻¹ Glu-MNPs : w/w ratios of 1, 2, 4, 6, 8 and 10 of EDA-KR ₂	(DOX)	Potential drug carriers	18
AuBP1 and AuBP2	AuBP1 and AuBP2	MNP@Si-COOH	COOH	70 nm	Hydrothermal reaction	3-Aminopropyltriethoxysilane (APTES) into 4-oxo-4-(3-(triethoxysilyl)propylamino) butanoic acid (OTPBA) <i>via</i> succinic anhydride conjugation, 4-Methylcatechol (MC)	Grafting from	EDC/NHS carbodiimide	—	—	Gold mining	10
L-Arginine-(RGD)	—	MNPS@MC	—	TEM-4.5 nm core DLS-10 nm	—	—	—	—	Estimation 100-200 peptides per particle.	—	—	121

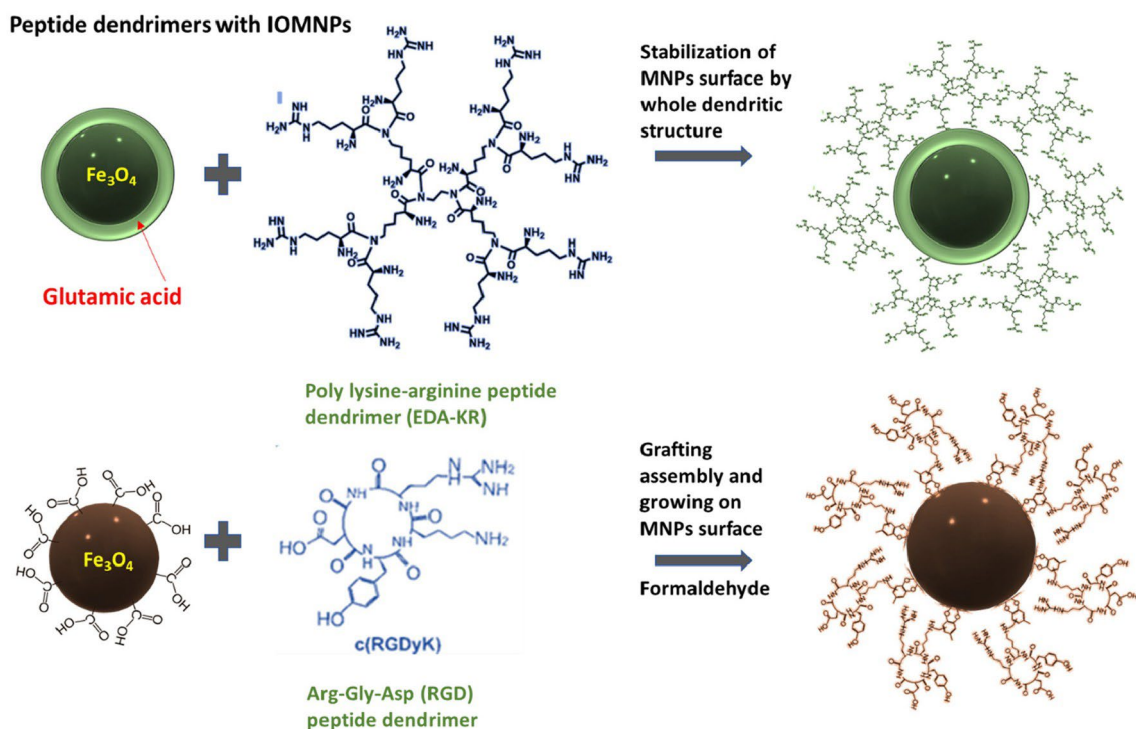


Fig. 9 Peptide dendrimers grafted on or stabilizing MNPs.

on produced nanoparticles from the reaction.¹²⁹ Considering the OH groups from TEG connecting with the open ring of glycidol establishes a stable coordination for further application (Fig. 10). Arsalani *et al.* initiated PG from APTES functionalized MNPs using *n*-butyllithium as an initiator¹²⁸ (see Table 10).

4.8 Dendritic hyperbranched polyesters (HBPE)

Magnetic nanoparticles were synthesized through a coprecipitation method, where iron oxide was precipitated from iron slats (precursors) and coated with poly citric acid (PCA) dendritic macromolecules using a bulk polymerization strategy. To enhance their properties for tumor cell targeting, the surface of the nanoparticles was further functionalized with poly(ethylene glycol) (PEG), followed by the incorporation of folic acid through a coupling reaction. This modification was achieved by reacting the hydroxyl end group of PEG with the carboxyl group of folic acid.⁸⁹ Another study developed a biocompatible magnetic drug carrier based on hyperbranched polyester (HBPE) modified with (2-dodecen-1-yl)succinic anhydride (DDSA) functional groups. The HBPE was modified to introduce hydrophilic $-\text{COOH}$ groups and serve as efficient acceptors of small MNPs (Fe_3O_4 and $\gamma\text{-Fe}_2\text{O}_3$) and isoniazid (INH). However, the carrier exhibited low loading capacity and encapsulation efficiency, likely due to the inhomogeneous structure of Fe_3O_4 /HBPE-DDSA/INH nanoparticles. A one-step method was developed to synthesize Fe_3O_4 /HBPE-DDSA/INH nanoparticles with controlled drug release characteristics. Orthogonal experiments were conducted to optimize the loading capacity and encapsulation efficiency of the

nanoparticles.^{65,67} In another approach, magnetite (Fe_3O_4) nanoparticles were covalently functionalized with a Polyester bis-MPA dendron, specifically a 2-hydroxyl, 1-azide dendrimer known as polyester dendron hydroxyl acid (PEDHA). The presence of C–H–O covalent bonds between the Fe_3O_4 nanoparticle and PEDHA dendrimer was confirmed by IR-absorption analysis.¹³⁰ Additionally, further investigation was carried out on the synthesis approaches and their influence on the morphology, chemistry, and magnetization of iron oxide nanophases within a highly branched polymer matrix. Various methods, including chemical reduction, polyol thermolysis, sonochemistry, and hybrid sonochemistry/polyol processes were employed to develop magnetically active iron oxide-based nanocomposites in a highly branched polyol matrix.¹³¹ The hyperbranched polymer was found to be an excellent stabilizer for iron oxide nanophases in all the different four samples that were prepared. Moreover, throughout the hybrid method and thermolytic process, the hyperbranched polyol exhibited favorable reducing agent properties. By utilizing these diverse synthesis approaches, it became feasible to precisely regulate the iron-based nanophases' shape, size, composition, and dispersity, enabling the creation of materials with high stability, low hemolytic activity, and favorable magnetic activity. The feasibility of deploying the synthesized composites as tomographic probes was demonstrated through NMR relaxation analysis.¹³² Another form of magnetic nanocomposite (NC) was created by incorporating magnetically responsive nanoparticles (Fe_3O_4) into a sunflower oil-modified hyperbranched polyurethane (HBPU) matrix. This was achieved using an

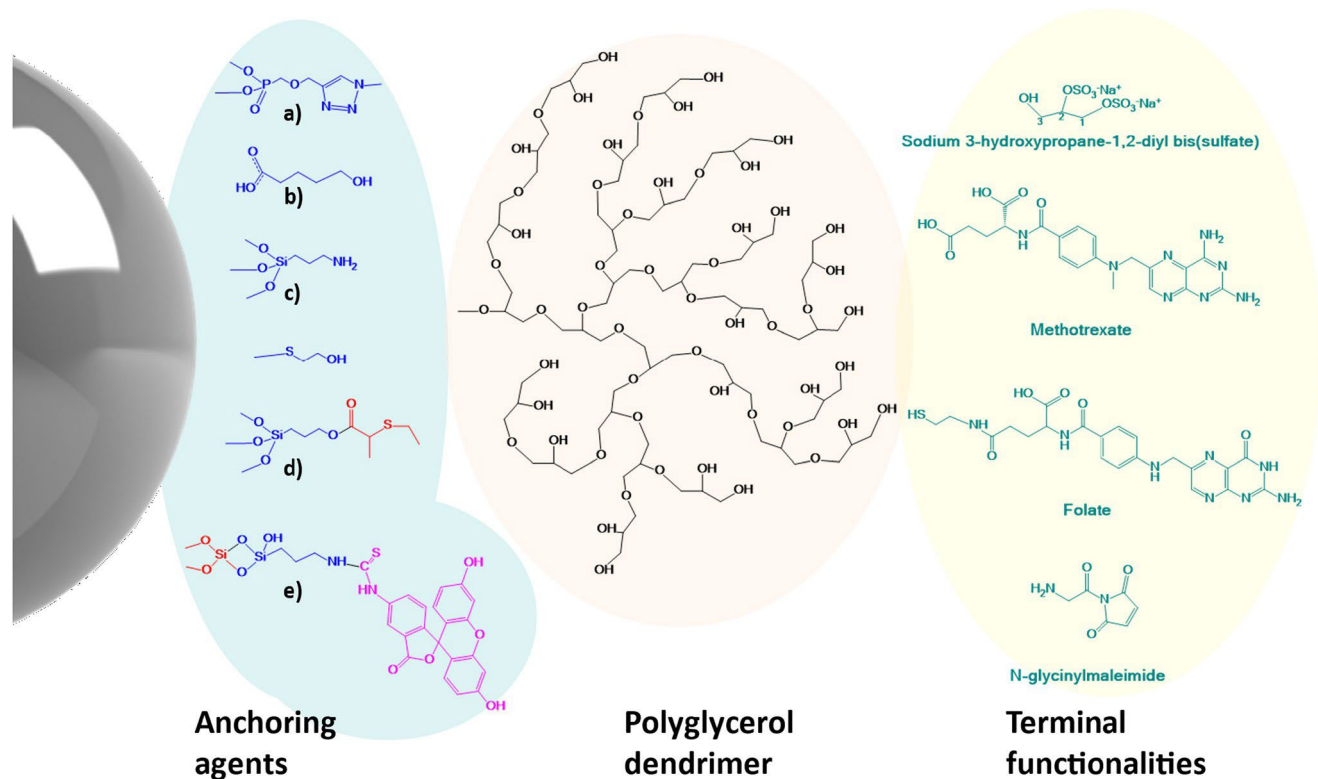


Fig. 10 Hyperbranched dendritic polyglycerol grafted MNPs. (a) Wang (2009),⁵³ (b) Wang (2013),¹²⁹ (c) Arsalani (2012),¹²⁸ (d) Nordmeyer (2014),¹² (e) Jafari *et al.* (2010),⁴⁰ (f) Wang (2011),⁴¹ (g) Li *et al.* (2013).²²

in situ polymerization technique, which allowed for better mixing of the nanoparticles throughout the HBPU due to its lower viscosity compared to other methods. Ultrasonication was employed to break up agglomerates, resulting in a uniform dispersion of the nanoparticles in the HBPU matrix. The uniform distribution was confirmed through imaging techniques, which showed small spherical particles of Fe_3O_4 with a mean diameter of 7.65 nm. The presence of void structures and surface functionality facilitated the interaction and encapsulation of the nanoparticles, leading to their stabilization within the HBPU matrix. The interaction between Fe_3O_4 and HBPU was primarily due to electrostatic and hydrogen bonding interactions, along with possible interactions between the carbonyl groups of urethanes and absorbed hydroxyl groups on the nanoparticles (Fig. 11 and Table 11). The resulting nanocomposite exhibited superparamagnetic-like behavior and demonstrated discernible improvements in terms of biocompatibility, antimicrobial properties, biodegradability, and shape recovery in comparison to the original HBPU material.¹³³

4.9 Pyridylphenylene dendrons and dendrimers

Polyphenylene pyridine dendrimers (or Pyridylphenylene) are cyclic dendrimers formed from phenylene and pyridine embeds repetitive units. They are characterized by their rigidity and minimal conformational changes by exceptionally allowing rotation around the C–C bonds of the inter-ring. These

dendrimers possess a high degree of thermal and chemical stability comparable to linear polyphenylenes but with enhanced solubility due to their ability to prevent the typical intermolecular packing observed in linear poly-*p*-phenylenes. A convergent synthesis approach of a polyphenylene dendrimer was first achieved by employing transition-metal-catalyzed aryl–aryl coupling reactions, whereas the earliest divergent preparation method was accomplished through repetitive Diels–Alder cycloaddition.^{135–137} The study involves the creation of multicore iron oxide mesocrystals through the thermal decomposition of iron acetyl acetonate with the aid of Pyridylphenylene dendron and dendrimer. MNPs colloidal clusters can also form mesocrystals, which are composed of individual nanocrystals arranged in a common crystallographic fashion without coalescing individual cores. The self-assembly of dendron/dendrimer leads to the formation of multicore morphologies (Fig. 12a). These mesocrystals exhibit cooperative magnetic behavior due to their single-crystalline ordering, and they have ambient blocking temperatures, which allow for fine-tuned control of magnetic properties through minor temperature changes. When the concentration of supersaturation is achieved, the nucleation of particles begins to form and grow to a specific size while aligning with each other to create larger structures. If particles merge through oriented attachment, they form individual crystals. However, if capping molecules or other factors prevent fusion, mesocrystals will form instead.¹³⁸

Table 10 Summarized details of magnetic polyglycerol dendritic and hyperbranched systems in literature

Dendrimer monomers	Dendrimer core	Dendrimer terminal group	MNPs size	MNPs synthesis	MNPs pre-surface functionalization	Dendritic attachment approach	Bond type between MNPs & dendrimer	MNPs : dendrimer ratio	Dendritic MNPs post-surface modification	Targeted application	Ref.
Glycidol	MNPs@OA	OH	12 nm	Coprecipitation <i>in situ</i> with Oleic acid	(Ligand exchange), 3-(trimethoxysilyl)propylmethacrylate (3-TMSPMA) (MPS)	Stabilization ("thiol-ene" click reaction)	MNP-O-Si-S-HPG-O-MTX	3 MNP : 20 HPG	Methotrexate (MTX) & folic acid (separately)	Targeted anticancer effects	22
Glycidol	MNPs@OA	OH		Thermal decomposition	(Ligand exchange), 6-hydroxy caproic acid & aluminum isopropoxide	Grafting assembly	MNPs-(OO)-R-O-HPG-OH	—	—	Magnetic resonance imaging contrast agent	53
Glycidol	Core-shell iron-gold (MNPs@Au)@S	OH	TEM9 nm to 20 nm	Reduction of Fe & Au salts	2-Mercaptoethanol	Grafting assembly	MNPs-Au-S-O-PG-OH	30 nm	—	— Non-toxic	40
Glycidol	MNPs@OA (monodispersed)	OH	12 nm	Thermal decomposition (nanocrystals)	(Ligand exchange), TEOS, APTES, & FITC	Grafting assembly	MNP-O-Si-O-Si-NH-FITC-HPG-OH	—	N-Glycylmaleimide & folic acid (folate-SH)	Real-time imaging in ovarian cancer resection	41
Glycidol	MNPs@APTES	OH		coprecipitation	APTES, then butyllithium (<i>n</i> -BuLi) to ionize amine group.	Grafting assembly	MNP-O-Si-NH-HPG-OH	—	—	Liver and kidney imaging/ scaffold for cellular and molecular imaging	128
Glycidol	MNPs@OH	OH	10 nm HPG-grafted MNPs	Thermal decomposition	Triethylene glycol	Grafting assembly	MNPs-O-HPG-OH	—	—	—	129
Glycidol	MNPs@OA	OH	11 ± 1 nm	Thermal decomposition	(Ligand exchange), phosphonate group (sodium(prop-2-ynyloxy)methylphosphonate)	Stabilization (dendron grafted to MNPs)	MNP-Pn ₁ -dPG-OH/ MNP-Pn ₃ -dPG-OH/ MNP-Pn ₃ -dPG-OSO ₃ ⁻	10 mg MNPs : 6 mM dPG	76% sulfate groups (statically), OSO ₃ ⁻ Na ⁺	Selective MRI contrast agent	12
Glycidol	MNPs@RNH ₂	OH	—	Solvothermal	Hexanediamine	Grafting assembly, (from MNPs)	Na ⁺ MNP-O-R-NH ₂ -HPG-OH	TEM: 21-30 nm, DLS: 22.0 ± 3.0 nm	—	Removal of (Ni, Cu and AL)	125

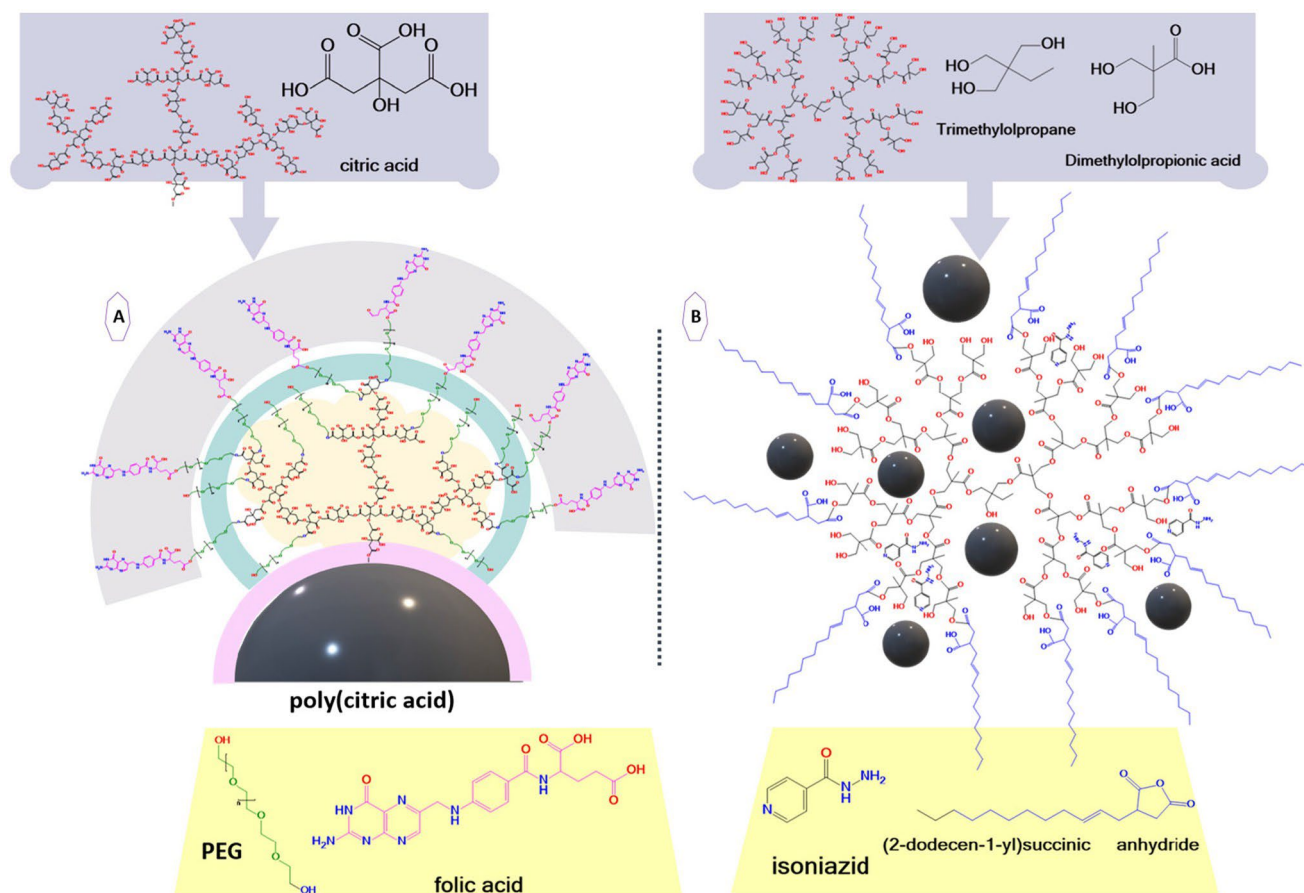


Fig. 11 Synthesis and modification of MNPs with HBPE; (a) ref. 65, (b) ref. 89, (c) ref. 67, and (d) ref. 131.

In further studies, MNPs were developed to serve as a support for catalysts that are magnetically retrievable. To achieve this, polyphenylene pyridyl dendrons were used to coat the MNPs, which allowed for coordination between catalytic Pd species and pyridyl groups, followed by PdNP formation upon reduction. The formation of Pd NPs was precisely controlled by both the generation and number of dodecyl chains on the dendron periphery. Additionally, it was found that the dendron generation had an impact on the internal structure of iron oxide multicore mesocrystals (Fig. 12c), providing sensitive nanoscale control of the associated magnetic properties. The size of the immobilized Pd NPs was found to be a determining factor in catalytic activity, leading to the proposal of an intelligent design strategy for novel catalysts. These nanomaterials demonstrated remarkable catalytic characteristics, accompanied by their facile recovery, recyclability for multiple cycles, and high stability, thereby rendering them immensely viable for hydrogenation and numerous other catalytic reactions that utilize Pd catalysts.¹³⁹

In Sorokina *et al.* (2019) study, the pyridylphenylene dendrons (D) were attached to the surface of magnetic silica ($\text{Fe}_3\text{O}_4\text{-SiO}_2$, MS) through the creation of ether or amide bonds. The type of bond formed depends on the structure of the flexible linkers present on the MS surface and the focal

groups of the dendrons.⁵⁰ Later, Kuchkina *et al.* (2020)¹⁴⁰ group were able to synthesize magnetic silica (MS) samples by incorporating magnetite (Fe_3O_4) nanoparticles (NPs) within commercially available mesoporous silica, where the NPs exhibited a size suitable for fitting into the pores. The X-ray diffraction (XRD) pattern confirmed the presence of a cubic spinel structure after using ethylene glycol as a reducing agent, with a mean crystallite size of 13.2 nm. The interconnectedness of the NPs along the pores resulted in the formation of larger crystals through oriented attachment. Subsequently, MS was functionalized with iodine (MS-I) and NH_2 groups (MS- NH_2) through reactions with IPTMS and APTES, respectively. The design of flexible linkers aimed to enhance the accommodation of rigid aromatic dendrons on the MS surface. For example, the preparation of MS-D1 involved the Williamson reaction between MS-I and D1, resulting in the formation of an inert ester group (Fig. 12e). On the other hand, MS-D2 was synthesized *via* peptide bonds utilizing standard peptide coupling with D2. The complexation of MS-G3 with Pd acetate resulted in the formation of different Pd forms, such as Pd^{2+} ions and Pd^0 nanoparticles. The interaction of MS-G3-PdAc with Pd acetate probably resulted in the creation of bidentate pyridine complexes at the outer part of the dendron. Meanwhile, the development of complexes

Table 11 Summarized details of magnetic hyperbranched polyester (HBPE) systems in literature

Dendrimer generation/size	Dendrimer monomers	Dendrimer core	Dendrimer terminal group	MNPs size	MNPs synthesis	MNPs pre-surface functionalization	Dendritic attachment approach	Bond type between MNPs & dendrimer	MNPs : dendrimer ratio	Dendritic MNPs post-surface modification	Targeted application	Ref.
Poly citric acid (PCA)	Citric acid	MNPs@COOH	COOH	10-49 nm	Coprecipitation	Citric acid (CA)	Grafting assembly (from)	Esterification	—	Poly(ethylene glycol) (PEG), and folic acid (FA)	Drug targeting and delivery	89
HBPE-DDSA	Tri-methylamine (TMP), dimethylolpropanoic acid (DMPA)	Tri-methylamine (TMP)	-OH, dodecanyl succinic anhydride	10 nm	Coprecipitation	—	Encapsulation and entrapping	Electrostatic interactions	MNPs : HBPE, 0.1 g : 0.05 g	Isoniazid (INH)	Drug-loading and delivery	67
	Trimethylolpropane (TMP) and Dimethylolpropanoic acid (DMPA)	Trimethylolpropane (TMP) and	(DDSA)	26 nm	One-step fabrication <i>in situ</i> within HBPE-DDSA	—	—	—	—	—	Drug-loading and delivery	65
PEDHA	Bis-MPA dendron, 2-hydroxyl, 1-azide dendrimer.	MNPs	-OH	—	Coprecipitation	—	Grafting onto	-O-CvO covalent linkages	3.5 g of MNPs : ~25 mg and 50 mg of	—	Demulsification of crude oil	130
G2	Aminocellulose	MNPs	-NH ₂	10 nm	—	Amino cellulose coating	Grafting assembly (from)	Amide bonding	—	PEG & niclosamide	Niclosamide delivery	131
G2 BOLTORN (BH20)	2,2-Dimethylol propionic acid (Bis-MPA)	2,2-Dimethylol propionic acid (Bis-MPA)	-OH	30 nm	Chemical reduction	Polyol thermolytic process, Sonochemistry	—	—	—	—	Tomographic probes	132
G4 Boltorn (BH40)	2,2-Dimethylol propionic acid (Bis-MPA)	2,2-Dimethylol propionic acid (Bis-MPA)	-OH	15-25 nm	Coprecipitation	Hybrid sonochemistry/polyol process	Grafting onto	Electrostatic interaction and physical attachment	1 : 1	—	Pb and Cu removal	134

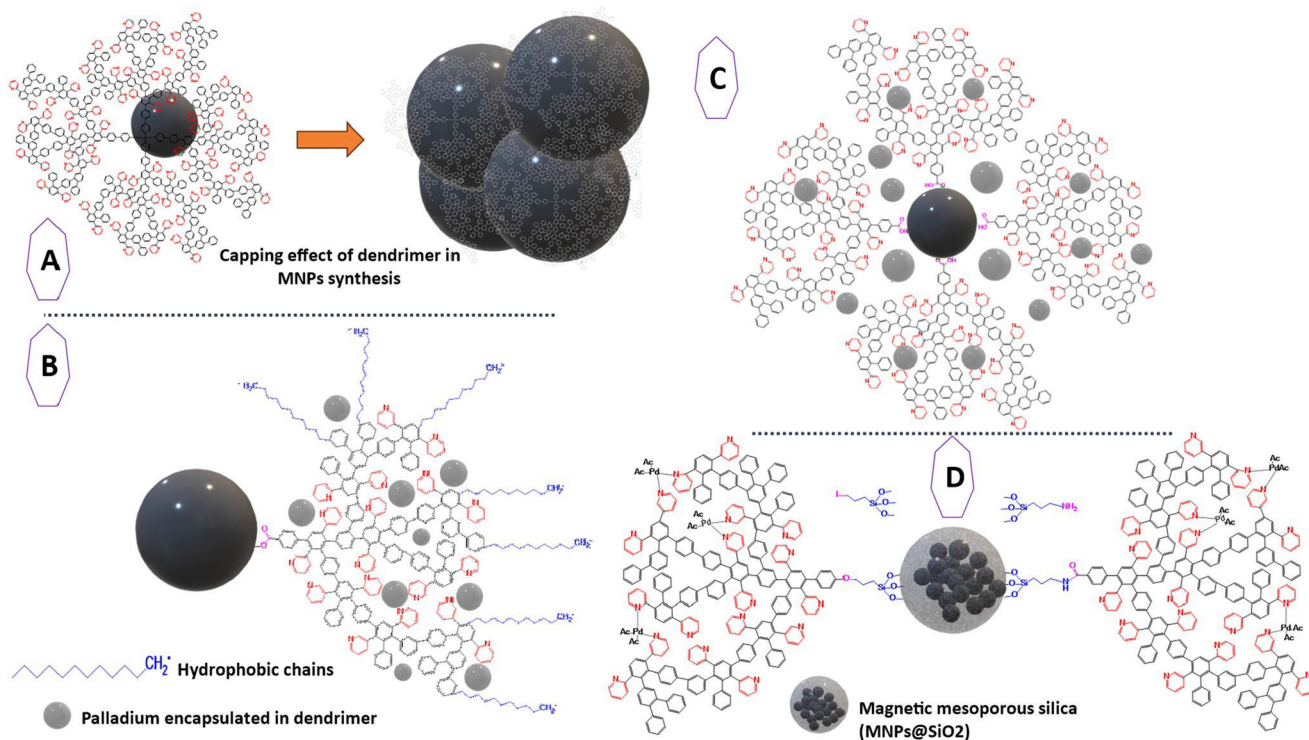


Fig. 12 Various conjugations and coordination of MNPs with poly(pyridyl phenylene) dendrons and dendrimers (a) ref. 141, (b) ref. 141, (c) ref. 139, (d) ref. 50 and 140.

within the interior of the dendron possibly involved the collaborative action of an electron donated by a lone pair of pyridine nitrogen and the π -electrons from an aromatic ring.¹⁴⁰ Further details are summarized in Table 12.

4.10 Carbosilane dendritic systems

Carbosilanes are a class of organosilicon compounds that contain both carbon and silicon atoms in their molecular structure. They are composed of a central silicon atom bonded to carbon and hydrogen atoms, and other functional groups. Carbosilanes can be synthesized through various methods, including the reaction of silicon hydrides with organic compounds containing carbon-carbon double or triple bonds, the reaction of dichlorosilanes with organolithium compounds, and the hydrolysis of alkoxy silanes. Regarding their connection with MNPs, carbosilanes can be functionalized with various organic molecules, such as amines or carboxylic acids, to provide reactive groups that can bind to the surface of MNPs. This allows for the creation of hybrid materials that simultaneously exhibit magnetic and organic properties^{143,144} (check Fig. 13). In addition, carbosilane dendrons decorated with carboxyl groups and alkoxy silane functional groups at the focal point were proven effective for the stabilization of MNPs using the co-precipitation technique. These dendrons are named according to the nomenclature "XG_nY_m", where X, G_n, Y, and m refer to the focal point, the generation of carbosilane dendron, the nature of peripheral groups, and the number of these groups, respectively. By reacting NH₂G_nA_m (A = allyl; n =

1, m = 2; n = 2, m = 4) with nearly equimolar amounts of 3-isocyanatopropyltriethoxysilane, a chemically stable urea group is formed, providing the necessary group at the focal point for grafting onto the MNPs surface. This results in the formation of compounds (EtO)₃SiG_nA_m [n = 1, m = 2 (1); n = 2, m = 4 (2)]. Additionally, two cationic CBS dendrons, (EtO)₃SiG_n(S-NMe³⁺)_m (G2, n = 2, m = 4 (1); G3, n = 3, m = 8 (2)), were synthesized to assess the impact cationic groups' number on the ligand. Furthermore, a cationic CBS dendrimer, G1Si(S-NMe³⁺)₇(S-Si(OEt)₃)(G1 3), was utilized to investigate the influence of the dendritic structure on the MNPs functionalization and their associated activity. The functionalization process occurs through the reaction between ligands containing a triethoxysilyl moiety and the hydroxyl groups existing on the MNPs' surface. This study employed three different CBS dendritic systems that were functionalized with ammonium groups (-NMe³⁺).^{145,146} The resulting hybrid materials exhibited enhanced magnetic properties and can be used in a variety of applications, such as protein extraction and purification,¹⁴⁷ viruses,¹⁴⁶ and bacteria¹⁴⁵ capturing (see Table 13).

4.11 Methoxyphenyl triallyl-based catalytic dendrons

Cyclo- and dicyclohexyldiphosphinopalladium catalytic dendrons are a unique type of dendrons where they are formed from Methoxyphenyl triallyl and phosphine monomers. Their work involves the synthesis of core-shell γ -Fe₂O₃/polymer superparamagnetic nanoparticles (MNPs), which were then

Table 12 Summarized details of magnetic poly(pyridyl phenylene) dendrons and dendrimers in literature

Dendrimer generation/size	Dendrimer monomers	Dendrimer core	Dendrimer terminal group	MNPs size	MNPs synthesis	MNPs pre-surface functionalization	Dendritic attachment approach	Bond type between MNPs & dendrimer	MNPs : dendrimer ratio	Dendritic MNPs post-surface modification	Targeted application	Ref.
G3 poly (phenylenepyridyl) dendron and dendrimer	Phenylene & pyridylene	Tetrakis(4-ethynylphen-1-yl) methane (Td)	Pyridyl periphery	23 nm	Thermal decomposition (Fe(acac) ₃) in presence of dendrimer	Poly (phenylenepyridyl) dendron Poly (phenylenepyridyl) dendrimer	Stabilization Fe NP		0.353 g (1 mmol) of Fe(acac) ₃ , 0.607 g (0.055 mmol) dendrimer	—	Iron oxide mesocrystals stabilization	138
G2, G3 dendrons	Phenylene & pyridylene	COOH focal group	Pyridyl periphery	18–30 nm (1.2 nm PdNP)	Thermal decomposition (Fe(acac) ₃) in presence of dendron	Poly (phenylenepyridyl) dendron	Stabilization	MNP–O–COO–Dend	1 mmol Fe (acac) ₃ : 0.2 mmol dendron	Dodecyl periphery/palladium NP.	Control nanoparticle formation and catalytic hydrogenation	141
G2, G3 dendrons and dendrimers	Phenylene & pyridylene	COOH focal group (for dendrons)	Pyridyl periphery	21.8 nm	Thermal decomposition (Fe(acac) ₃) in presence of dendron	Poly (phenylenepyridyl) dendron	Stabilization	MNP–O–COO–dendron	0.353 g (1 mmol) of Fe(acac) ₃ , 0.140 g (0.11 mmol) of dendron	Palladium NP.	Catalytic hydrogenation	142
G2, G3 dendrons	Phenylene & pyridylene	COOH focal group	Pyridyl periphery	21.8 ± 3.3 nm	Thermal decomposition (Fe(acac) ₃) in presence of dendron	—	Stabilization	MNP–O–COO–dendron	0.353 g (1 mmol) of Fe(acac) ₃ , 0.140 g (0.11 mmol) of dendron	Palladium NP.	Continuous-flow Suzuki cross-coupling reactions	139
G2 dendrons	Phenylene & pyridylene	OH focal group/COOH focal group	Pyridyl periphery	13.2 nm	Reduction of Fe(NO ₃) ₃ in presence of silica gel (magnetic silica MS)	Mesoporous silica then: 1. MS-I (3-iodopropyl) trimethoxysilane (IPTMS) 2. MS-NH ₂ (APTES)	Stabilization	Fe ₃ O ₄ –SiO ₂ –I–O–dendron/ Fe ₃ O ₄ –SiO ₂ –NH ₂ –COO–dendron	0.36 g MS-I : 0.56 g D1/0.33 g MS-NH ₂ : 0.15 g D2	Palladium acetate into (Pd ²⁺ ions, PdNP)	Catalytic reactions	50
G3 dendrons	Phenylene & pyridylene	COOH focal group	Pyridyl periphery	4.9 ± 0.5 nm	Reduction of Fe(NO ₃) ₃ in presence of silica gel (magnetic silica MS)	Mesoporous silica formin magnetic silica MS/(APTES)	Stabilization	Fe ₃ O ₄ –SiO ₂ –NH ₂ –COO–dendron	0.43 g MS-NH ₂ : 0.28 g G3	Palladium acetate into (Pd ²⁺ ions, PdNP)	Suzuki–Miyaura reactions of Br-arenes and phenylboronic acid	140

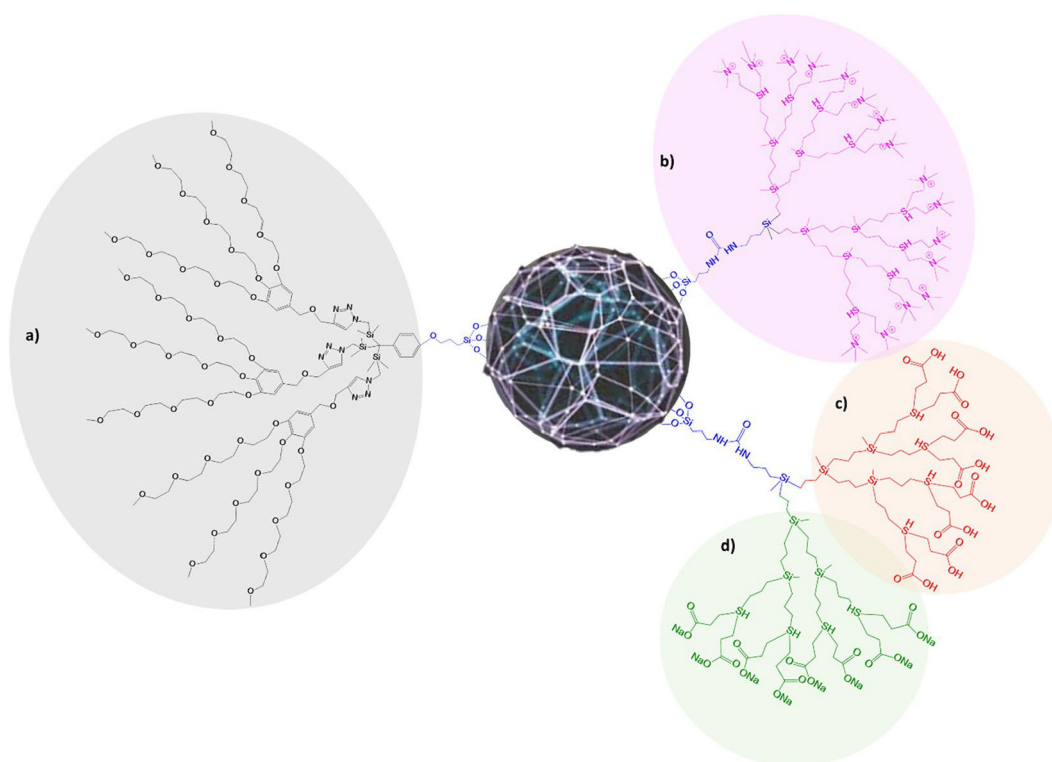


Fig. 13 (a) Structure of MNPs coated by silane anchoring agents followed by dendritic PEG ligands,^{143,144,148,148} (b) ref. 146, (c) ref. 147, (d) ref. 145.

modified with four metallodendrons containing dicyclohexyl-diphosphinopalladium complexes (see Fig. 14). The grafting of the dendrons onto the MNPs was achieved through a peptide reaction between the carboxyl groups on MNPs' polymer shell and the terminal primary amino group of the dendron. The most optimal conditions for this attachment process were found to be in an aqueous environment, particularly when using nonionic surfactants with a lower hydrophilic-lipophilic balance, such as Triton X405 (Tx) or a combination of MeOH and Tx (1 : 2 ratio) in an organic/aqueous environment. The efficiency of grafting was shown to be affected by the type of coupling agents, and CHMC selected as the most suitable agent for the grafting process. The produced nanocatalysts in this study were also optimized for the Suzuki C-C cross-coupling reaction.^{149,150}

4.12 Phosphonate-containing dendrimers

The field of phosphonates and related multifunctional hybrids has experienced significant growth due to their potential applications in medicine and nano-biomaterial research. Various hydrophilic dendritic or linear phosphonic acids have been successfully synthesized with high yields to functionalize metal oxide nanoparticles. Through ligand exchange methods, these phosphonic acids have been effectively attached to iron or manganese oxide nanoparticles, resulting in stable and biocompatible nano-colloids that are primarily eliminated through the kidneys. This collection of phosphonates opens up possibilities for developing advanced hybrid materials with enhanced *in vivo* performance and sensitivity. Moreover, phos-

phonate-containing dendrimers and copolymers have also been synthesized and utilized for functionalizing MNPs, expanding their applications^{151,152} (Fig. 15 and Table 14). In one study, a conjugate of dopamine and bisphosphonate was developed to modify magnetite Fe₃O₄ nanoparticles for the removal of UO₂²⁺ ions. The synthesis involved a series of reactions starting from compound 1 (3-(3,4-bis(benzyloxy) phenethylcarbamoyl) propanoic acid) and compound 2 (tetraethyl 3-amino-propane-1,1-bisphosphonate), resulting in the formation of compound 3. Further modifications led to compound 4, which was then linked to Fe₃O₄ nanoparticles through Fe-O bonds. The resulting water-soluble product, compound 5, demonstrated a high affinity for UO₂²⁺ and efficiently removed UO₂²⁺ from both water and blood.¹⁵³ In another study, small-sized dendrons were synthesized and grafted onto MNPs to achieve colloidal stability and tunable organic coating characteristics. The successful grafting of dendrons depended on the functional groups present, with oppositely charged groups proving to be challenging. However, the use of carboxylate dendrons on MNPs resulted in excellent stability under physiological conditions and iso-osmolar media. These dendronized probes exhibited enhanced *in vivo* contrast compared to polymer-coated MNPs (Lamanna *et al.*, 2011).¹⁵⁵ Furthermore, a study conducted research on biocompatible phosphonated monomers and dendrons used as functional coatings for metal oxide nanoparticles. These molecules were designed with varying properties such as size, hydrophilicity, biocompatibility, and the number of anchoring phosphonate groups. This library of hydrophilic phosphonic acids

Table 13 Magnetic Carboxilane dendritic system

Dendrimer generation/size	Dendrimer monomers	Dendrimer core	Dendrimer terminal group	MNPs size	MNPs synthesis	Dendritic attachment approach	Bond type between MNPs & dendrimer	Dendritic MNPs post-surface modification	Targeted application	Ref.
G1, G2	Amine, allyl group, isocyanate, and 3-mercaptopropionic acid	MNP (attached to trioxysilane focal group)	COOH		Coprecipitation	Grafting onto MNP	MNPs-O-Si...S-COOH	COONa	HIV-1 capture and diagnosis	146
G2,	Amine, allyl group, isocyanate, and Ammonium (NMe ₃ ⁺)	MNP (attached to trioxysilane focal group)	Ammonium (NMe ₃ ⁺)	11 ± 2 nm	Coprecipitation	Grafting onto MNPs	MNPs-O-Si...NMe ₃ ⁺	—	Bacteria captor	145
G1,	Amine, allyl group, isocyanate, and 3-mercaptopropionic acid	MNP (attached to trioxysilane focal group)	SCOOH	12-14 nm	Coprecipitation	Grafting onto MNPs	MNPs-O-Si...S-COOH	—	Protein purification	147

offers promising opportunities for exploring dendronized nanohybrids as theragnostic agents.¹⁵¹

4.13 Magnetic graphene oxide with dendrimers

Graphene oxide (GO) is a graphene-derived material, characterized by its high specific surface area and the presence of diverse oxygen-containing functional groups, such as carboxyl, hydroxyl, and epoxy groups. These functional groups provide active attachment sites for further functionalization and modification. Compared to other carbonaceous nanomaterials, GO is known for its environmental friendliness and better biocompatibility. To improve the surface properties of GO, MNPs can be functionalized on the GO surface. Different types of dendrimers, with their distinct end functional groups and cavity sizes, can selectively adsorb specific target molecules. Therefore, the combination of magnetic GO and dendrimers holds promise as environmentally friendly nanomaterials.¹⁵⁶ In one study, magnetic graphene oxide functionalized with ethylenediamine (EDA) was prepared employing a simple one-pot solvothermal technique. The grafting reaction and growth of PAMAM dendrimers were achieved by performing a Michael addition of methyl acrylate (MA) to the amino groups on the GO/MNPs surface, followed by amidation of the terminal ester groups with EDA. The content of amino groups and steric hindrance of the dendrimers increase with generation growth, requiring an increase in the amount of MA, EDA, and reaction time for the complete reaction.⁵¹ Another approach involved the amidation method to prepare graphene oxide-modified magnetic polyamidoamine dendrimers (MNPs-PAMAM-G2.0-GO) nanoparticles. This method utilized EDC and NHS as bi-functionalizing cross-linkers. MNPs and MNPs-PAMAM-Gn were synthesized using a reported method, and further amidation coupling with GO was performed using NHS and EDC.¹⁵⁷ In a different study, a new type of dendrimer synthesized from ethylenediamine and maleic anhydride, was propagated from MNPs loaded with GO. The resulting magnetic graphene oxide grafted polymaleicamide dendrimer (GO/Fe₃O₄-*g*-PMAAM) nanohybrids were fabricated using a divergent approach and magnetic separation techniques. The surface of GO/Fe₃O₄ nanohybrids modified by 3-aminopropyltriethoxysilane (APTES) was grafted with various generations of (PMAAM). The incorporation of MNPs into GO facilitated the grafting reaction and allowed for easy product collection through magnetic separation. GO also played a role in preventing the agglomeration of MNPs, while PMAAM dendrimers protected against the oxidation of MNPs. The Pb(II) ions adsorption capacity of the GO/MNPs-*g*-PMAAM nanohybrids can be regulated by changing the terminal groups and generations of the PMAAM dendrimers. The fabrication process involved preparing GO/Fe₃O₄ nanohybrids using an inverse coprecipitation method, modifying them with APTES, and then synthesizing different generations of GO/MNPs-*g*-PMAAM using ethylenediamine and maleic anhydride as functional monomers.¹⁵⁸ More details are represented in Fig. 16 and Table 15.

These are just a few examples of the dendrimers grafted onto or conjugated with MNPs. The choice of dendrimer will depend on the specific desired properties of the resulting conjugate.

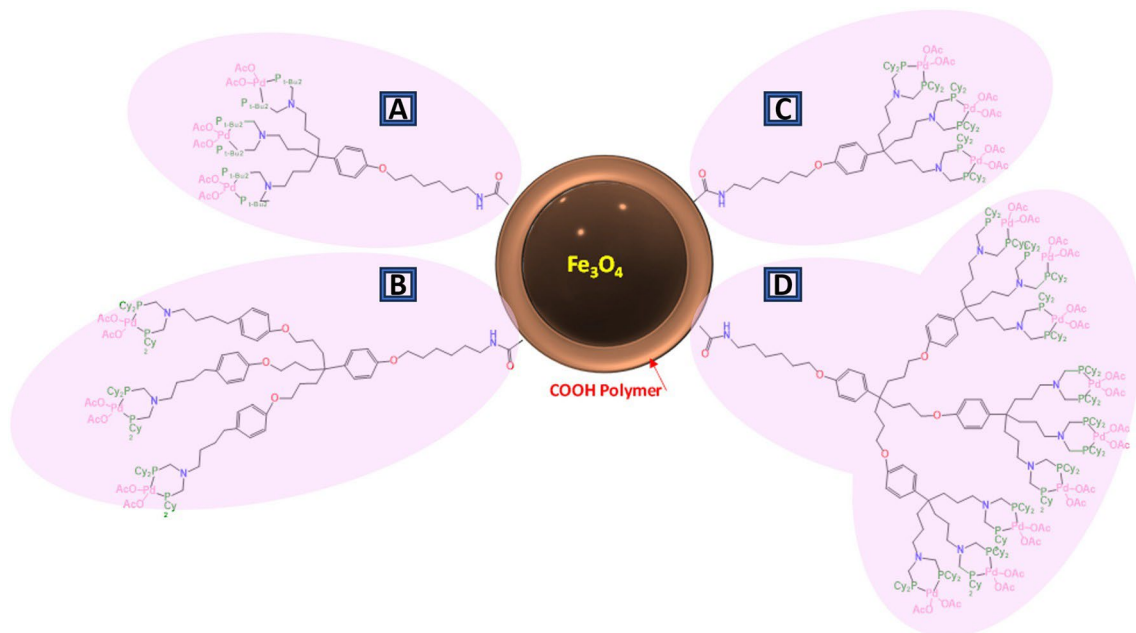


Fig. 14 Magnetic methoxyphenyl triallyl-based catalytic dendrons with various generation and dendronization processes.^{149,150}

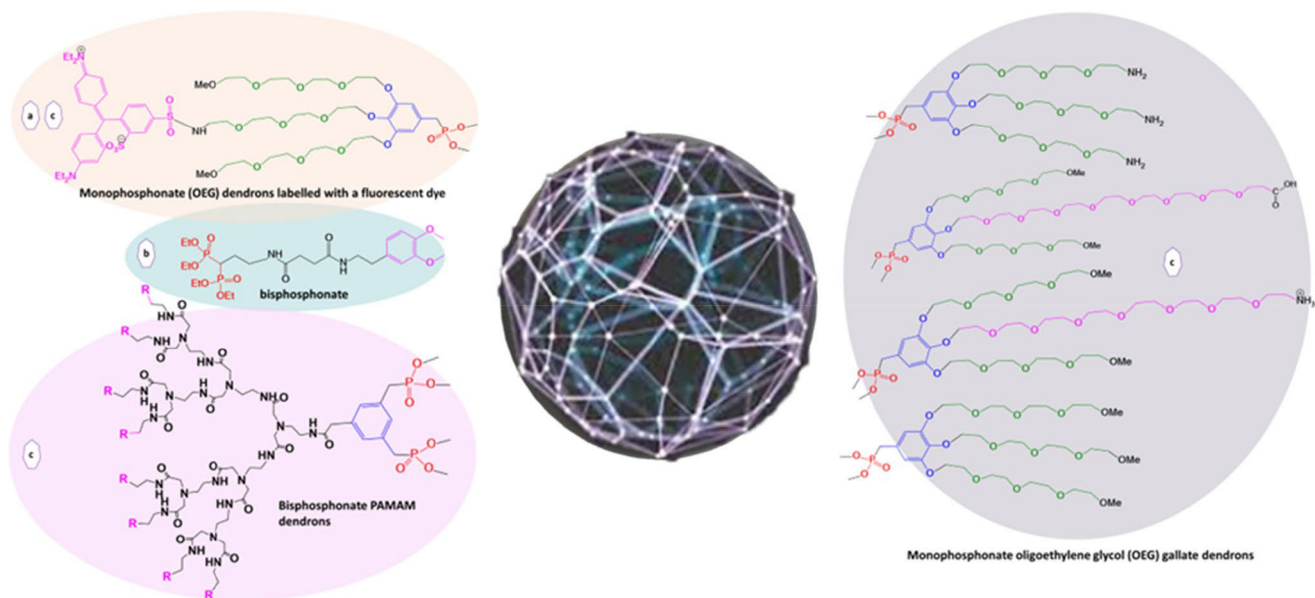


Fig. 15 Surface modification of MNPs with dendritic dopamine and bis-phosphonates (A) ref. 151, (B) ref. 154, (C) retro-syntheses of final dendritic phosphonic acids. (Phosphonic acids 2 and 3 bearing a longer and functional oligoethylene.)

5. Factors between MNPs and dendrimer

5.1 Preparation methods

Various methods can be used to prepare magnetic nanoparticles (MNPs) bound with dendrimers, each producing distinctive shapes and sizes. These include conventional techniques like reflux, stirring, and innovative methods like soni-

cation, hydrothermal synthesis, microwave-assisted synthesis, electrosynthesis, and ligand exchange. Sonication uses ultrasonic waves to generate pressure fluctuations in a solution of metal salts, dendrimers, and reducing agents, leading to dendrimer-bound MNPs. This method provides unique morphologies and sizes of nanoparticles^{75,77,82} (see TEM results in Fig. 17a). The hydrothermal process involves high temperatures and pressures in a sealed vessel to combine metal salts, dendrimers, reducing agents, and surfactants, creating dendri-

Table 14 Summarized details of Phosphonate-based dendrimers and dendrons with MNPs

Dendrimer generation/size	Dendrimer monomers core	Dendrimer terminal group	MNPs size	MNPs synthesis	MNPs pre-surface functionalization	Dendritic attachment approach	Bond type between MNPs & dendrimer	MNPs : dendrimer ratio	Dendritic MNPs post-surface modification	Targeted application	Ref.
G1	Dendritic-oligoethylene glycol gallate (OEG) dendrons	COOH -NH ₂	10 nm	Coprecipitation (within dendrimer)	—	Covalent bonding (grafting onto)	Mono-bis-phosphonate	—	—	Theranostics (cancer treatment)	151
—	monophosphonate Dendritic-PAMAM bisphosphonate Dopamine (DA) from (3-(3,4-bis(benzyloxy)phenethylcarbamoyl)propanoic acid) and tetraethyl 3-amino-propane-1,1-bisphosphonate Dendritic-oligoethylene glycol gallate (OEG) dendrons mono/bis-phosphonate	-OH -OMe PO ₃ Na ₂	—	Thermal decomposition Thermal decomposition	—	Grafting onto, sonication stabilization	Catechol/ MNP-O-DA- NH-bis (PO ₃ Na ₂)	2 mg ml ⁻¹ MNPs : 1 mg l ⁻¹	—	Remove Uranyl Ions from Water and Blood	154
—	—	NH ₂ , COOH	11.5 nm	Coprecipitation	—	Stabilization (dendron grafting onto)	Mono-bis-phosphonate	5 mg MNPs : 4 mg : dendron	Alexa 647	Multimodal imaging and biodistribution	155

mer-coated MNPs with functional groups^{79,107} (see Fig. 17b). Microwave-assisted synthesis accelerates reactions by heating the solution with microwave irradiation, enabling rapid preparation of dendrimer-bound MNPs with varied morphologies²⁴ (Fig. 17c). Electrosynthesis, applying an electric potential to a submerged electrode, deposits MNPs with dendrimers onto the substrate, offering precise control over nanoparticle shape and size.¹⁶¹ Finally, ligand exchange replaces original ligands on pre-synthesized MNPs with dendrimers containing functional groups, allowing for scalable and versatile synthesis such as oleic acid to different anchoring groups like catechol or catecholamine (dopamine),²¹ silane,^{22,41} carboxylate dendrimers,³⁶ or phosphonate¹² (Fig. 17d). These diverse methods reveal how preparation techniques shape the properties of dendrimer-functionalized MNPs for various applications.

5.2 Generation effect

The generation of dendrimers, which refers to the number of branching points repeated or propagated in the dendrimer structure, has a significant effect on the binding to MNPs due to the size and shape of the dendrimer. Typically, higher generation dendrimers have a larger size and greater number of functional groups, resulting in increased binding to the MNP surface. Dendrimers with higher generations tend to exhibit greater binding to MNPs due to the increased number of functional groups available for interaction. However, excessive dendrimer size and surface functionalization can lead to steric hindrance, limiting the number of dendrimers that can bind to the MNP surface. As the generation increases, the dendrimers' amino group content and steric hindrance also increase. This means that in order to ensure a complete reaction process, there is a need to increase the number of monomers (*e.g.*, MA, EDA) and reaction time.⁵¹ Moreover, the generation of dendrimers can also affect the distribution and orientation of dendrimers on the MNP surface,¹¹ which in turn can affect the properties of the resulting nanocomposites, such as stability, magnetic properties, and adsorption capacity.

To comprehend the behavior of MNPs after assembly with dendrimers, the magnetism of MNPs was studied. Superparamagnetism is a state wherein the thermal energy within a system surpasses the energy barrier that holds the magnetization of a particle in a specific direction. As the system undergoes cooling, thermal energy decreases while the energy barrier increases, causing the magnetization to align along the easy axis, thereby creating a net dipole. This process occurs at a temperature known as the blocking temperature, which is closely linked to the volume of the MNPs. Using small-angle X-ray scattering (SAXS), it was observed that the average spacing between particles in assemblies is dependent on the generation of PAMAM dendrimers employed, ranging from generation 1 to 6.5. By combining particles with different dendrimers, the spacing between them was increased by approximately 2.4 nm at the extremes. This structural manipulation led to a considerable shift of more than 50 K in the blocking temperature. In contrast to theoretical expectations of a uniform r^3 dependence between interparticle spacing and

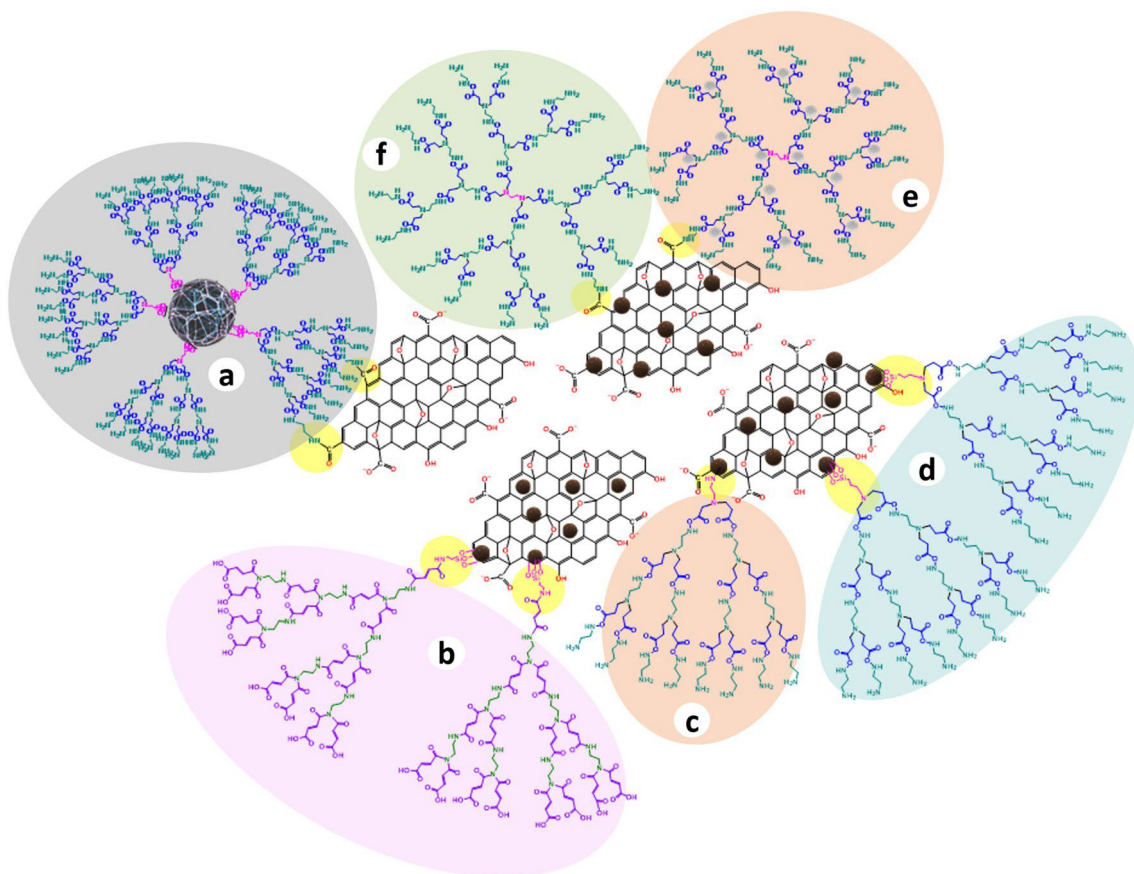


Fig. 16 Emerging magnetic graphene oxide with the dendritic systems (a) MNPs–PAMAM dendrimer was bound covalently as a whole system to the surface of graphene oxide sheet,¹⁵⁷ (b) PMAAM dendrimer was grafted from GO/MNPs using ethylenediamine and maleic anhydride as functional monomers,⁵² (c) PAMAM dendrimer was grafted from GO/MNPs using MA/EDA as the dendritic monomers (silane coupling agent was used for coordination for a, b & c systems,⁵¹ d) ref. 156, e and (f) grafting onto stabilization interaction between PAMAM and GO/MNPs through EDC/NHS carbodiimide bonding with encapsulation of Pd NPs in (e) ref. 159, (f) ref. 160.

blocking temperature, the collected data indicated two distinct regimes. Initially, there appeared to be an interdependence of approximately r^6 , followed by a significant leveling off at larger interparticle distances. Furthermore, when particles were assembled with the largest dendrimer, their magnetic behavior mirrored that of particles free of magnetic interactions. This suggests that the assembled particles were completely decoupled within the dense aggregate.¹¹

The optimal generation of dendrimers for binding to MNPs and achieving good stability with functionality depends on several factors, including the size and surface properties of the MNPs, the desired functionalization, and the specific application. In general, lower generation dendrimers (such as G1 or G2) tend to have better stability with MNPs due to their smaller size and lower number of functional groups, which can reduce steric hindrance and increase the accessibility of functional groups for interaction with the MNP surface. However, lower generation dendrimers may have lower functionalization capacity and weaker binding strength to the MNP surface, which may limit their use in certain applications. On the other hand, higher generation dendrimers

(such as G4 or G5) may offer better functionalization capacity and stronger binding to the MNP surface due to their larger size and higher number of functional groups. However, the steric hindrance and crowding effects can lead to reduced stability and aggregation of the resulting nanocomposites. Therefore, the optimal generation of dendrimer for binding to MNPs and achieving good stability with functionality depends on a careful balance between these factors, as well as the specific requirements of the intended application. A systematic evaluation of the dendrimer–MNP architecture is needed to identify the optimal dendrimer generation and surface functionalization for achieving the desired stability, functionality, and performance.

5.3 pH effect on binding mode and shape of dendrimers coating

The pH value has a significant effect on the shape and conformation of dendrimers and their binding modes with MNPs in terms of coating and functionality. At different pH values, the protonation or deprotonation of functional groups on the dendrimer surface can affect the electrostatic interactions, hydro-

Table 15 Magnetic graphene oxide with various type of dendrimer and dendritic interactions

Dendrimer generation/size	Dendrimer monomers	Dendrimer core	Dendrimer terminal group	MNPs synthesis	MNPs pre-surface functionalization	Dendritic attachment approach	Bond type between MNPs & dendrimer	MNPs : dendrimer ratio	Dendritic MNPs post-surface modification	Targeted application	Ref.
PAMAM G0.5-G4	Ethylenediamine (EDA), methyl acrylate (MA)	GO@MNP@NH (GO)	NH ₂	One-pot solvothermal method (loading MNPs on the surface of graphene oxide GO)	EDA	Grafting from assembly	GO@MNps@NH ₂	—	—	Removal of Hg (ii)	51
Polymaleicamide (PMAAM) G3.5	Maleic anhydride (MAH), ethanediamine (EDA)	GO@MNP@Si-NH (GO)	COOH	Inverse coprecipitation	(3-Aminopropyl) triethoxysilane	Grafting from assembly	GO@MNps@Si-NH ₂	—	—	Removal of Pb (ii)	52
PAMAM G3	Ethylenediamine (EDA), methyl acrylate (MA)	GO@MNP@Si-NH (GO)	NH ₂	Coprecipitation	GO-(3-aminopropyl) triethoxysilane (APTES)	Grafting from assembly	GO@MNps@Si-NH ₂	—	—	Sorbent of the synthetic dyes tartrazine, quinoline yellow, sunset yellow and carmoisine	156
PAMAM G2	Ethylenediamine (EDA), methyl acrylate (MA)	EDA	NH ₂	Coprecipitation <i>in situ</i> with GO	1-Ethyl-3-(3-dimethylaminopropyl) carbodiimide hydrochloride (EDC) and <i>N</i> -hydroxysuccinimide (NHS) EDC/NHS	Grafting onto stabilization	Carbodiimide	150.0 mg of GO-MNPs : 1.5 mL PAMAM	—	Carbon electrode (GCE) coating for simultaneous detection of Pb (ii) and Cd(ii) in environmental waters	160
PAMAM G2	Ethylenediamine (EDA), methyl acrylate (MA)	MNP@Si-NH ₂	NH ₂	Coprecipitation	-(3-Aminopropyl) triethoxysilane (APTES)	Grafting from (PAMAM on MNPs), grafting onto (on GO)	MNPs@PAMAM-G2.0@GO	—	—	Electrochemical sensor for the determination of H ₂ O ₂ in real water samples	159
										Magnetic solid phase extraction (MSPE) of polycyclic aromatic hydrocarbons (PAHs) from water	157

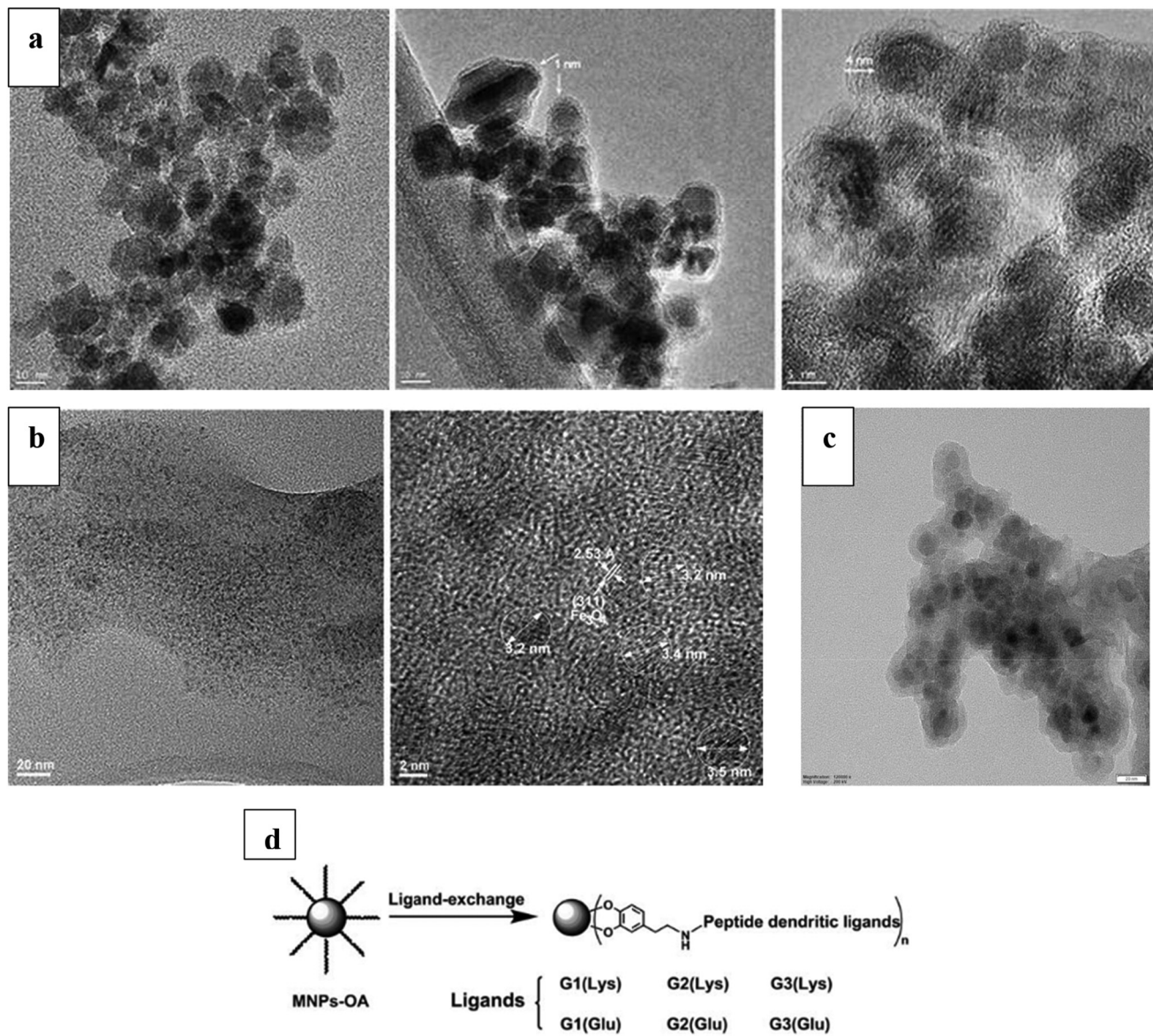


Fig. 17 (a) PAMAM Dendrimer G7 coated on MNPs *via* sonication process,⁷⁷ (b) HRTEM images of MNPs with PAMAM-SAH G4 *via* hydrothermal process,⁷⁹ (c) microwave assisted synthesis of PAMAM-MNPs (HRTEM image of Fe₃O₄).

gen bonding, and steric hindrance, leading to changes in the shape and charge density of the dendrimer. At low pH values, the negatively charged groups on the dendrimer surface are protonated, resulting in a positive charge and increased electrostatic repulsion between the dendrimer branches. This repulsion leads to a more extended conformation of the dendrimer, exposing more functional groups for interaction with the MNP surface. The positively charged dendrimer can also electrostatically interact with the negatively charged MNP surface, resulting in a stable coating and enhanced functionality. In contrast, at high pH values, the carboxylic acid groups on the dendrimer surface are deprotonated, resulting in a negative charge and increased electrostatic attraction between the dendrimer branches. This attraction leads to a more compact conformation of the dendrimer, reducing the accessi-

bility of functional groups for interaction with the MNP surface. The negatively charged dendrimer can also electrostatically repel the negatively charged MNP surface, resulting in reduced coating stability and functionality. Moreover, the pH value can also affect the binding modes between dendrimers and MNPs through coordination interactions. For example, at low pH values, the protonation of amino groups on the dendrimer surface can enhance the coordination of metal ions on the MNP surface, leading to a higher binding capacity and selectivity for metal ion removal. As the pH value plays a critical role in determining the shape and charge density of dendrimers and their binding modes with MNPs in terms of coating and functionality, the optimal pH value for dendrimer-MNP interaction depends on the specific application and the desired properties of the resulting nano-

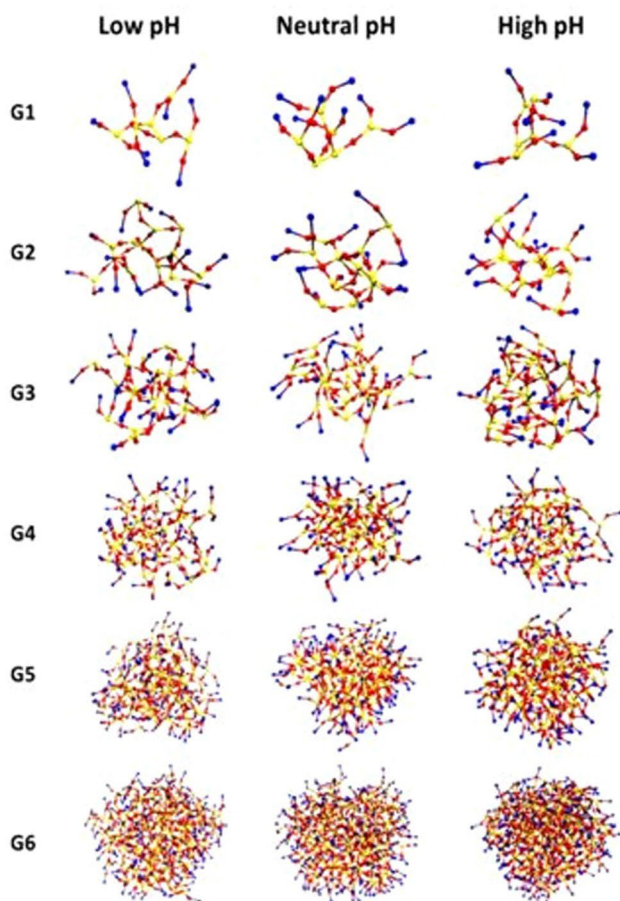


Fig. 18 Effect of pH on dendrimer charge at different generations^{162,163} copy rights.

composites (biomedical systems, water treatment, *etc.*). A summary of this section is represented in Fig. 18.

5.4 Doping and intervention of MNPs

In modern nanomaterial research, the functionalization of dendrimers with MNPs is profoundly influenced by strategic changes in the chemical composition and structural configurations of MNPs. Notably, doping these nanoparticles with various metal ions substantially modifies their intrinsic magnetic properties, which is pivotal for enhancing their interaction with dendrimers. Aptamer-dendrimer functionalized magnetic nano-octahedrons were utilized in which doping provided notable enhancements in drug and gene delivery capacities alongside improved contrasts in near-infrared and magnetic resonance imaging modalities.¹⁶⁴ Furthermore, Bhalla *et al.* (2021) demonstrated that the doping of spinel ferrites could effectively tune their magnetic and plasmonic properties without altering the work function, thus maintaining stable band gaps with customized plasmonic responses.¹⁶⁵ Additionally, the inversion number in ferrites, which dictates the cation distribution within the crystal lattice, directly impacts the magnetic properties and consequently, the surface characteristics essential for dendrimer functionalization.

These changes in the inversion number are critical as they influence the overall effectiveness of dendrimer-MNP conjugates in various applications, ranging from targeted therapeutic delivery to advanced imaging techniques. Through such structural modifications, the functional properties of MNPs can be meticulously tailored, enhancing their utility across a spectrum of biomedical and technological applications.

5.5 Potential functionality groups

The potential functionalities attached to the conjugated MNPs-Dendrimer have a great impact on the application due to differences in the size, shape, charge, and functional groups of the MNP-dendrimer. The size and shape of MNPs-dendrimers can influence the accessibility and density of functional groups on the dendrimer surface. Larger dendrimers, such as higher generation dendrimers, may have more functional groups, resulting in higher binding capacity and functionalization. The functional groups on dendrimers can play a crucial role in their binding and functionalization of MNPs. Dendrimers with functional groups such as carboxylate, amine, and thiol groups can bind to the surface of MNPs through coordination or electrostatic interactions, resulting in stable coatings and functionalization. Additionally, dendrimers with functional groups such as hydroxyl, epoxy, and alkyl groups can provide sites for further functionalization with other molecules, enhancing their functionality. In general, the choice of dendrimer type can impact the binding and functionalization of MNPs through several mechanisms. Moreover, surface modification of dendrimer-coated MNPs with various molecules can enhance their stability, biocompatibility, targeting, imaging, or therapeutic properties for various applications. Some of the commonly used molecules for surface modification of dendrimer-coated MNPs are discussed in Table 16.

6. Research limitations and challenges

Coordinating MNPs with dendrimers involves several challenges, including surface reactivity, size mismatches, steric hindrance, stability and aggregation issues, compatibility of surface functional groups, controlled conjugation, and concerns over biocompatibility and toxicity. MNPs like magnetite and maghemite have reactive surfaces prone to oxidation, complicating stable dendrimer conjugation. Matching the sizes of nanoscale MNPs and larger macromolecular dendrimers is difficult, affecting efficient conjugation and stability. Dendrimers' densely packed functional groups can cause steric hindrance, limiting surface coverage and attachment. MNPs' tendency to aggregate, exacerbated by dendrimer presence, can hinder their application in magnetic targeting or imaging. Achieving compatibility and controlled arrangement of dendrimers on MNPs is crucial for desired functionalities but challenging due to competing functional groups. Finally, ensuring biocompatibility and safety of these conjugates for biological applications is critical, as both MNPs and dendri-

Table 16 Terminal group functionalities and active sites

Potential functionalization	Examples	Application	Ref.		
Polymers	Polyethyleneimine (PEI)	Enhancement of transfection efficiency	90 110		
	Polyethylene glycol (PEG)	Increase of stability and biocompatibility	17 78		
	Chitosan (DGEBA) epoxy resin	Amphoteric adsorption and biocompatibility Improving thermal and mechanical properties of resin network	93 82		
Peptides	RGD peptides Gold binding peptides	Specific target binding	39 10		
Aptamers	DNA & RNA	Gene editing and targeting	90 14, 95, 111 and 112		
Fluorescent dyes	Fluorescein isothiocyanate (FITC)	Fluorescent reporters for potential MRI contrast enhancement	57 and 71 41 166 88 and 120 28		
	Carboxytetramethylrhodamine (TAMRA). With coumarin 6				
Protective molecules	Fluorenyl methoxycarbonyl (Fmoc) Tertbutoxycarbonyl (Boc)	Control of the branching degree and the dendrimer size	18 and 28 21 and 151 151		
	<i>tert</i> -Butyl (tBu) ether Gold nanoparticles	Electrical conductivity	23 34 8		
Metal ions	Silver ions and NPs Palladium Pd	Catalytic reactions Catalytic activities	44 34 50, 138 and 140–142 73		
	Titanium oxides (TiO ₂) Zinc doped	Photocatalysts			
Small molecules	Drugs Dithiocarbamate (DTC) Doxorubicin hydrochloride (DOX) Niclosamide Rosuvastatin (RST; Crestor) Methotrexate (MTX) Beta naphthol	Targeted drug delivery	167 17, 77 and 168 28 and 131 169 22 and 120 98		
		Others Murexide	Metallochromic indicator, effective scavenger for hydroxyl and radical superoxides	47	
			Precious metal targeting and adsorption	76	
			Folic acid	Receptor-mediated (or active) targeted imaging of tumor cells	41, 57 and 71
		Temperature sensitive conjugates	Isopropylacrylamide (NIPAM)	Thermo-response	170 171
		Antibodies	Carbohydrate antigen-125 (CA125)	Immuno-sensing probes	58

mers may exhibit toxicological properties, requiring careful testing and consideration.

7. Future directions

In the field of MNPs coordination of with dendrimers, several areas of future work can be explored. Here are some potential directions:

- **Enhanced stability and control:** Developing strategies to improve the stability of conjugated MNPs and achieve better control over the surface coverage and spatial arrangement of dendrimers. This can involve designing new dendrimers with specific functionalities or modifying the surface of MNPs to enhance stability and prevent aggregation.

- **Surface engineering and multifunctionality:** Exploring advanced surface engineering techniques to introduce mul-

iple functionalities onto the surface of MNPs conjugated with dendrimers. This may include incorporating targeting ligands, therapeutic agents, imaging probes, or stimuli-responsive moieties to enable multifunctional properties, such as targeted drug delivery, imaging, or controlled release.

- **Biocompatibility and toxicity assessment:** Conducting comprehensive studies to evaluate the biocompatibility and potential toxicity of dendrimer–MNPs. This involves in-depth investigations into their interactions with biological systems, including cellular uptake, biodistribution, and long-term effects. The goal is to develop safe and biocompatible nanomaterials for various biomedical applications.

- ***In vivo* applications:** Advancing the translation of dendrimer–conjugated MNPs into practical *in vivo* applications. This includes preclinical and clinical studies to assess their efficacy and safety in targeted drug delivery, magnetic resonance imaging (MRI), hyperthermia therapy, and other biomedical

applications. Optimizing the properties and functionalities of these nanoparticles for specific disease targets can significantly impact their clinical potential.

- Scalability and manufacturing: Developing scalable and cost-effective manufacturing methods for dendrimer-conjugated MNPs. The ability to produce these coordinated nanoparticles in large quantities while maintaining their desired properties is crucial for their widespread use and commercial viability.

- Novel dendrimer designs: There is a huge potential of designing and synthesizing dendrimers with tailored properties specifically for conjugation to MNPs. This may involve exploring new dendrimer architectures, functional groups, or surface modification strategies to optimize the conjugation process, improve stability, and enable new functionalities.

- Integration with other nanomaterials: Investigating the integration of dendrimer-conjugated MNPs with other nanomaterials or nanosystems, such as liposomes, polymers, or carbon nanomaterials. Synergistic combinations of different nanomaterials can lead to enhanced properties and functionalities, expanding the potential applications in areas like therapeutics (therapy and diagnostics combined).

8. Conclusion

The process of functionalization of MNPs and conjugation with dendrimers is a promising approach for efficient and effective utilization in various applications. Dendrimers provide stability and functionalization sites for targeted applications such as adsorption, catalytic activities, sensing, imaging, and superparamagnetic properties, while also allowing for control over the size and surface chemistry of the resulting magnetic nanocomposites. The underlying mechanisms of coordination and conjugation involve electrostatic interactions, covalent bonding, and hydrophobic interactions. Despite the potential benefits of dendrimer-conjugated MNPs, there are still challenges that need to be addressed. These challenges include the potential toxicity of dendrimers, the complex interplay between dendrimer size and MNP surface area, and the difficulty in controlling dendrimer distribution and orientation on the MNP surface. To overcome these challenges, the use of biocompatible dendrimers and advanced characterization techniques is recommended. The insights provided by this review paper will be valuable for researchers working on the development and application of dendrimer-MNPs systems. Further research is required to optimize and develop new dendrimer-MNP architectures and to unlock the full potential of these nanocomposites in environmental remediation, catalysis industry, water treatment, and biomedical and therapeutic fields.

Conflicts of interest

There are no conflicts of interest to declare.

Acknowledgements

The authors gratefully acknowledge the financial support provided by Qatar Research Development and Innovation (QRDI), research grant (MME03-1015-210003). One of the authors would like to thank Qatar University for the support provided through the Graduate Assistantship program.

References

- 1 A. H. Lu, E. L. Salabas and F. Schüth, *Angew. Chem., Int. Ed.*, 2007, 46, 1222–1244.
- 2 M. J. Ansari, M. M. Kadhim, B. A. Hussein, H. A. Lafta and E. Kianfar, *Bionanoscience*, 2022, 12, 627–638.
- 3 M. Salehipour, S. Rezaei, J. Mosafer, Z. Pakdin-Parizi, A. Motaharian and M. Mogharabi-Manzari, *J. Nanopart. Res.*, 2021, 23, 48.
- 4 F. Chen, N. Haddour, M. Frenea-Robin, Y. Chevolut and V. Monnier, *ChemistrySelect*, 2018, 3, 2823–2829.
- 5 M. S. Gruzdev, U. V. Chervonova, V. E. Vorobeva, A. A. Ksenofontov and A. M. Kolker, *RSC Adv.*, 2019, 9, 22499–22512.
- 6 I. N. Kurniasih, J. Keilitz and R. Haag, *Chem. Soc. Rev.*, 2015, 44, 4145–4164.
- 7 X. Wu, X. He, L. Zhong, S. Lin, D. Wang, X. Zhu and D. Yan, *J. Mater. Chem.*, 2011, 21, 13611–13620.
- 8 T. Fernandes, N. C. T. Martins, A. L. Daniel-da-Silva and T. Trindade, *Spectrochim. Acta, Part A*, 2022, 283, 121730.
- 9 S. Zhang, Y. Zhang, J. Liu, Q. Xu, H. Xiao, X. Wang, H. Xu and J. Zhou, *Chem. Eng. J.*, 2013, 226, 30–38.
- 10 W.-Z. Shen, S. Cetinel, K. Sharma, E. R. Borujeny and C. Montemagno, *J. Nanopart. Res.*, 2017, 19, 74.
- 11 B. L. Frankamp, A. K. Boal, M. T. Tuominen and V. M. Rotello, *J. Am. Chem. Soc.*, 2005, 127, 9731–9735.
- 12 D. Nordmeyer, P. Stumpf, D. Gröger, A. Hofmann, S. Enders, S. B. Riese, J. Dervede, M. Taupitz, U. Rauch, R. Haag, E. Rühl and C. Graf, *Nanoscale*, 2014, 6, 9646–9654.
- 13 M. H. Beyki, F. Feizi and F. Shemirani, *React. Funct. Polym.*, 2016, 103, 81–91.
- 14 Y. Zhou, Z. Tang, C. Shi, S. Shi, Z. Qian and S. Zhou, *J. Mater. Sci. Mater. Med.*, 2012, 23, 2697–2708.
- 15 J. Yang, Y. Luo, Y. Xu, J. Li, Z. Zhang, H. Wang, M. Shen, X. Shi and G. Zhang, *ACS Appl. Mater. Interfaces*, 2015, 7, 5420–5428.
- 16 J. Chang, Z. Zhong, H. Xu, Z. Yao and R. Chen, *Chin. J. Chem. Eng.*, 2013, 21, 1244–1250.
- 17 S. Nigam, S. Chandra, D. F. Newgreen, D. Bahadur and Q. Chen, *Langmuir*, 2014, 30, 1004–1011.
- 18 S. Nigam and D. Bahadur, *Colloids Surf., B*, 2017, 155, 182–192.
- 19 B. Lesiak, N. Rangam, P. Jiricek, I. Gordeev, J. Tóth, L. Kövér, M. Mohai and P. Borowicz, *Front. Chem.*, 2019, 7, 642.
- 20 A. Boni, L. Albertazzi, C. Innocenti, M. Gemmi and A. Bifone, *Langmuir*, 2013, 29, 10973–10979.

- 21 R. Zhu, W. Jiang, Y. Pu, K. Luo, Y. Wu, B. He and Z. Gu, *J. Mater. Chem.*, 2011, 21, 5464.
- 22 M. Li, K. G. Neoh, R. Wang, B. Y. Zong, J. Y. Tan and E. T. Kang, *Eur. J. Pharm. Sci.*, 2013, 48, 111–120.
- 23 E. Murugan and J. N. Jebaranjitham, *Chem. Eng. J.*, 2015, 259, 266–276.
- 24 K. Lakshmi and R. Rangasamy, *J. Mol. Struct.*, 2021, 1224, 129081.
- 25 W. Xie, Y. Xiong and H. Wang, *Renewable Energy*, 2021, 174, 758–768.
- 26 D. K. Kim and J. W. Lee, *J. Korean Ceram. Soc.*, 2018, 55, 625–634.
- 27 T. Hyeon, S. S. Lee, J. Park, Y. Chung and H. Bin Na, *J. Am. Chem. Soc.*, 2001, 123, 12798–12801.
- 28 P. Parlanti, A. Boni, G. Signore and M. Santi, *Molecules*, 2020, 25, 2252.
- 29 A. Boni, G. Bardi, A. Bertero, V. Cappello, M. Emdin, A. Flori, M. Gemmi, C. Innocenti, L. Menichetti, C. Sangregorio, S. Villa and V. Piazza, *Nanoscale*, 2015, 7, 7307–7317.
- 30 A. Walter, A. Garofalo, A. Parat, H. Martinez, D. Felder-Flesch and S. Begin-Colin, *Nanotechnol. Rev.*, 2015, 4, 581–593.
- 31 X. Shi, T. P. Thomas, L. A. Myc, A. Kotlyar and J. R. Baker Jr., *Phys. Chem. Chem. Phys.*, 2007, 9, 5712.
- 32 D. Niculaes, A. Lak, G. C. Anyfantis, S. Marras, O. Laslett, S. K. Avugadda, M. Cassani, D. Serantes, O. Hovorka, R. Chantrell and T. Pellegrino, *ACS Nano*, 2017, 11, 12121–12133.
- 33 A. N. Avan, S. Demirci-Çekiç and R. Apak, *ACS Omega*, 2022, 7, 44372–44382.
- 34 E. Murugan, J. Nimita, M. Ariraman, S. Rajendran, J. Kathirvel, C. R. Akshata and K. Kumar, *ACS Omega*, 2018, 3, 13685–13693.
- 35 A. Pourjavadi, A. Abedin-Moghanaki and S. H. Hosseini, *Int. J. Environ. Sci. Technol.*, 2016, 13, 2437–2448.
- 36 X. He, X. Wu, X. Cai, S. Lin, M. Xie, X. Zhu and D. Yan, *Langmuir*, 2012, 28, 11929–11938.
- 37 K. Lakshmi and R. Rangasamy, *J. Mol. Struct.*, 2021, 1224, 129081.
- 38 V. Švorčík, K. Kolářová, P. Slepíčka, A. Macková, M. Novotná and V. Hnatowicz, *Polym. Degrad. Stab.*, 2006, 91, 1219–1225.
- 39 J. Yang, Y. Luo, Y. Xu, J. Li, Z. Zhang, H. Wang, M. Shen, X. Shi and G. Zhang, *ACS Appl. Mater. Interfaces*, 2015, 7, 5420–5428.
- 40 T. Jafari, A. Simchi and N. Khakpash, *J. Colloid Interface Sci.*, 2010, 345, 64–71.
- 41 L. Wang, K. G. Neoh, E.-T. Kang and B. Shuter, *Biomaterials*, 2011, 32, 2166–2173.
- 42 M. Mirzaie, A. Rashidi, H. A. Tayebi and M. E. Yazdanshenas, *J. Chem. Eng. Data*, 2017, 62, 1365–1376.
- 43 S. Aliannejadi, A. H. Hassani, H. A. Panahi and S. M. Borghei, *Microchem. J.*, 2019, 145, 767–777.
- 44 U. Kurtan and A. Baykal, *Mater. Res. Bull.*, 2014, 60, 79–87.
- 45 D. Chen, T. Awut, B. Liu, Y. Ma, T. Wang and I. Nurulla, *e-Polym.*, 2016, 16, 313–322.
- 46 Y. Tong, Q. Zhou, Y. Sun, X. Sheng, B. Zhou, J. Zhao and J. Guo, *Talanta*, 2021, 224, 121884.
- 47 S. Ekinci, Z. İlter, S. Ercan, E. Çınar and R. Çakmak, *Heliyon*, 2021, 7, e06600.
- 48 Y. Yuan, Y. Wu, H. Wang, Y. Tong, X. Sheng, Y. Sun, X. Zhou and Q. Zhou, *J. Hazard. Mater.*, 2020, 386, 121658.
- 49 E. Esmaeili, M. Khalili, A. N. Sohi, S. Hosseinzadeh, B. Taheri and M. Soleimani, *J. Cell. Physiol.*, 2019, 234, 12615–12624.
- 50 S. A. Sorokina, N. V. Kuchkina, B. P. Lawson, I. Y. Krasnova, N. A. Nemygina, L. Z. Nikoshvili, V. N. Talanova, B. D. Stein, M. Pink, D. G. Morgan, E. M. Sulman, L. M. Bronstein and Z. B. Shifrina, *Appl. Surf. Sci.*, 2019, 488, 865–873.
- 51 Y. X. Ma, D. Xing, W. J. Shao, X. Y. Du and P. Q. La, *J. Colloid Interface Sci.*, 2017, 505, 352–363.
- 52 Y. X. Ma, Y. L. Kou, D. Xing, P. S. Jin, W. J. Shao, X. Li, X. Y. Du and P. Q. La, *J. Hazard. Mater.*, 2017, 340, 407–416.
- 53 L. Wang, K. G. Neoh, E. T. Kang, B. Shuter and S. C. Wang, *Adv. Funct. Mater.*, 2009, 19, 2615–2622.
- 54 H.-R. Kim, J.-W. Jang and J.-W. Park, *J. Hazard. Mater.*, 2016, 317, 608–616.
- 55 P. Parlanti, A. Boni, G. Signore and M. Santi, *Molecules*, 2020, 25, 2252.
- 56 D. Rosario-Amorin, M. Gaboyard, R. Clérac, L. Vellutini, S. Nlate and K. Heuzé, *Chem. – Eur. J.*, 2012, 18, 3305–3315.
- 57 X. Shi, S. H. Wang, S. D. Swanson, S. Ge, Z. Cao, M. E. Van Antwerp, K. J. Landmark and J. R. Baker, *Adv. Mater.*, 2008, 20, 1671–1678.
- 58 X.-H. Fu, *Anal. Lett.*, 2010, 43, 455–465.
- 59 L. M. Bronstein and Z. B. Shifrina, *Chem. Rev.*, 2011, 111, 5301–5344.
- 60 B. Hayati, A. Maleki, F. Najafi, H. Daraei, F. Gharibi and G. McKay, *J. Hazard. Mater.*, 2017, 336, 146–157.
- 61 X. Zhang, Y. Dai and G. Dai, *Polym. Chem.*, 2020, 11, 964–973.
- 62 F. Zhao and W. Li, *Sci. China: Chem.*, 2011, 54, 286–301.
- 63 X. Peng, Q. Pan and G. L. Rempel, *Chem. Soc. Rev.*, 2008, 37, 1619.
- 64 N. E. Domracheva, V. I. Morozov, M. S. Gruzdev, R. A. Manapov, A. V. Pyataev and G. Lattermann, *Macromol. Chem. Phys.*, 2010, 211, 791–800.
- 65 T. Lu, Y. Wu, C. Zhao, F. Su, J. Liu, Z. Ma and Q. Han, *Mater. Sci. Eng., C*, 2018, 93, 838–845.
- 66 Y. Shi, J. Du, L. Zhou, X. Li, Y. Zhou, L. Li, X. Zang, X. Zhang, F. Pan, H. Zhang, Z. Wang and X. Zhu, *J. Mater. Chem.*, 2012, 22, 355–360.
- 67 C. Zhao, Q. Han, H. Qin, H. Yan, Z. Qian, Z. Ma, X. Zhang and X. Li, *J. Biomater. Sci., Polym. Ed.*, 2017, 28, 616–628.
- 68 N. E. Domracheva, V. E. Vorobeveva, M. S. Gruzdev, Y. N. Shvachko and D. V. Starichenko, *Inorg. Chim. Acta*, 2017, 465, 38–43.

- 69 M. S. Gruzdev, A. G. Ramazanova, V. V. Korolev, U. V. Chervonova, O. V. Balmasova and A. M. Kolker, *Russ. J. Inorg. Chem.*, 2020, 65, 640–645.
- 70 V. V. Korolev, M. S. Gruzdev, A. G. Ramazanova, O. V. Balmasova and U. V. Chervonova, *Liq. Cryst.*, 2021, 48, 588–597.
- 71 S. H. Wang, X. Shi, M. Van Antwerp, Z. Cao, S. D. Swanson, X. Bi and J. R. Baker, *Adv. Funct. Mater.*, 2007, 17, 3043–3050.
- 72 S. L. Zhou, J. Li, G. B. Hong and C. T. Chang, *J. Nanosci. Nanotechnol.*, 2013, 13, 6814–6819.
- 73 L.-J. Kim, J.-W. Jang and J.-W. Park, *Appl. Catal., B*, 2014, 147, 973–979.
- 74 C.-M. Chou and H.-L. Lien, *J. Nanopart. Res.*, 2011, 13, 2099–2107.
- 75 R. Khodadust, G. Unsoy, S. Yalcin, G. Gunduz and U. Gunduz, *J. Nanopart. Res.*, 2013, 15, 1488.
- 76 C.-H. Yen, H.-L. Lien, J.-S. Chung and H.-D. Yeh, *J. Hazard. Mater.*, 2017, 322, 215–222.
- 77 K. Rouhollah, M. Pelin, Y. Serap, U. Gozde and G. Ufuk, *J. Pharm. Sci.*, 2013, 102, 1825–1835.
- 78 M. Salimi, S. Sarkar, M. Hashemi and R. Saber, *Nanomaterials*, 2020, 10, 2310.
- 79 M. A. Deriu, L. M. Popescu, M. F. Ottaviani, A. Danani and R. M. Piticescu, *J. Mater. Sci.*, 2016, 51, 1996–2007.
- 80 S. Chandra, M. D. Patel, H. Lang and D. Bahadur, *J. Power Sources*, 2015, 280, 217–226.
- 81 A. Hassanein, M. Hafiz, M. K. Hassan, M. M. Ba-Abbad, M. AL-Ejji, R. Alfahel, K. A. Mahmoud, M. Talhami and A. H. Hawari, *Desalination*, 2023, 564, 116800.
- 82 F. Jafari-Soghieh, B. Maleki and H. Behniafar, *High Perform. Polym.*, 2019, 31, 24–31.
- 83 G. Chizari Fard, M. Mirjalili, A. Almasian and F. Najafi, *J. Taiwan Inst. Chem. Eng.*, 2017, 80, 156–167.
- 84 F. Chen, N. Haddour, M. Frenea-Robin, Y. Chevolut and V. Monnier, *ChemistrySelect*, 2018, 3, 2823–2829.
- 85 I. Hussain, N. Muhammad, Q. Subhani, D. Shou, M. Jin, L. Yu, G. Lu, X. Wen, A. Intisar and Z. Yan, *TrAC, Trends Anal. Chem.*, 2022, 157, 116810.
- 86 A. Zarei, S. Saedi and F. Seidi, *J. Inorg. Organomet. Polym. Mater.*, 2018, 28, 2835–2843.
- 87 S. F. Kokaz, P. K. Deb, P. Borah, R. Bania, K. N. Venugopala, A. B. Nair, V. Singh, N. A. Al-Shar'i, W. Hourani, G. Gupta and R. K. Tekade, *Nanoeng. Biomater.*, 2022, 215–243.
- 88 B. Pan, D. Cui, Y. Sheng, C. Ozkan, F. Gao, R. He, Q. Li, P. Xu and T. Huang, *Cancer Res.*, 2007, 67, 8156–8163.
- 89 A. Mashhadi Malekzadeh, A. Ramazani, S. J. Tabatabaei Rezaei and H. Niknejad, *J. Colloid Interface Sci.*, 2017, 490, 64–73.
- 90 W.-M. Liu, Y.-N. Xue, N. Peng, W.-T. He, R.-X. Zhuo and S.-W. Huang, *J. Mater. Chem.*, 2011, 21, 13306.
- 91 A. Pourjavadi, S. H. Hosseini, S. T. Hosseini and S. A. Aghayeemeibody, *Catal. Commun.*, 2012, 28, 86–89.
- 92 P. Wang, Q. Ma, D. Hu and L. Wang, *React. Funct. Polym.*, 2015, 91–92, 43–50.
- 93 H. R. Kim, J. W. Jang and J. W. Park, *J. Hazard. Mater.*, 2016, 317, 108–116.
- 94 R. M. Triano, M. L. Paccagnini and A. M. Balija, *SpringerPlus*, 2015, 4, 511.
- 95 X. Liang, Y. Ge, Z. Wu and W. Qin, *J. Chem. Technol. Biotechnol.*, 2017, 92, 819–826.
- 96 M. R. Knecht and R. M. Crooks, *New J. Chem.*, 2007, 31, 1349–1353.
- 97 V. Khatibikamal, H. A. Panahi, A. Torabian and M. Baghdadi, *Microchem. J.*, 2019, 145, 508–516.
- 98 A. Torabian, H. Ahmad Panahi, G. R. Nabi Bid Hendi and N. Mehrdadi, *J. Environ. Health Sci. Eng.*, 2014, 12, 105.
- 99 H. Bagheri, M. Manouchehri and M. Allahdadlalouni, *Microchim. Acta*, 2017, 184, 2201–2209.
- 100 S. Ekinci, Z. İlter, S. Ercan, E. Çınar and R. Çakmak, *Heliyon*, 2021, 7, e06600.
- 101 K.-J. Kim and J.-W. Park, *J. Mater. Sci.*, 2017, 52, 843–857.
- 102 S. L. Zhou, J. Li, G.-B. Hong and C.-T. Chang, *J. Nanosci. Nanotechnol.*, 2013, 13, 6814–6819.
- 103 Z. Y. Wang, J. B. Xie, Y. G. Wang and Y. Li, *Sci. Rep.*, 2020, 10, 5396.
- 104 B. González, E. Ruiz-Hernández, M. J. Feito, C. López De Laorden, D. Arcos, C. Ramírez-Santillán, C. Matesanz, M. T. Portolés and M. Vallet-Regí, *J. Mater. Chem.*, 2011, 21, 4598–4604.
- 105 N. E. Domracheva, A. V. Pyataev, R. A. Manapov and M. S. Gruzdev, *ChemPhysChem*, 2011, 12, 3009–3019.
- 106 J. Li, L. Zheng, H. Cai, W. Sun, M. Shen, G. Zhang and X. Shi, *Biomaterials*, 2013, 34, 8382–8392.
- 107 H. Cai, X. An, J. Cui, J. Li, S. Wen, K. Li, M. Shen, L. Zheng, G. Zhang and X. Shi, *ACS Appl. Mater. Interfaces*, 2013, 5, 1722–1731.
- 108 M. Ortega-Muñoz, S. Plesselova, A. V. Delgado, F. Santoyo-Gonzalez, R. Salto-Gonzalez, M. D. Giron-Gonzalez, G. R. Iglesias and F. J. López-Jaramillo, *Polymers*, 2021, 13, 1599.
- 109 H. Zhao, C. Zhang, D. Qi, T. Lü and D. Zhang, *J. Dispersion Sci. Technol.*, 2019, 40, 231–238.
- 110 S. S. Rohiwal, N. Dvorakova, J. Klima, M. Vaskovicova, F. Senigl, M. Slouf, E. Pavlova, P. Stepanek, D. Babuka, H. Benes, Z. Ellederova and K. Stieger, *Sci. Rep.*, 2020, 10, 4619.
- 111 J. W. Park, K. H. Bae, C. Kim and T. G. Park, *Biomacromolecules*, 2011, 12, 457–465.
- 112 G. Liu, J. Xie, F. Zhang, Z. Wang, K. Luo, L. Zhu, Q. Quan, G. Niu, S. Lee, H. Ai and X. Chen, *Small*, 2011, 7, 2742–2749.
- 113 Y. Shi, J. Du, L. Zhou, X. Li, Y. Zhou, L. Li, X. Zang, X. Zhang, F. Pan, H. Zhang, Z. Wang and X. Zhu, *J. Mater. Chem.*, 2012, 22, 355–360.
- 114 M. S. Draz, B. A. Fang, P. Zhang, Z. Hu, S. Gu, K. C. Weng, J. W. Gray and F. F. Chen, *Theranostics*, 2014, 4, 872–892.
- 115 H. Cai, X. An, J. Cui, J. Li, S. Wen, K. Li, M. Shen, L. Zheng, G. Zhang and X. Shi, *ACS Appl. Mater. Interfaces*, 2013, 5, 1722–1731.

- 116 D. Gajjar, R. Patel, H. Patel and P. M. Patel, *Chem. Sci. Trans.*, 2014, 3, 897–908.
- 117 M. Pawlaczyk and G. Schroeder, *Int. J. Mol. Sci.*, 2021, 22, 11353.
- 118 R. Ahangarani-Farahani and M. A. Bodaghifard, *J. Mater. Sci.: Mater. Electron.*, 2022, 33, 25674–25686.
- 119 R. Ahangarani-Farahani, M. A. Bodaghifard and S. Asadbegi, *Sci. Rep.*, 2022, 12, 19469.
- 120 A. Landarani-Isfahani, M. Moghadam, S. Mohammadi, M. Royvaran, N. Moshtael-Arani, S. Rezaei, S. Tangestaninejad, V. Mirkhani and I. Mohammadpoor-Baltork, *Langmuir*, 2017, 33, 8503–8515.
- 121 J. Xie, K. Chen, H. Y. Lee, C. Xu, A. R. Hsu, S. Peng, X. Chen and S. Sun, *J. Am. Chem. Soc.*, 2008, 130, 7542–7543.
- 122 A. Ito, K. Ino, T. Kobayashi and H. Honda, *Biomaterials*, 2005, 26, 6185–6193.
- 123 M. Cherri, M. Ferraro, E. Mohammadifar, E. Quaas, K. Achazi, K. Ludwig, C. Grötzinger, M. Schirner and R. Haag, *ACS Biomater. Sci. Eng.*, 2021, 7, 2569–2579.
- 124 C. Avitabile, L. Moggio, G. Malgieri, D. Capasso, S. Di Gaetano, M. Saviano, C. Pedone and A. Romanelli, *PLoS One*, 2012, 7, e35774.
- 125 F. Almomani, R. Bhosale, M. Khraisheh, A. kumar and T. Almomani, *Appl. Surf. Sci.*, 2020, 506, 144924.
- 126 T. Heek, C. Fasting, C. Rest, X. Zhang, F. Würthner and R. Haag, *Chem. Commun.*, 2010, 46, 1884–1886.
- 127 D. Ernenwein, A. M. Vartanian and S. C. Zimmerman, *Macromol. Chem. Phys.*, 2015, 216, 1729–1736.
- 128 N. Arsalani, H. Fattahi, S. Laurent, C. Burtea, L. Vander Elst and R. N. Muller, *Contrast Media Mol. Imaging*, 2012, 7, 185–194.
- 129 L. Wang, D. Su, L. Zeng, N. Liu, L. Jiang, X. Feng, K. G. Neoh and E. T. Kang, *Dalton Trans.*, 2013, 42, 13642–13648.
- 130 A. A. Umar, I. M. Saaid, A. Halilu, A. A. Sulaimon and A. A. Ahmed, *J. Mater. Res. Technol.*, 2020, 9, 13411–13424.
- 131 A. Ahmad, A. Gupta, M. M. Ansari, A. Vyawahare, G. Jayamurugan and R. Khan, *ACS Biomater. Sci. Eng.*, 2020, 6, 1102–1111.
- 132 A. Khannanov, A. Burmatova, K. Ignatyeva, F. Vagizov, A. Kiiamov, D. Tayurskii, M. Cherosov, A. Gerasimov, E. Vladimir and M. Kuttyreva, *Int. J. Mol. Sci.*, 2022, 23, 14764.
- 133 B. Das, M. Mandal, A. Upadhyay, P. Chattopadhyay and N. Karak, *Biomed. Mater.*, 2013, 8, 035003.
- 134 S. Habib, R. Akoume, E. Mahdi, M. Al-Ejji, M. K. Hassan and A. H. Hawari, *J. Water Process Eng.*, 2024, 60, 105280.
- 135 F. Morgenroth and K. Müllen, *Tetrahedron*, 1997, 53, 15349–15366.
- 136 Z. B. Shifrina, M. S. Rajadurai, N. V. Firsova, L. M. Bronstein, X. Huang, A. L. Rusanov and K. Muellen, *Macromolecules*, 2005, 38, 9920–9932.
- 137 T. M. Miller, T. X. Neenan, E. W. Kwock and S. M. Stein, *Macromol. Symp.*, 1994, 77, 35–42.
- 138 D. G. Morgan, B. S. Boris, N. V. Kuchkina, E. Y. Yuzik-Klimova, S. A. Sorokina, B. D. Stein, D. I. Svergun, A. Spilotros, A. Kostopoulou, A. Lappas, Z. B. Shifrina and L. M. Bronstein, *Langmuir*, 2014, 30, 8543–8550.
- 139 T. H. Rehm, C. Hofmann, P. Löb, Z. B. Shifrina, D. G. Morgan and L. M. Bronstein, *Chem. Ing. Tech.*, 2016, 88, 1338–1338.
- 140 N. V. Kuchkina, S. A. Sorokina, B. P. Lawson, A. S. Torozova, L. Z. Nikoshvili, E. M. Sulman, O. L. Lependina, B. D. Stein, M. Pink, D. G. Morgan, L. M. Bronstein and Z. B. Shifrina, *React. Funct. Polym.*, 2020, 151, 104582.
- 141 N. V. Kuchkina, D. G. Morgan, A. Kostopoulou, A. Lappas, K. Brintakis, B. S. Boris, E. Y. Yuzik-Klimova, B. D. Stein, D. I. Svergun, A. Spilotros, M. G. Sulman, L. Z. Nikoshvili, E. M. Sulman, Z. B. Shifrina and L. M. Bronstein, *Chem. Mater.*, 2014, 26, 5654–5663.
- 142 E. Y. Yuzik-Klimova, N. V. Kuchkina, S. A. Sorokina, D. G. Morgan, B. Boris, L. Z. Nikoshvili, N. A. Lyubimova, V. G. Matveeva, E. M. Sulman, B. D. Stein, W. E. Mahmoud, A. A. Al-Ghamdi, A. Kostopoulou, A. Lappas, Z. B. Shifrina and L. M. Bronstein, *RSC Adv.*, 2014, 4, 23271–23280.
- 143 D. Wang, C. Deraedt, L. Salmon, C. Labrugere, L. Etienne, J. Ruiz and D. Astruc, *Synfacts*, 2015, 11, 0447–0447.
- 144 L. M. Bronstein, *ChemCatChem*, 2015, 7, 1058–1060.
- 145 S. Quintana-Sánchez, A. Barrios-Gumiel, J. Sánchez-Nieves, J. L. Copa-Patiño, F. J. de la Mata and R. Gómez, *Mater. Sci. Eng., C*, 2021, 133, 112622.
- 146 A. Barrios-Gumiel, D. Sepúlveda-Crespo, J. L. Jiménez, R. Gómez, M. Á. Muñoz-Fernández and F. J. de la Mata, *Colloids Surf., B*, 2019, 181, 360–368.
- 147 I. M. Prados, A. Barrios-Gumiel, F. J. de la Mata, M. L. Marina and M. C. García, *Anal. Bioanal. Chem.*, 2022, 414, 1677–1689.
- 148 D. Wang, C. Deraedt, L. Salmon, C. Labrugère, L. Etienne, J. Ruiz and D. Astruc, *Chem. – Eur. J.*, 2015, 21, 1508–1519.
- 149 D. Rosario-Amorin, M. Gaboyard, R. Clérac, L. Vellutini, S. Nlate and K. Heuzé, *Chem. – Eur. J.*, 2012, 18, 3305–3315.
- 150 D. Rosario-Amorin, X. Wang, M. Gaboyard, R. Clérac, S. Nlate and K. Heuzé, *Chem. – Eur. J.*, 2009, 15, 12636–12643.
- 151 A. Garofalo, A. Parat, C. Bordeianu, C. Ghobril, M. Kueny-Stotz, A. Walter, J. Jouhannaud, S. Begin-Colin and D. Felder-Flesch, *New J. Chem.*, 2014, 38, 5226–5239.
- 152 J.-F. Berret and A. Graillot, *Langmuir*, 2022, 38, 5323–5338.
- 153 L. Wang, Z. Yang, J. Gao, K. Xu, H. Gu, B. Zhang, X. Zhang and B. Xu, *J. Am. Chem. Soc.*, 2006, 128, 13358–13359.
- 154 L. Wang, Z. Yang, J. Gao, K. Xu, H. Gu, B. Zhang, X. Zhang and B. Xu, *J. Am. Chem. Soc.*, 2006, 128, 13358–13359.
- 155 G. Lamanna, M. Kueny-Stotz, H. Mamlouk-Chaouachi, C. Ghobril, B. Basly, A. Bertin, I. Miladi, C. Billotey, G. Pourroy, S. Begin-Colin and D. Felder-Flesch, *Biomaterials*, 2011, 32, 8562–8573.
- 156 Z. Lotfi, H. Z. Mousavi and S. Maryam Sajjadi, *Microchim. Acta*, 2017, 184, 4503–4512.

- 157 Y. Tong, S. Li, Y. Wu, J. Guo, B. Zhou, Q. Zhou, L. Jiang, J. Niu, Y. Zhang, H. Liu, S. Yuan, S. Huang and Y. Zhan, *Chemosphere*, 2022, 296, 134009.
- 158 Y. X. Ma, Y. L. Kou, D. Xing, P. S. Jin, W. J. Shao, X. Li, X. Y. Du and P. Q. La, *J. Hazard. Mater.*, 2017, 340, 407–416.
- 159 M. Baghayeri, H. Alinezhad, M. Tarahomi, M. Fayazi, M. Ghanei-Motlagh and B. Maleki, *Appl. Surf. Sci.*, 2019, 478, 87–93.
- 160 M. Baghayeri, H. Alinezhad, M. Fayazi, M. Tarahomi, R. Ghanei-Motlagh and B. Maleki, *Electrochim. Acta*, 2019, 312, 80–88.
- 161 M. Aghazadeh, I. Karimzadeh and M. R. Ganjali, *Curr. Nanosci.*, 2018, 15, 169–177.
- 162 S. S. Gillani, M. A. Munawar, K. M. Khan and J. A. Chaudhary, *J. Iran. Chem. Soc.*, 2020, 17, 2717–2736.
- 163 J. W. J. Knapen, A. W. van der Made, J. C. de Wilde, P. W. N. M. van Leeuwen, P. Wijkens, D. M. Grove and G. van Koten, *Nature*, 1994, 372, 659–663.
- 164 Z. Chen, Y. Peng, Y. Li, X. Xie, X. Wei, G. Yang, H. Zhang, N. Li, T. Li, X. Qin, S. Li, C. Wu, F. You, H. Yang and Y. Liu, *ACS Nano*, 2021, 15, 16683–16696.
- 165 N. Bhalla, S. Taneja, P. Thakur, P. K. Sharma, D. Mariotti, C. Maddi, O. Ivanova, D. Petrov, A. Sukhachev, I. S. Edelman and A. Thakur, *Nano Lett.*, 2021, 21, 9780–9788.
- 166 F. Y. Cheng, S. P. H. Wang, C. H. Su, T. L. Tsai, P. C. Wu, D. Bin Shieh, J. H. Chen, P. C. H. Hsieh and C. S. Yeh, *Biomaterials*, 2008, 29, 2104–2112.
- 167 L. Danyang, N. Lanli, D. Yimin, Z. Jiaqi, C. Tianxiao and Z. Yi, *J. Mater. Sci.: Mater. Electron.*, 2019, 30, 1161–1174.
- 168 P. Parlanti, A. Boni, G. Signore and M. Santi, *Molecules*, 2020, 25, 2252.
- 169 H. Mirzapour, H. A. Panahi, E. Moniri and A. Feizbakhsh, *Microchim. Acta*, 2018, 185, 440.
- 170 Y.-L. Han, H.-R. Kim, H.-K. Kim and J.-W. Park, *Chemosphere*, 2022, 307, 135988.
- 171 S. Luo, J. Xu, Z. Zhu, C. Wu and S. Liu, *J. Phys. Chem. B*, 2006, 110, 9132–9139.